Biochemical and biophysical characterisation of the Cohesin complex

Kyle Muir

Communauté
UNIVERSITÉ Grenoble Alpes

THÈSE

Pour obtenir le grade de

DOCTEUR DE LA COMMUNAUTÉ UNIVERSITÉ GRENOBLE ALPES

Spécialité : Biologie Structurale et Nanobiologie

Arrêté ministériel : 25 mai 2016

Présentée par

Kyle MUIR

Thèse dirigée par **Daniel PANNE**

préparée au sein du **Laboratoire européen de biologie moléculaire**
dans **l'École Doctorale Chimie et Sciences du Vivant**

Caractérisation biochimique et biophysique du complexe cohésine

Biochemical and biophysical characterisation of the Cohesin complex

Thèse soutenue publiquement le **15 février 2016**,
devant le jury composé de :

Monsieur DANIEL PANNE
DIRECTEUR DE RECHERCHE, EMBL GRENOBLE, Directeur de thèse
Monsieur CARLO PETOSA
DIRECTEUR DE RECHERCHE, CNRS DELEGATION ALPES, Président
Madame JOANNA TIMMINS
CHARGE DE RECHERCHE, CNRS DELEGATION ALPES, Examinateur
Monsieur STEPHAN GRUBER
DIRECTEUR DE RECHERCHE, MPI - BIOCHIMIE (MARTINSRIED) ALLEMAGNE, Rapporteur
Monsieur ANDREA MUSACCHIO
PROFESSEUR, MPI. (DORTMUND) - ALLEMAGNE, Rapporteur
Monsieur CHRISTIAN HÄRING
DIRECTEUR DE RECHERCHE, EMBL HEIDELBERG - ALLEMAGNE, Examinateur

For May

Gie me ae spark o' Nature's fire,
That's a' the learning I desire

Table of Contents

List of Abbreviations

A	Alanine
Å	Ångstrom
aa	Amino acid
ABC	Adenosine triphosphate binding cassette
Ac	Acetyl
AcK	Acetyl-lysine
APC/C	Anaphase promoting complex/cyclosome
ATP	Adenosine triphosphate
bp	Basepairs
Cdc	Cell-division cycle protein
Cdk	Cyclin-dependent kinase
ChIP-Seq	Chromatin immunoprecipitation sequencing
Co	Cobalt
CoA	Coenzyme A
CTCF	CCCTC-binding factor
D	Aspartic acid
Da	Daltons
D_{max}	Maximum diameter
DEN	Deformable elastic network
DNA	Deoxyribonucleic acid
DTT	Dithiothrietol
E	Glutamic acid
Eco/Esco/Eso	Establishment of cohesion
EDTA	Ethylenediaminetetraacetic acid
EM	Electron microscopy
EMSA	Electrophoretic mobility shift assay
F	Phenylalanine
FACS	Fluorescence-activated cell sorting
FL	Full-length

G	Glycine
GCN	General control nonderepressible
GFP	Green fluorescent protein
GST	Glutathione S-transferase
H	Histidine
HA	Haemagluttanin
HAT	Histone acetyltransferase
hd	Head
HDAC	Histone deacetylase
HEAT	Huntington, EF3, PP2A, TOR1
Hepes	4-(2-hydroxyethyl)-1-piperazineethanesulfonic acid
His-tag	Polyhistidine-tag
HCL	Hydrochloric acid
HTX	High-throughput crystallography
I	Isoleucine
IMAC	Immobilised metal ion chromatography
IPTG	Isopropyl--β-thio-galactoside
KEN	Lysine, glutamic acid, asparagine
K	Lysine
kDa	Kilodalton
L	Leucine
M	Methionine
mAU	Milliabsorbance units
MES	2-(N-morpholino)ethanesulfonic acid
µl	Microlitres
ml	Millilitres
µM	MicroMolar
mM	MilliMolar
MPD	2-Methyl-2,4-pentanediol
N	Asparagine

NaCl	Sodium chloride
NCS	Non-crystallographic symmetry
nm	nanometres
OD	Optical density
ORF	Open reading frame
P	Proline
PCNA	Proliferating cell nuclear antigen
PCR	Polymerase chain reaction
Pds	Precocious dissociation of sisters
PK	V5 epitope
Plk	Polo-like kinase
PP2A	Protein phosphatase 2A
PDB	Protein databank
Q	Glutamine
R	Arginine
R_g	Radius of gyration
RNAi	Ribonucleic acid interference
S	Serine
SAD	Single wavelength anomalous diffraction
SAXS	Small-angle X-ray scattering
Scc	Sister chromatid cohesion
SCF	Skp, Cullin, F-box containing complex
ScpA	Segregation and condensation protein A
SDS-PAGE	Sodium dodecyl sulphate-polyacrylamide gel electrophoresis
SEC	Size-exclusion chromatography
SeMet	Selenomethionine
Sgo	Shugoshin
Smc	Structural maintenance of chromosomes
T	Threonine
TCEP	Tris(2-carboxyethyl)phosphine

tet	Tetracycline
TEV	Tobacco etch virus
TLS	Translation/libration/screw
Tris	Tris(hydroxymethyl)aminomethane
TRP	Tryptophan
ts	Temperature-sensitive
URA	Uracil requiring
V	Valine
W	Tryptophan
Wapl	Wings apart-like protein homologue
w/w	Weight by weight
X	X-ray
Y	Tyrosine
zf	Zinc finger

List of Figures

Abstract

Sister chromatid cohesion is a fundamental prerequisite to faithful genome segregation. Cohesion is precisely regulated by accessory factors that modulate the stability with which the cohesin complex embraces chromosomes. One of these factors, Pds5, engages cohesin through Scc1 and participates both in the enhancement of cohesion, and conversely in mediating the release of cohesin from chromatin. In this thesis the crystal structure of a complex between budding yeast Pds5 and Scc1 is presented, thus elucidating the molecular basis of Pds5 function. Pds5 forms an elongated HEAT repeat that binds to Scc1 via a conserved surface patch. Complementary cell biological and biochemical characterisation of this structure demonstrates that the integrity of the Pds5–Scc1 interface is indispensable for the recruitment of Pds5 to cohesin, and that its abrogation results in loss of sister chromatid cohesion and cell viability, in a manner correlative to weakened binding strength. The results presented in this thesis therefore suggest that Pds5 is a constitutively bound, core subunit of cohesin.

Résumé en Français

L'appariement des chromatides sœurs est un prérequis fondamental pour la ségrégation fidèle du génome. Cet assemblage est précisément régulé par plusieurs facteurs modulant la solidarité entre le complexe formant la cohésine et les chromosomes. Un de ces facteurs, Pds5, engage la cohésine par le biais de Scc1 et participe à la fois au renforcement de la cohésion, et inversement à la libération de la cohésine de la chromatine. Dans cette thèse, la structure cristalline du complexe entre les protéines de levure Pds5 et Scc1 est présentée. Celle-ci permet la compréhension de la fonction moléculaire de Pds5. Pds5 forme un « heat-repeat » allongé qui se lie à Scc1 via une interface dont sa séquence reste conservée. Suite à la caractérisation biologique et biochimique de cette structure, cette thèse démontre que l'intégrité de l'interface entre Pds5 et Scc1 est indispensable pour le recrutement de Pds5 à la cohésine et que son abrogation conduit à la perte de la cohésion entre les chromatides sœurs ainsi que la perte de la viabilité cellulaire. Les résultats présentés dans cette thèse suggèrent donc que Pds5 est constitutivement lie au cœur de la sous-unité de la cohésine.

Introduction

Résumé en Français

Dans les trois principaux règnes de la vie: Eucaryote, Procaryote et *Archaea* l'information génétique qui définit la cellule et donc l'organisme doit être fidèlement transmise de génération en génération. Infailliblement, le maintien précis du génome lors de la réplication et la ségrégation de celui-ci dans les cellules filles est donc impératif pour le succès et même l'existence de toute espèce.

Dans de nombreux organismes procaryotes, la réplication et la ségrégation sont étroitement couplées temporellement. Dans de nombreux cas, ils coïncident avec nucléoïdes doubles étant rapidement compactés et captifs, ou tout simplement transportés, vers les pôles opposés de la cellule avant de fission binaire de l'organisme. Cependant, dans les organismes eucaryotes, la réplication se produit bien avant la division cellulaire. Pour cette raison, de nouveaux mécanismes ont évolué pour assurer l'appariement (ou la cohésion), la dissociation et la ségrégation correcte des chromatides sœurs.

Le processus de cohésion des chromatides sœurs répond à deux problèmes fondamentaux dans la cellule eucaryote. Tout d'abord, il permet, de mani**è**re tout à fait élégante, le couplage de la réplication de l'ADN avec le jumelage de chromatides sœurs. En effet, la cohésion n'est possible qu'une fois que l'état diploïde de la cellule est atteint. D'autre part, la cohésion confère une résistance à la tension requise pour la bi-orientation et fixation des chromatides sœurs aux centrosomes situés sur les pôles opposés de la cellule, en compensant les forces exercées par microtubules du fuseau sur cinétochores sœurs.

L'exécution correcte de ce processus permet d'éviter une mauvaise ségrégation et l'aneuploïdie dû à un appariement incorrect des chromosomes. Aussi, les mécanismes de ségrégation peuvent se dérouler de manière appropriée pour assurer une transmission fid**è**le des chromosomes aux cellules filles.

La cohésion de chromatides sœurs est médiée par un complexe protéique appelé cohésine. Ce mécanisme est ancien d'un point de vue évolutif et se compose d'un

sous-complexe annulaire formé par deux protéines 'structural maintenance of chromosomes' (SMC), Smc1 et Smc3, qui sont apparu chez les procaryotes, et Scc1, apparenté à la famille des protéines kleisin, partagent certaines caractéristiques structurales avec leurs équivalents procaryotes.

Pendant le cycle cellulaire, la cohésine subit plusieurs cycles fonctionnels. Initialement, la cohésine est liée à des proteines accessoires. Durant la réplication de l'ADN, lorsque les paires de chromosomes apparaissent, la cohésion de chromatides sœurs est établie par l'acétylation du complexe par Eco1, un acétyl-transférase spécifique. La cohésion est ensuite maintenue jusqu'à la division cellulaire où sa dissociation permise par un processus en deux étapes. La première étape est précisément régulée par une série de protéines accessoires: Scc3, Pds5, et le facteur de dissociation Wapl Ces proteines ont été proposées pour la modulation de la stabilité de l'ensemble cohésine sur la chromatine. L'association de ces protéines avec cohésine est permise par Scc1, qui agit comme un hub pour le recrutement des facteurs de régulation de la cohésion. La seconde, et dernière étape dans le cycle de la cohésion est la destruction de la cohésine encore lié à la chromatine. Ceci est effectué par le clivage de la sous-unité Scc1 par la protéase Separase durant la transition entre la métaphase à l'anaphase, permettant ainsi la libération des chromatides sœurs et leur ségrégation dans les cellules filles

1.1 Sister chromatid cohesion

Across the three domains of life: *Bacteria*, *Archaea*, and *Eukaryota*, the genetic information which defines the cell and thus the organism must be faithfully inherited from generation to generation. Unfailingly accurate genome maintenance, replication, and segregation into daughter cells therefore are imperative to the success and indeed the continued existence of any species.

In many prokaryotic organisms, replication and segregation are tightly temporally coupled, and in many instances coincide, with duplicated nucleoids being swiftly compacted and tethered, or simply transported, to opposite poles of the cell prior to binary fission of the organism. In eukaryotic organisms however, replication can occur significantly in advance of cell division, thus additional mechanisms have evolved to ensure proper pairing (or cohesion), dissociation and segregation of sister chromatids.

The process of sister chromatid cohesion addresses two fundamental problems in the Eukaryotic cell. Firstly, it enables, quite elegantly, the coupling of DNA replication with the subsequent pairing of sister chromatids, such that cohesion only arises when the diploid state of the cell is achieved. Secondly, cohesion confers resistance to the tension required for the biorientation and amphitelic attachment of sister chromatids to centrosomes located on opposite poles of the cell, by counteracting forces exerted by spindle microtubules on sister kinetochores.

The correct execution of this process thusly ensures both that missegregation and aneuploidy do not arise through aberrant chromosome pairing, and that the segregation machinery may assemble appropriately to ensure the fidelity of chromosome transmission to daughter cells.

Early investigations led to the proposal of a mechanism wherein sister chromatid cohesion is enforced by replication-coupled catenation of sister DNAs and resolved by enzymatic de-catenation (Murray and Szostak, 1985). However, it transpired that cells arrested in metaphase do not maintain such intertwined DNA structures, yet still possess paired chromatids (Guacci et al., 1994, Koshland and Hartwell, 1987).

Furthermore, the discovery that a cell-cycle regulated programme of proteolysis (Holloway et al., 1993), and the discovery of the E3 ubiquitin ligase responsible for targeting relevant substrates (the APC/C) (King et al., 1995, Sudakin et al., 1995), facilitate the metaphase-to-transition to permit cell division, were crucial in establishing that sister chromatid cohesion most likely had a mechanism that was predominantly orchestrated by proteins.

The basic apparatus which mediates sister chromatid cohesion is evolutionarily ancient and principally consists of an annular complex formed by two structural maintenance of chromosomes (SMC) proteins, which arose in prokaryotes, and their cognate kleisin proteins, which share some structural features with their prokaryotic equivalents (Gruber et al., 2003, Haering and Jessberger, 2012, Haering and Hochwagen, 2002, Gligoris et al., 2014, Huis in 't Veld et al., 2014, Peters and Nishiyama, 2012, Anderson et al., 2002).

In Eukaryotic organisms, evolution has produced at least three separate families of SMC complexes, each with distinct roles in chromosome condensation, sister chromatid cohesion and DNA repair, referred to as condensin, cohesin, and SMC5/6 respectively (Hirano, 2006). For the purpose of this thesis, I will focus primarily on cohesin, its mechanisms, and regulation, with brief allusion to aspects of the other SMC complexes where relevant.

The first SMC gene (initially an acronym of ‘stability of minichromosomes’; later revised to ‘structural maintenance of chromosomes’ according to taste) gene was initially named three decades ago in *Saccharomyces Cerevisiae* (Larionov et al., 1985). Thereafter the gene product, Smc1, was characterised further and established as an essential chromosome segregation factor (Strunnikov et al., 1993).

The discovery of the cohesin complex arose from parallel studies designed to identify regulators of chromosome architecture (Guacci et al., 1997), and mutants capable of executing sister-chromatid disjunction in the absence of APC/C function, which is otherwise required for chromosome segregation, respectively (Michaelis et al., 1997).

The latter study, in particular, demonstrated that Scc1, Smc3 and Smc1 localise to chromosomes to facilitate sister chromatid cohesion. Subsequently, cohesin complexes were also identified in diverse Eukaryotic organisms, and the functions of previously identified genes reconciled with the identification of this novel complex, underscoring the functional conservation of this proteinaceous mode of sister chromatid cohesion and dissolution (Losada et al., 1998, Darwiche et al., 1999, Jessberger et al., 1996, Birkenbihl and Subramani, 1992).

1.2. The general architecture of the cohesin complex

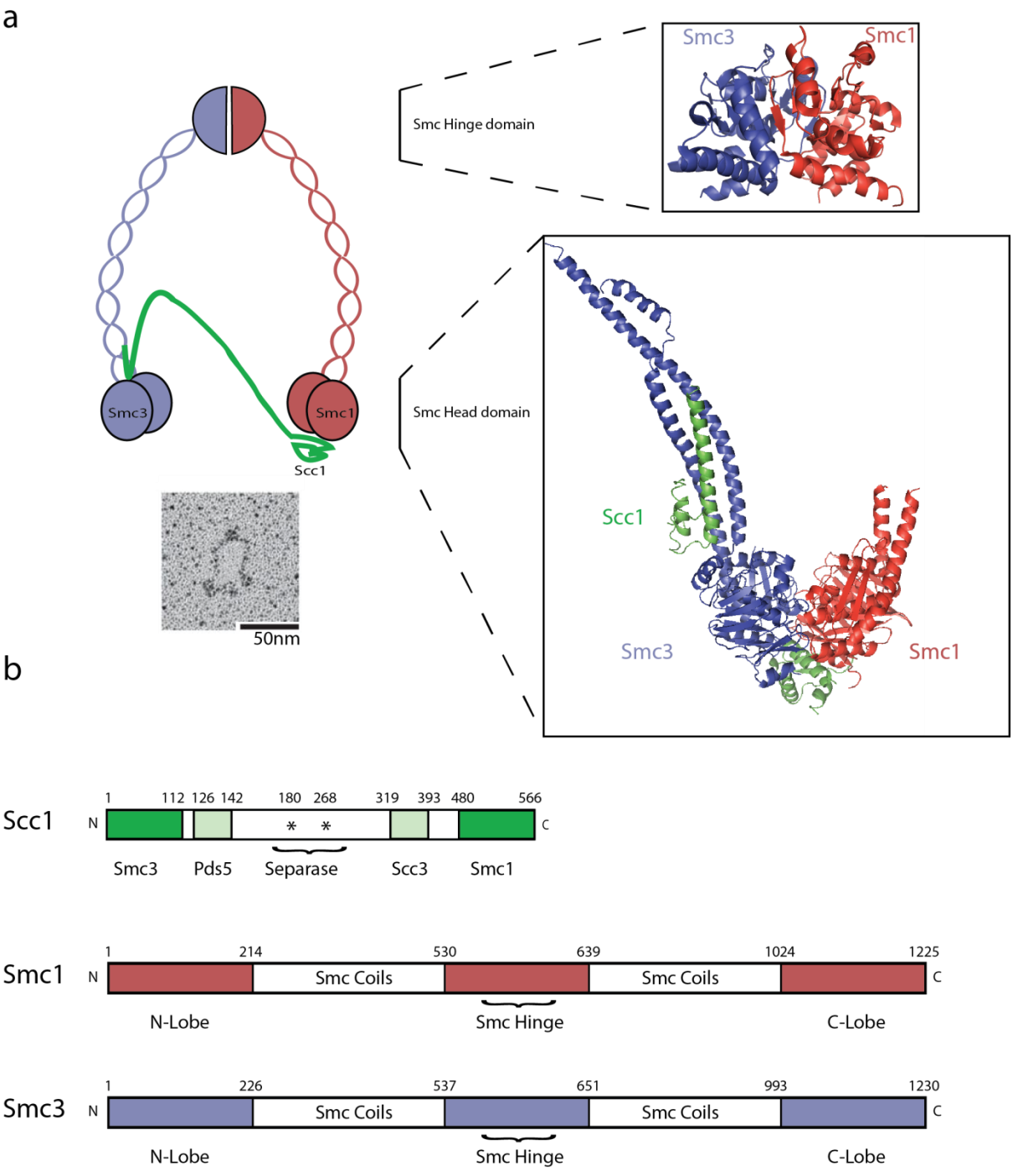

Figure 1 | Architecture of the cohesin trimer. (a) Schematic illustration of cohesin. The Smc3-Smc1-Scc1 cohesin trimer forms a ring (depicted as a cartoon in the upper left), with

corresponding rotary shadowing EM of the cohesin tetramer shown below (Huis in 't Veld et al., 2014). Smc3 and Smc1 interact through their hinge domains to form a toroidal heterodimer (upper panel; PDB 2WD5). The N terminus of Scc1 forms a 4 alpha-helical bundle with the coiled coil domain of Smc3 (PDB 4UX3); the C terminus of Scc1 folds into a winged-helix domain which associates with the underside of the Smc1 ATPase head (PDB 1W1W). (b) Domain architecture and sequence boundaries of Scc1, Smc1, and Smc3. Scc1 is a modular protein scaffold with binding regions for Smc3, Pds5, Scc3, and Smc1 (from N to C terminus). Two separase sites are located in the centre of Scc1. The Smc proteins follow analogous ATPase N-lobe, coils, hinge, coils, ATPase C-lobe domain configuration.

The core cohesin complex in budding yeast comprises an annular trimer composed of two SMC proteins, Smc1 and Smc3, and the alpha–kleisin subunit Mcd1/Scc1 (figure 1a). Each SMC protein contains a functional ABC-like ATPase head, comprised of two lobes contributed by N– and C–terminal domains, and a central hinge domain, through which Smc3 and Smc1 heterodimerize, which are separated by ~40 nm through the antiparallel packing of the intervening coiled–coil region. The ATPase heads are arranged such that the Walker A and B motifs of one head engage ATP, through its phosphate and ribose groups respectively, so that its γ-phosphate group is positioned in proximity to the signature C-motif of an adjacent head (Haering et al., 2004, Gligoris et al., 2014). Consequently, the heads do not hydrolyse ATP independently, but must do so in tandem with an opposing SMC head.

Finally the N– and C–terminal domains of Scc1 associate with the Smc3, and Smc1 head, respectively (Figure 1. a-b), thus closing the ring. Scc1 is a member of a highly conserved, from bacteria to humans, family of proteins called ‘kleisins’ (a portmanteau derivative of the Greek ‘kleísimo’, meaning ‘closure’), which are highly modular in nature and, in addition to facilitating ring closure, per their namesake, by bridging SMC heads, have been described to thus also serve as binding platforms for regulatory factors (Schleiffer et al., 2003, Haering and Hochwagen, 2002, Kulemzina et al., 2012, Murayama and Uhlmann, 2014, Piazza et al., 2014).

The resulting assemblies are large tripartite rings, which are thought to entrap sister chromatids, most likely in a topological manner (Gligoris et al., 2014, Gruber et al.,

2003, Haering et al., 2008, Huis in 't Veld et al., 2014). Rotary shadowing EM experiments, of both native and recombinant cohesin confirm this ring-like architecture (Anderson et al., 2002, Haering et al., 2002, Huis in 't Veld et al., 2014). However the structure of chromosome-bound cohesin remains to be determined.

The functional importance of this circular architecture is, at least, twofold; firstly it confers a considerable diameter to the complex, which is presumably important in mediating chromatin entrapment, and secondly, it provides several heterotypic interfaces through which DNA may pass (Haering and Hochwagen, 2002, Gruber et al., 2003, Huis in 't Veld et al., 2014). The prevailing consensus in the field holds that DNA entry into the ring requires dissociation of the Smc1-Smc3 hinges, as artificial closure of this interface inhibits the accumulation of cohesin on chromatin (Gruber et al., 2006). Release of cohesin from DNA, however, appears to be governed by two modes: the cleavage of Scc1 at the metaphase to anaphase transition, which naturally is irreversible, and the transient dissociation of the Smc3-Scc1 interface (Uhlmann et al., 1999, Chan et al., 2012, Buheitel and Stemmann, 2013, Eichinger et al., 2013).

1.3. Cohesion and the cell cycle

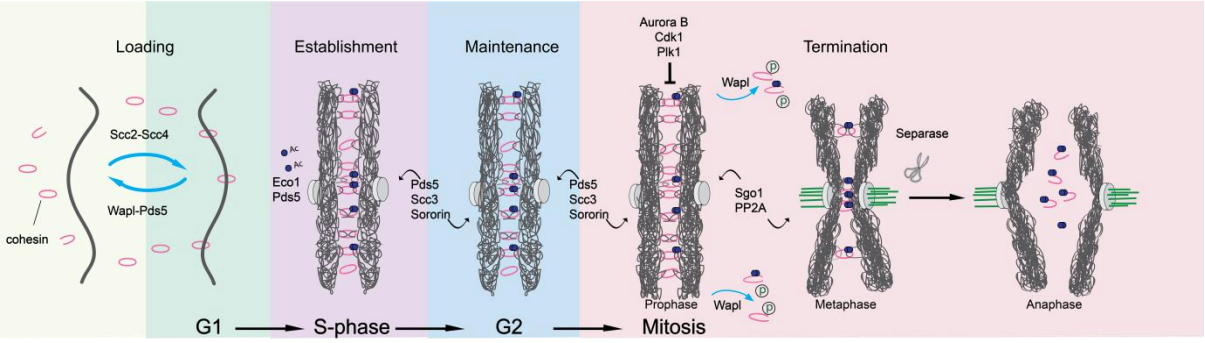

Figure 2 | Regulation of cohesion throughout the cell cycle. In Metazoan telophase, cohesin (pink) is loaded by Scc2-Scc4. Loading continues in G1 phase. During G1, cohesin dynamics are enforced by the antagonistic loading and unloading activities of Scc2-Scc4 and Wapl-Pds5 respectively. Cohesion establishment occurs in S-phase and coincides with acetylation (acetyl-lysine is depicted as blue spheres) of Smc3 by Eco1, in a manner involving Pds5. From S-phase to Mitosis, Pds5, Scc3, and Sororin co-operate to maintain cohesion. At the onset of mitosis, mitotic kinases phosphorylate cohesin, rendering these complexes

vulnerable to removal by Wapl. Centromeric cohesion is protected by Sgo1-PP2A until the metaphase-to-anaphase transition. Upon successful biorientation and spindle attachment, cohesin is cleaved by separase to permit progression into anaphase. Chromosomes subsequently segregate into daughter cells and the cell-cycle restarts. Figure adapted from Haarhuis et al., 2014 and Singh et al., 2015.

Sister chromatid cohesion is a fundamental prerequisite to faithful genome segregation, and so the establishment of and dissolution of cohesion is precisely regulated by accessory factors that modulate the stable association of the cohesin complex with chromosomes. Therefore, as will be described in this section, cohesin undergoes several functional transitions concurrent with the stages of the chromosome cycle of the cell.

At the commencement of the cell-cycle, cohesin is assembled onto chromosomes by an accessory loading complex, and is antagonised by release factors. Turnover of the complex on DNA remains dynamic until stable cohesion is established in S-phase by the cohesin acetyltransferase, which is thought to neutralise release function by acetylating a subset of centromeric and telomeric cohesin. Acetylated cohesin then remains robustly associated with chromosomes throughout interphase until it is proteolytically cleaved following G2 by specific protease, releasing sister chromatids to be segregated into daughter cells, and permitting progression through anaphase to a new cell cycle.

A schematic representation of the regulation of cohesin throughout the cell-cycle is presented in figure 2.

1.3.1. Cohesin loading and positioning

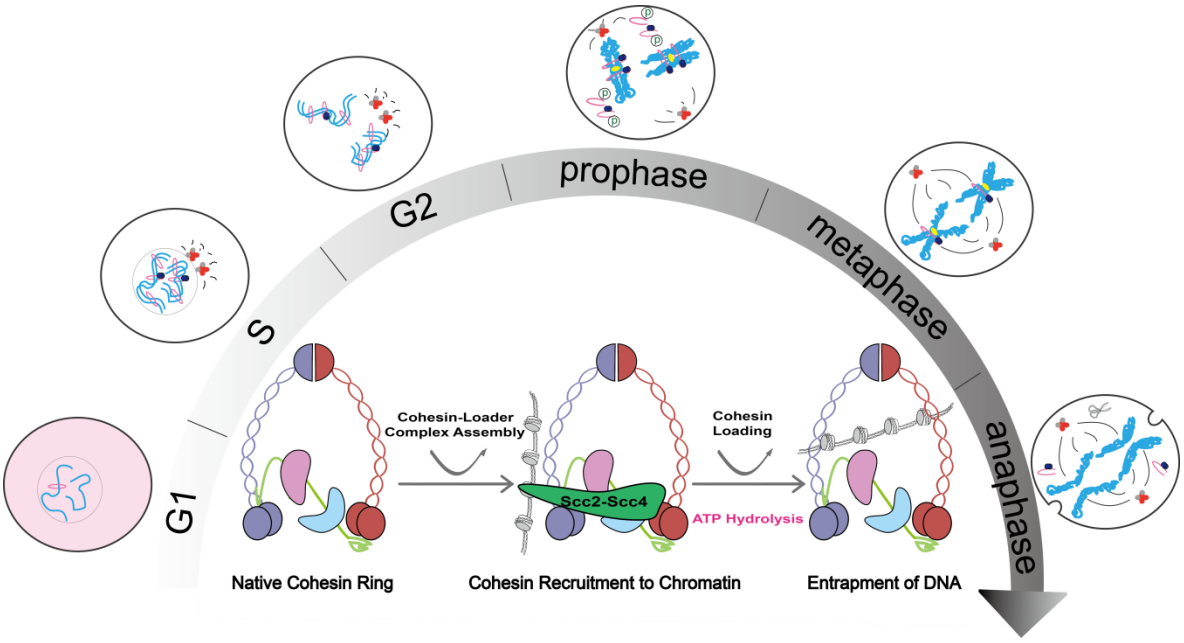

Figure 3 | Cohesin loading. At the commencement of the cell-cycle, cohesin is recruited to chromatin by the Scc2-Scc4 loading complex (indicated in green as a single entity), which may utilise the energy produced from ATP hydrolysis by the SMC heads to facilitate entrapment of chromatin by the cohesin ring (the loading reaction). Also shown are Pds5 (violet) and Scc3 (blue). The chromosome cycle is depicted inside spheres above a hemispherical arrow indicating the stage of the cell-cycle represented. The stage of the cell-cycle under consideration is highlighted in pink, and is accompanied by a more detailed illustration of concurrent cohesin behaviour. Cohesin rings are again shown in pink, with and without KAc, chromosomes are depicted in blue, centrosomes are shown in red and grey.

The loading of cohesin onto chromosomes commences in telophase in metazoans, and in G1 in yeast, in a manner dependent on ATP hydrolysis by Smc1–Smc3, on binding of the Scc3 subunit to a central region on Scc1, and on the accessory Scc4–Scc2 complex, which facilitates recruitment of cohesin to chromatin and its subsequent loading on to chromatin respectively (figure 3) (Hinshaw et al., 2015, Chao et al., 2015, Murayama and Uhlmann, 2014, Ladurner et al., 2014, Sumara et al., 2000, Losada et al., 2000, Ciosk et al., 2000). In yeast, these loading sites converge in pericentromeric chromatin, to which Scc2-Scc4 is recruited by an as yet unknown mechanism, whereas

in humans no such loading sites have been determined as of yet (Ciosk et al., 2000, Blat and Kleckner, 1999, Megee et al., 1999). In the absence of its loader, cohesin is able to load onto plasmid DNA in the presence of ATP (Murayama and Uhlmann, 2014). It is possible that a specialised chromatin environment may be required for cohesin loading (Bernard et al., 2001); ChIP-seq studies indicate that the Scc2-Scc4 complex accumulates at and is maintained in regions of naked DNA (Lopez-Serra et al., 2014). As Scc4 appears to be responsible for the targeting to cohesin, it was also recently proposed that this may involve a specific chromosomal receptor (Chao et al., 2015).

In the absence of a functional ATPase activity, cohesin accumulates and turns over rapidly at pericentromeric regions (Hu et al., 2011), however, in yeast, cohesin which has fulfilled loading is then relocated to so-called cohesin-associated regions, possibly by RNA polymerase II and its associated factors, of which the majority coincide with sites of convergent transcription. (Bausch et al., 2007, Lengronne et al., 2004, Tanaka et al., 1999, Glynn et al., 2004, Megee et al., 1999, Blat and Kleckner, 1999).

The chromosomal localisation of cohesin in mammals is emerging as a determining factor of large-scale modulation of genome biology, and appears to be correspondingly more complex. Whilst the positioning of cohesin in metazoans has been reported to be regulated by additional factors such as CTCF (Wendt et al., 2008, Parelho et al., 2008), and may dictate processes as diverse as the global addresses of transcription factors (Yan et al., 2013), execution of transcriptional regulation (Kagey et al., 2010), and X-chromosome inactivation (Minajigi et al., 2015), the modes, mechanisms and consequences of this function are yet to be fully understood.

1.3.2. Establishment of cohesion

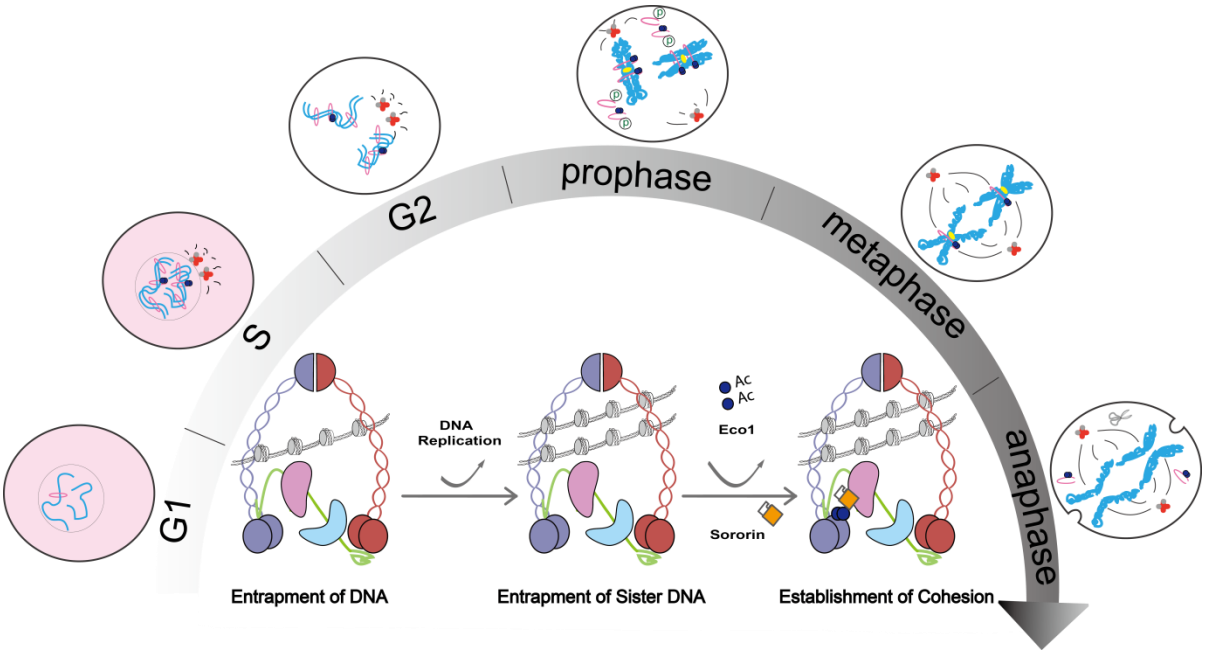

Figure 4 | Establishment of cohesion in S-phase. Sister DNAs are replicated and entrapped by cohesin. Eco1 then acetylates the Smc3 head, promoting Sororin recruitment (in Metazoans; depicted as a padlock), and the establishment of cohesion.

Live imaging studies indicate that there are at least 3 populations of cohesin found within cells: a transiently bound fraction, with a residence time of seconds, a dynamic population, which loads and unloads within minutes, and a third population which remains bound for an extended period of time and presumably corresponds to the pool of cohesin concerned with sister-chromatid cohesion, only arising in S-phase (Chan et al., 2012, Gerlich et al., 2006, Ladurner et al., 2014, Gause et al., 2010). The first population likely corresponds to cohesin which associates with, but does not load on to chromatin, whereas the second and third populations appear to depend on the ability of cohesin to hydrolyse ATP, suggesting that they correspond to cohesin which has successfully effected the loading process to entrap chromatin (Hu et al., 2011, Ladurner et al., 2014). Therefore, current evidence indicates that there are two chromosomal populations of cohesin: an exceptionally stable population, which emerges in S-phase and is dependent on acetylation of Smc3, and a more dynamic population, which is less

well understood and, as mentioned previously, may be responsible for functions of the cohesin complex which extend beyond its role in sister chromatid cohesion.

Turnover of the complex on DNA remains dynamic until S phase, when stable cohesion is established by the acetylation of two adjacent, evolutionarily conserved lysine residues on the Smc3 head (K112-113 in yeast, K105-106 in humans), by the cohesin acetyltransferase Eco1 (Establishment of Cohesion 1) (figure 4) (Ben-Shahar et al., 2008, Unal et al., 2008, Zhang et al., 2008, Skibbens et al., 1999, Toth et al., 1999, Ivanov et al., 2002).

Eco1 is ordinarily expressed prior to and degraded after S-phase, following the coordinated action of several kinases, which sequentially phosphorylate Eco1 in an elaborate AND-gated coincidence detection circuit, and Cdc4-SCF (Lyons and Morgan, 2011, Lyons et al., 2013, Borges et al., 2010). Thus activity of the enzyme is timed to coincide with the replication of sister-chromatids.

Acetylation *in vivo* occurs preferentially on chromatin-bound cohesin (Unal et al., 2008, Mishra et al., 2010), however it has proven possible to recapitulate this reaction *in vitro,* and so the precise determinants of when and how cohesin becomes acetylated remain somewhat mysterious (Ladurner et al., 2014).

However, several lines of evidence infer a direct coupling between the acetylation of Smc3, and thus cohesion establishment, to replication. It was found that Eco1 coimmunoprecipitates and co-localises with elements of replication factor C (RFC), a heteropentamer which facilitates the assembly of the DNA polymerase processivity factor PCNA (proliferating cell nuclear antigen) on to DNA, in addition to potentially directly interacting with PCNA itself (Kenna and Skibbens, 2003, Lengronne et al., 2006, Moldovan et al., 2006), suggesting at least that Eco1 associates with the replication fork. The identification of cohesion defects arising from depletion or perturbation of non-essential elements of replication forks, and of replicative DNA polymerases further establishes that cohesion is indeed somehow directly coupled to replication (Edwards et

al., 2003, Borges et al., 2013). Intriguingly, the Eco1 equivalent in fission yeast, Eso1, is physically fused to DNA polymerase η in this organism (Tanaka et al., 2000).

The loading of cohesin onto DNA in Xenopus extracts has been proposed to depend on elements of the pre-replication apparatus, and may indeed facilitate replication licensing (Gillespie and Hirano, 2004, Takahashi et al., 2004), furthermore implying a mutually beneficial relationship between the two processes. Notably, this is supported by studies which indicate that ATP hydrolysis is a prerequisite for both the loading and acetylation of cohesin (Arumugam et al., 2003, Hu et al., 2011, Ladurner et al., 2014, Murayama and Uhlmann, 2014).

Finally, depletion of functional Eco1 has also been shown to reduce the rate at which the replication fork, and thus sister-chromatid synthesis proceeds (Terret et al., 2009).

Collectively, these data emphasise a model wherein timely establishment of sister chromatid cohesion is achieved by directly linking acetylation of Smc3 to replication of the sisters.

Accordingly, cohesin complexes which have loaded in G2 do not participate in cohesion, emphasising that the establishment of cohesion is truly confined to S-phase (Uhlmann and Nasmyth, 1998). The only exception to this appears to be DNA-damage induced cohesion which appears to require *de novo* acetylation of cohesin, however it is not currently clear how targeting of Eco1 to sites of DNA damage is achieved (Strom et al., 2007, Unal et al., 2007, Sjogren and Nasmyth, 2001).

The mechanistic details of how acetylation of the Smc3 head confers such dramatic stabilisation of cohesin on chromatin remain elusive, however it has been proposed that it may act to modulate the ATPase activity of the complex (Heidinger-Pauli et al., 2010, Gligoris et al., 2014, Ladurner et al., 2014). Accordingly, acetyl-mimicking mutations rescue inviability of temperature-inactivation of a temperature-sensitive Eco1 allele, *eco1-1*, in yeast, but appear to induce significant cohesion defects (Ben-Shahar et al., 2008, Unal et al., 2008). Yet, this hypothesis remains somewhat controversial, as both acetylated and acetyl-mimic cohesin complexes maintain essentially wild-type levels of

ATP hydrolysis (Ladurner et al., 2014). A recent structure of the yeast Smc3 head revealed that the targets of Eco1, K112-K113, are located on the external surface of the Smc3 N-lobe, which led the authors to speculate that the positioning of these residues enables direct coupling of acetylation to an alpha helix which resides in close proximity to the Walker B motif, and may thus affect ATP engagement by Smc3 (Gligoris et al., 2014). It was not directly reported whether or not this influences ATP hydrolysis by cohesin. Instead it was determined that an R61Q mutation in this 'coupling' helix of Smc3 perturbs accumulation of cohesin at pericentric regions in G2, a process which is reliant on ATP hydrolysis. Given that the R61 residue participates in a hydrogen bonding network with nearby backbone atoms, it remains entirely possible that the phenotype observed is the product of a steric effect.

Further insights arose from parallel yeast studies designed to identify suppressor mutants of loss of Eco1 function through inactivation of a temperature-sensitive strain. Initial studies in fission yeast determined that the deletion of Pds5 rescued lethality of Eso1 deletion, implying that the function of acetylation may be to counteract functions of cohesin-associated proteins which are refractory to the establishment of cohesion (Tanaka et al., 2001). It was subsequently demonstrated that deletion of Wapl, and the presence of certain point mutants within Smc3, Pds5, Scc3, Eco1, and Wapl, render Eco1, which is an otherwise essential gene, dispensable for cell viability (Ben-Shahar et al., 2008, Rowland et al., 2009, Shintomi and Hirano, 2009, Sutani et al., 2009). This work led to the proposal that Pds5, Scc3, and Wapl might constitute a network of 'anti-establishment' or 'releasing' factors which might facilitate the release cohesin in the absence of Eco1 function (Rowland et al., 2009, Shintomi and Hirano, 2009, Sutani et al., 2009, Nasmyth, 2011). It is important to note that unlike, Pds5 and Scc3, Wapl has not been described to participate in cohesion promoting activities, and appears to associate with cohesin substoichiometrically, implying a transient, perhaps catalytic mode of release (Chan et al., 2012). Therefore, Wapl has been proposed to constitute a 'cohesin inhibitor', and is most likely the key agent in driving this release activity (Chan et al., 2012, Lopez-Serra et al., 2013, Ouyang et al., 2013, Tedeschi et al., 2013).

Thus establishment of cohesion might not be fully explained by modulation of Smc3's ATPase activity, but may require further regulatory mechanisms which are controlled by cohesin-associated factors. Indeed, metazoan organisms require a further factor called Sororin, for which a yeast analogue has not yet been identified, whose recruitment is enhanced by Smc3 acetylation, and which is proposed to enhance stability of cohesion by antagonising recruitment of the dissociation factor Wapl (Nishiyama et al., 2010, Rankin et al., 2005, Minamino et al., 2015).

The discovery that fusion of Smc3 to Scc1 can overcome this release activity led to the proposal that the Smc3-Scc1 interface constitutes a DNA 'exit-gate', and that the stable establishment of cohesion might therefore depend on the closure of this gate (Chan et al., 2012, Buheitel and Stemmann, 2013, Eichinger et al., 2013). The structure of this interface reveals that Scc1 forms a 4 α-helix bundle with the base of Smc3's coiled coils, which strongly resembles the assembly formed by the bacterial Condensin homologue (Burmann et al., 2013, Gligoris et al., 2014). The opening and closure of such interfaces therefore is likely to be a universal determinant of dynamic transactions between DNA and SMC complexes.

Curiously, the Smc3-Scc1 interface is relatively distant from the acetylation sites and the ATPase pocket of Smc3, thus it is not yet clear how the acetylation status of cohesin might prevent opening of this interface to confer sister chromatid cohesion, or conversely how antagonistic factors such as Wapl may drive its dissociation. However, it is highly probable that cohesion establishment by acetylation may involve the as of yet ill-defined adaptor mechanisms of associated regulators such as Pds5, Sororin, and Scc3, which may potentially act in concert to translate energy produced during the ATP hydrolysis cycle to promote different functional outcomes.

Whatever the mechanism, it is clear that acetylated cohesin may remain robustly associated with chromosomes, apparently resisting dissociation until proteolytic cleavage of their Scc1 subunits by the cysteine protease Separase at the metaphase–to–anaphase transition, releasing sister chromatids for their segregation into the

daughter cells (Peters and Nishiyama, 2012, Rowland et al., 2009, Sutani et al., 2009, Tedeschi et al., 2013, Gerlich et al., 2006).

1.3.3. Dynamic cohesin release and discovery of the prophase pathway

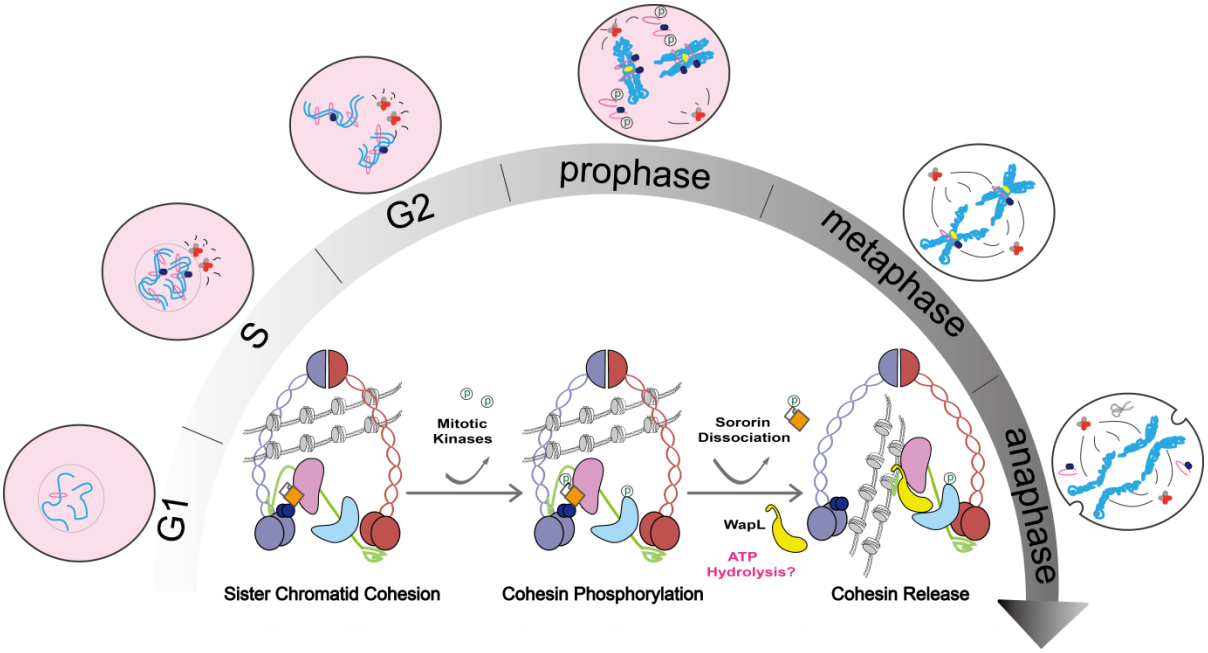

Figure 5 | Cohesin release in prophase. Mitotic kinases, as described in the text, phosphorylate the cohesin subunits Sororin and Scc3, which causes Sororin dissociation and enables Wapl to promote release of cohesin from chromatin. The prophase cohesin release pathway affects both acetylated and non-acetylated (not shown) complexes. Energy for the release process has been speculated to derive from ATP hydrolysis.

Liberation of non-acetylated cohesin from chromatin throughout the cell-cycle appears to be mediated through disruption of the Smc3–Scc1 interface and allows the complex to participate in a dynamic cycle of DNA entrapment and release (Eichinger et al., 2013, Buheitel and Stemmann, 2013, Chan et al., 2012). Cohesin release is exquisitely regulated by a series of accessory proteins: Scc3, Pds5, and the dissociation factor Wapl, which have been proposed to collectively modulate the stability of cohesin on chromatin. The association of these proteins with cohesin occurs through Scc1, which acts as a nexus for the recruitment of regulatory factors (Roig et al., 2014, Hara et al., 2014, Chan et al., 2012, Sutani et al., 2009, Rowland et al., 2009). The appropriate

regulation of this release activity is a critical determinant of genome architecture in species ranging from yeast to humans (Tedeschi et al., 2013, Lopez-Serra et al., 2013, Guacci and Koshland, 2012, Yan et al., 2013) and is presumably also essential to the roles of cohesin which lie outside the establishment of sister chromatid cohesion.

The first indication of a dynamic release pathway arose from initial studies of cohesin in vertebrate organisms which revealed the existence of a ‘prophase pathway’ wherein the bulk of cohesin is removed from chromosome arms in prophase in advance of cell division (Losada et al., 1998, Losada et al., 2000, Sumara et al., 2000, Waizenegger et al., 2000). In Metazoans, the majority of cohesin is removed from chromosome arms in prophase, with only a subset of telomeric and centromeric cohesion being maintained prior to cleavage by Separase (Buheitel and Stemmann, 2013, Hara et al., 2014, Nishiyama et al., 2010, Peters and Nishiyama, 2012, Losada et al., 2000, Sumara et al., 2000, Waizenegger et al., 2000, Liu et al., 2013b).

In contrast to yeast, in which cohesin complexes are dismantled by proteolysis at the metaphase-to-anaphase transition, the first studies of vertebrate cohesin revealed that the majority of such complexes dissociate from chromatin at the onset of mitosis(Losada et al., 1998). As immuno-depletion of cohesin in the same study resulted in sister-chromatid separation, evidently a certain population must remain bound to facilitate cohesion. However, the discovery of the prophase pathway introduced a certain ambiguity in the role of cohesin in this process in vertebrates. Subsequent work revealed that this dissociation occurs independently of Scc1 cleavage by Separase, and instead is driven by the phosphorylation of cohesin subunits (Losada et al., 2000, Sumara et al., 2000, Waizenegger et al., 2000). These studies also established that a small pool of centromeric cohesin remains protected from this prophase pathway, the putative mechanism for which will be discussed in the next section (Losada et al., 2000, Waizenegger et al., 2000). Shortly thereafter, it was determined that the kinases Plk1 and Aurora B were required for the prophase pathway, and that this pathway is essential for sister chromatid resolution, implying as was later confirmed, that the majority of cohesin removed via this pathway dissociates therefore

from chromosome arms and not the centromere (Losada et al., 2002, Sumara et al., 2002, Gimenez-Abian et al., 2004). Whereas Plk1 directly phosphorylates Scc3 and Scc1, and was shown thereby to reduce the stability of chromatin engagement by cohesin, the relevant targets of Aurora B did not become apparent until later on (Sumara et al., 2002, Nishiyama et al., 2013a, Losada et al., 2000, Hauf et al., 2005).

However, the utility of any such release pathway would be compromised if cohesin displaced thus were to simply immediately reload onto chromatin. Hence, the Scc2-Scc4 loading complex is also inactivated in mitosis in a Cdk1-dependent manner, thus further biasing the equilibrium toward unloading of cohesin (Gillespie and Hirano, 2004, Watrin et al., 2006). The re-emergence of Scc2-Scc4 coincides with, and is necessary for the loading of metazoan cohesin in telophase (Sumara et al., 2000, Losada et al., 2000, Watrin et al., 2006).

Unsurprisingly, the discovery of a cell-cycle regulated cohesin displacement pathway strongly implied the existence of a cohesin inhibition factor, and thus triggered concomitant research. These efforts resulted in the attribution of these release activities to the protein Wapl, which was formerly identified in *Drosophila* as a regulator of hererochromatin architecture and genome inheritance, and as an oncogenic factor in humans and mice (Oikawa et al., 2004, Kueng et al., 2006, Verni et al., 2000, Dobie et al., 2001, Gandhi et al., 2006).

Initial studies indicated that Wapl is recruited to cohesin in a manner that appears to be largely dependent on the stable association of Scc1 and Scc3, and is thus positioned within relatively close proximity to the Smc3-Smc1 ATPase modules (Gandhi et al., 2006, Kueng et al., 2006, Shintomi and Hirano, 2009, Kulemzina et al., 2012, Ouyang et al., 2013, Hara et al., 2014, Huis in 't Veld et al., 2014). There is some evidence that Wapl associates to form a subcomplex with Pds5, and that this subcomplex mediates cohesin release, however the nature of this interaction appears to vary between the methods employed to test it. The Pds5-Wapl complex has alternately been reported as a direct, and indirect assembly, as it is enhanced by the addition of other factors such as Scc3 and Scc1 (Kueng et al., 2006, Rowland et al., 2009, Sutani et al., 2009,

Nishiyama et al., 2010, Chan et al., 2012, Kulemzina et al., 2012, Huis in 't Veld et al., 2014, Ouyang et al., 2013, Shintomi and Hirano, 2009, Carretero et al., 2013). Notably, Wapl recruitment is only modestly depleted by the absence of Pds5 in mice cells, whereas depletion or the deletion of select elements of Scc1 significantly impairs co-immunoprecipitation of Pds5 and Wapl, indicating that they associate through mutual interactors (Shintomi and Hirano, 2009, Kueng et al., 2006, Carretero et al., 2013). Human Wapl is therefore able to interact with the cohesin complex, yet the nature of this association remains somewhat unclear, and seems to require the cooperative action of multiple cohesin subunits.

The experimental depletion of Wapl by RNAi causes severe defects in sister chromatid resolution in prophase, which is accompanied by, and presumably caused by, increased retention of cohesin along chromosome arms (Gandhi et al., 2006, Kueng et al., 2006, Haarhuis et al., 2013). Furthermore the reduction or deletion of Wapl results in an increase in the residence time and quantity of chromatin-bound cohesin, from yeast and to humans (Kueng et al., 2006, Chan et al., 2012, Lopez-Serra et al., 2013, Tedeschi et al., 2013, Feytout et al., 2011). Thus Wapl constitutes a *bona fide*, and generally conserved, cohesin release factor, which acts on the complex directly to promote its removal from chromatin, most prominently in prophase. The finding that Wapl depletion does not influence Scc3 phosphorylation, a hallmark and requirement of the prophase pathway, nor does it cause enhanced accumulation of cohesin on chromatin through aberrant activation of the Scc2-Scc4 loader further emphasises that Wapl must somehow drive release through a direct means (Gandhi et al., 2006, Kueng et al., 2006).

Whilst the nature of their association is unclear, it is generally accepted that functional Wapl and Pds5 are both required for cohesin release and sister chromatid resolution in mitosis (Shintomi and Hirano, 2009, Carretero et al., 2013, Ouyang et al., 2013, Losada et al., 2005, Gandhi et al., 2006, Kueng et al., 2006). As mentioned previously, Pds5 is unusual in that it is implicated in both cohesion establishment and release activities (Hartman et al., 2000, Panizza et al., 2000, Tanaka et al., 2001, Sumara et al., 2002,

Wang et al., 2003, Losada et al., 2005, Rowland et al., 2009, Shintomi and Hirano, 2009, Sutani et al., 2009, Chan et al., 2012, Carretero et al., 2013, Chan et al., 2013). In yeast, this release function appears to be confined to the N terminal section of the protein, as several point mutants distributed across this domain are able to neutralise Wapl-induced cohesin release (Rowland et al., 2009, Sutani et al., 2009, Chan et al., 2012).

In higher eukaryotes, this Wapl-Pds5 release activity is regulated by an additional factor called Sororin, a metazoan-specific protein which associates with cohesin through Pds5 and is required for sister chromatid cohesion (Rankin et al., 2005, Lafont et al., 2010, Nishiyama et al., 2010, Carretero et al., 2013, Nishiyama et al., 2013a, Schmitz et al., 2007). Sororin is able to displace Wapl from Pds5 *in vitro*, however *in vivo*, the engagement of Sororin and Pds5 antagonises Wapl-mediated release without impairing its recruitment to cohesin (Nishiyama et al., 2010, Ouyang et al., 2013). Hence, it is probable that Sororin promotes the stability of cohesin on chromatin by attenuating release-related activities of Pds5, and the mode and consequences of Wapl-cohesin interactions.

The protection conferred to Sororin-bound cohesin complexes is enriched for those which harbour acetylated Smc3, and is antagonised by the concerted actions of mitotic kinases, including Cdk1 and Aurora B, which render it incompetent to compete Wapl from Pds5 and result in its dissociation from cohesin (Nishiyama et al., 2010, Dreier et al., 2011, Nishiyama et al., 2013a).

Thus, in summary, it is increasingly apparent who the players are in this process, however there remains a paucity of mechanistic details of how phosphorylation may promote an increased propensity for cohesin to dissociate from chromosomes. Whilst most apparent in prophase, the mechanisms underlying this pathway most likely define a general and central principle through which the dynamic association of cohesin with chromatin is modulated (see figure 5 for a schematic summary).

1.3.4. Maintenance of cohesion

Cohesion establishment in S phase is essential for correct sister-chromatid pairing and subsequent segregation. However these processes are temporally rather distant, and thus there is an apparent requirement for the cell to maintain cohesion throughout G2 until sister chromatid congression and separation are achieved.

Whilst the mechanistic details of these processes are yet to be fully revealed, several cohesin-associated factors have been implicated in maintenance of cohesion, as will be discussed. Pds5 has been shown to be necessary for cohesion maintenance in budding yeast and vertebrates, where temperature inactivation and immunodepletion of Pds5 respectively result in progressive loss of cohesion (Hartman et al., 2000, Panizza et al., 2000, Losada et al., 2005, Carretero et al., 2013, Chan et al., 2013). Investigation of the Pds5 orthologue in fission yeast suggested that it might be dispensable for the normal life-cycle of this organism, however this may reflect idiosyncrasies of cohesion establishment and maintenance in this yeast, as experimentally extended G2/M arrest results in loss of cohesion (Tanaka et al., 2001, Vaur et al., 2012). It has been proposed that Pds5 may act to establish and maintain cohesion by protecting Smc3 acetylation by Eco1 (Vaur et al., 2012, Carretero et al., 2013, Chan et al., 2013). However as deacetylation of cohesin appears to depend on its removal from chromatin, and as such complexes still retain Pds5-binding sequences, and thus, theoretically, Pds5, following cleavage of Scc1 by Separase, the mode by which this protection might occur is unclear (Borges et al., 2010, Xiong et al., 2010, Huis in 't Veld et al., 2014). Conversely, the means through which maintenance of cohesion is conferred by Pds5 in fission yeast does not appear to depend solely on acetylation or the neutralisation of Wapl, as Pds5 remains essential for this process even in the absence of Eco1 and Wapl (Feytout et al., 2011, Vaur et al., 2012).

At the centromere, the prophase pathway is antagonised by the actions of a complex formed between the cohesin protector shugosin (Sgo1) and the protein phosphatase PP2A, and directly maintains hypophosphorylation of Cohesin subunits (Marston et al.,

2004, McGuinness et al., 2005, Gandhi et al., 2006, Kitajima et al., 2006, Kueng et al., 2006, Shintomi and Hirano, 2009, Xu et al., 2009, Liu et al., 2013a, Liu et al., 2013b, Hara et al., 2014). Sgo1 was one of the first cohesion factors identified, and is indispensable for centromeric cohesion (Kerrebrock et al., 1992, Tang et al., 1998, Marston et al., 2004).

Notably, localisation of Sgo1 to the centromere is enforced by mitotic kinases including Bub1, Aurora B, and Cdk1, and a failure in this process results in loss of cohesion and mitotic arrest (Kitajima et al., 2005, Tang et al., 2004, Resnick et al., 2006) .

Sgo1 is thought to protect cohesion by facilitating dephosphorylation of Scc3, Sororin and Securin (thus maintaining inhibition of Separase), and in so doing confers stability to cohesin complexes (Kitajima et al., 2006, Shintomi and Hirano, 2009, Liu et al., 2013b, Nishiyama et al., 2013b, Hara et al., 2014, Hellmuth et al., 2014, Clift et al., 2009). A recent study of the human Scc3-Scc1 complex additionally indicates that aspects of the Wapl N-terminus are able to directly compete with Sgo1 for binding to Scc3-Scc1, which may explain the antagonism reported between Wapl and Sgo1 functions previously (Hara et al., 2014, Gandhi et al., 2006, Kueng et al., 2006). Furthermore, Sgo1, and thus PP2A, are principally enriched at the centromeres in quantities that are apparently sufficient to prevent cohesin removal by Wapl, hence it is possible that the purpose of this competition is to ensure robust cohesion is confined to appropriate chromosomal loci (Hara et al., 2014, Nishiyama et al., 2013a, Tedeschi et al., 2013, Liu et al., 2013b). Remarkably, cohesion loss in cells artificially suspended in metaphase for extended periods can be counteracted by depleting Wapl or interfering with its ability to associate with Cohesin, suggesting that acetylation and Sororin binding reduce but do not entirely abolish release activity (Daum et al., 2011, Hara et al., 2014).

Sgo1 has also been implicated as a sensor of kinetochore tension, and so it is thus critically positioned to ensure cohesion is maintained until biorientation and amphitelic spindle attachments are correctly established, at which juncture Sgo1-PP2A actually dissociates from cohesin and permits its destruction by Separase (Indjeian et al., 2005, Campbell and Desai, 2013, Xu et al., 2009, Peplowska et al., 2014, Tsukahara et al.,

2010, Liu et al., 2013a, Alexandru et al., 2001, Hauf et al., 2005, Nerusheva et al., 2014). As Sgo1 is required for localisation of PP2A to the centromere, the implication here is that Scc3-Scc1 may also indirectly constitute a key facilitator of PP2A function (Kitajima et al., 2006, Hara et al., 2014). This also suggests that the Wapl-Scc3 release interaction appears to dictate chromosomal positioning of cohesion. Similarly, Pds5 was recently implicated in control of the spindle assembly checkpoint and is required for the correct localisation of Aurora B (Carretero et al., 2013, Yamagishi et al., 2010). Thus the interplay between Sgo1 and cohesin functions, quite elegantly, as a switch to finely couple cohesion maintenance and dissolution to the molecular mechanisms that drive chromosome segregation.

1.3.4. Termination of cohesion

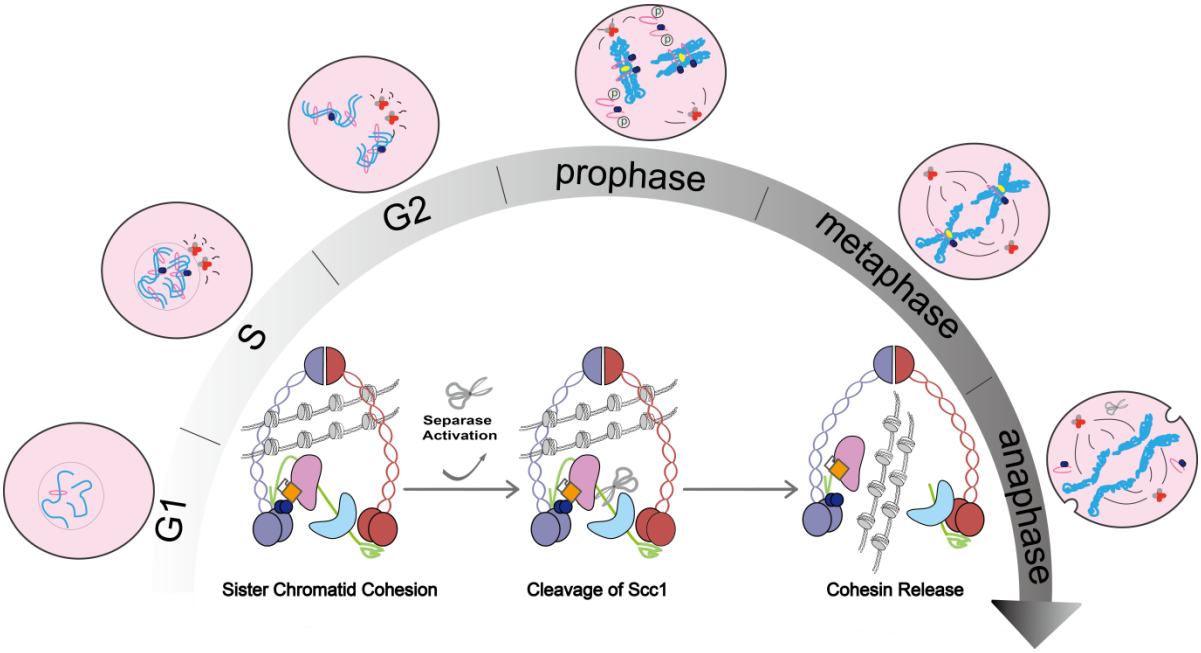

Figure 6 | Termination of cohesion. Cohesion dissolution is achieved at the metaphase-to-anaphase transition. Cohesin persisting at the centromere is destroyed by the cleavage of Scc1 by Separase, and thus sister chromatids are released for segregation.

In Metazoans, as discussed, most cohesion is dismantled in early mitosis through the actions of the prophase pathway which facilitates the dissociation of all but a modest yet very robust pool of centromeric cohesin. The maintenance of this centromeric fraction of

cohesin is critical to ensure effective biorientation and its timely dissolution by the protease Separase is essential to permit genome segregation. Thus the termination of cohesion, in higher eukaryotes, occurs via a two-step process wherein the integrity of most cohesin is firstly preserved through a Wapl-controlled release pathway (figure 5), and is totally abolished by a second step contingent on proteolytic cleavage of Scc1 by Separase, and the consequent destruction of the ring (figure 6).

In addition to pairing sister chromatids through topological entrapment, cohesin also generates catenanes, which must be resolved if chromosomes are to be subsequently segregated (Farcas et al., 2011, Haering et al., 2008). The human genome comprises over 3.2Gbp of DNA distributed across 23 chromosomes, each of which occupies a unique territory, and thus there are substantial mechanical challenges which must be addressed if interphase chromatin is to be neatly disentangled and condensed in advance of cell division (Lieberman-Aiden et al., 2009, Sanyal et al., 2012). In Metazoans, the efficiency of decatenation appears to be heavily reliant on the proper functioning of the prophase pathway. The disastrous consequences of perturbing this process are evident upon Wapl deletion. Such cells are inviable, and exhibit extended projections of highly condensed loops from the central bodies of their chromosomes, which were dubbed ‘vermicillo’ due to their worm-like appearance, and are densely populated by Cohesin (Tedeschi et al., 2013). In the absence of Wapl-mediated release, cohesin and the chromosomal structures enforced by the complex persist, and cause extensive architectural aberrations including anaphase bridges, which can lead to aneuploidy and even chromosome breakage (Haarhuis et al., 2013, Tedeschi et al., 2013). Thus it was recently proposed that one of the major functions of the prophase pathway is to permit efficient decatenation of chromatin such that chromosomes adopt the condensed X-shaped architecture conducive to genome segregation (Haarhuis et al., 2014) .

Advances in our understanding of the three-dimensional topology of our genome may also provide some clues as to why the prophase pathway is central to the successful execution of genome segregation in Metazoans. As the activity of Separase appears to

be confined to chromatin-bound fractions, Wapl may spare cohesin from destruction by displacing it from chromosomes (Tedeschi et al., 2013, Waizenegger et al., 2000, Sun et al., 2009).

Furthermore it is probable that the modulation of chromatin structure is required for the implementation of specific gene regulation programmes, in which cohesin actively participates, and so a mechanism which preserves a significant reserve of intact cohesin, rather than forcing the cell to resynthesise this 0.5MDa complex, has an obvious utility in permitting the immediate continuation of these processes in newly divided daughter cells (Wendt et al., 2008, Yan et al., 2013, Dowen et al., 2014, Minajigi et al., 2015).

The function of Separase is inhibited throughout the cell-cycle by a specific inhibitory protein, Securin, which is itself targeted for ubiquitin-mediated proteolysis by the APC/C shortly in advance of the metaphase-to-anaphase transition (Cohen-Fix et al., 1996, Funabiki et al., 1996, Zou et al., 1999). The process of Securin degradation is very finely modulated by the coordinated actions of Cdk1, which phosphorylates a site close to the KEN box on Securin, inhibiting the APC/C, and Cdc14, which dephosphorylates Securin and is itself activated by Separase, leading to highly synchronous sister-chromatid separation (Holt et al., 2008, Stegmeier et al., 2002, Pereira and Schiebel, 2003).

Cohesion is thusly terminated at the metaphase-to-anaphase transition by inactivation of the Separase inhibitor Securin, by the APC/C. Whilst not essential, phosphorylation of Scc1 expedites the process of cleavage (Hauf et al., 2005, Alexandru et al., 2001, Hornig and Uhlmann, 2004), and is presumably important therefore in promoting efficient chromosome segregation.

Cleaved cohesin released in this manner is then deacetylated following its removal from chromatin by Hos1 or HDAC8 in yeast and humans respectively (Deardorff et al., 2012, Borges et al., 2010, Xiong et al., 2010, Chan et al., 2013). It has been reported that this deacetylation is required for the efficient recycling of the Smc1 and Smc3 components

for the subsequent cell cycle, as the simultaneous suppression of Hos1 function and novel Smc1 and Smc3 is sufficient to impair sister-chromatid cohesion in newly divided cells, presumably by restricting the availability of non-acetylated cohesin (Borges et al., 2010, Xiong et al., 2010). Additionally, impaired HDAC8 function has been identified as causative in individuals with Cornelia de Lange syndrome, a developmental disorder, and cells isolated from these patients exhibit extended retention of cleaved Scc1 and Sororin in G2, implying that, similar to yeast, the pathology may be caused by inefficient recycling of cohesin components for a fresh cohesin cycle (Deardorff et al., 2012). However, it is not yet apparent how Separase cleavage fragments of Scc1 are removed from their respective SMC partner, and it is important to note that non-acetylation of Smc3 alone is apparently not sufficient to cause displacement of these cleavage products from cohesin, indicating that the efficient recycling of SMC proteins requires mechanisms in addition to deacetylation of Smc3 (Huis in 't Veld et al., 2014). Although there is some evidence that the C-terminal Separase cleavage fragment is subsequently degraded by the proteasome, it is not apparent that the N-terminal section is similarly processed (Rao et al., 2001)

1.4. Cohesin regulatory factors

1.4.1. Eco1

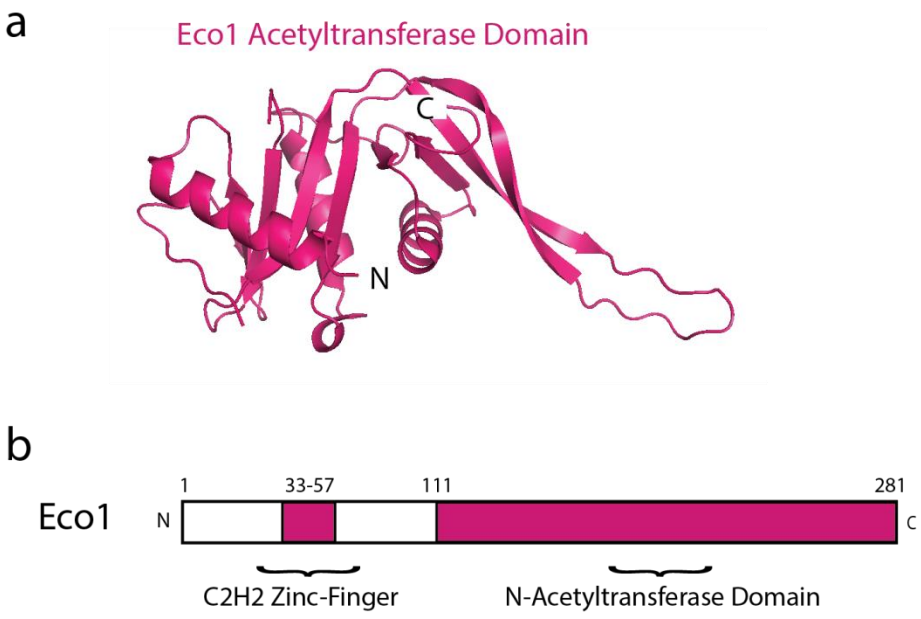

Figure 7 | Structure and domain organisation of Eco1. (a) The acetyltransferase domain of human Esco1 (magenta; PDB 4MXE) with labelled N and C termini. (b) Domain organisation of yeast Eco1.

Yeast Eco1, Establishment of Cohesion 1, is a 281 amino-acid acetyltransferase required for sister-chromatid cohesion at S-Phase, and during DNA double-stranded break repair (Toth et al., 1999, Tanaka et al., 2000, Ivanov et al., 2002, Bellows et al., 2003, Hou and Zou, 2005, Zhang et al., 2008, Chan et al., 2012, Unal et al., 2007, Strom et al., 2007). Eco1 has been reported to acetylate Smc3 and Scc1 *in vivo* (Ben-Shahar et al., 2008, Unal et al., 2008, Zhang et al., 2008, Heidinger-Pauli et al., 2009). Pds5 and Scc3 were also reported to be acetylated *in vitro*, but this has not been reported to occur *in vivo* (Ivanov et al., 2002, Unal et al., 2008).

The N-terminus of the protein is relatively divergent between yeast and metazoans, where two isoforms, Esco1/2, exist to coordinate general and pericentric/telomeric cohesion respectively. Conserved features of the protein include a C2H2 type zinc-finger, and C-terminal GCN5-like N-acetyltransferase domain (Ivanov et al., 2002). The structure of the acetyltransferase domain of human Esco1, which was released by the structural genomics consortium and is not accompanied by any functional characterisation, indicates that it forms a dimer in the asymmetric unit of the crystal, and there is further evidence that the protein oligomerises in yeast (Onn et al., 2009).

1.4.2. Scc3

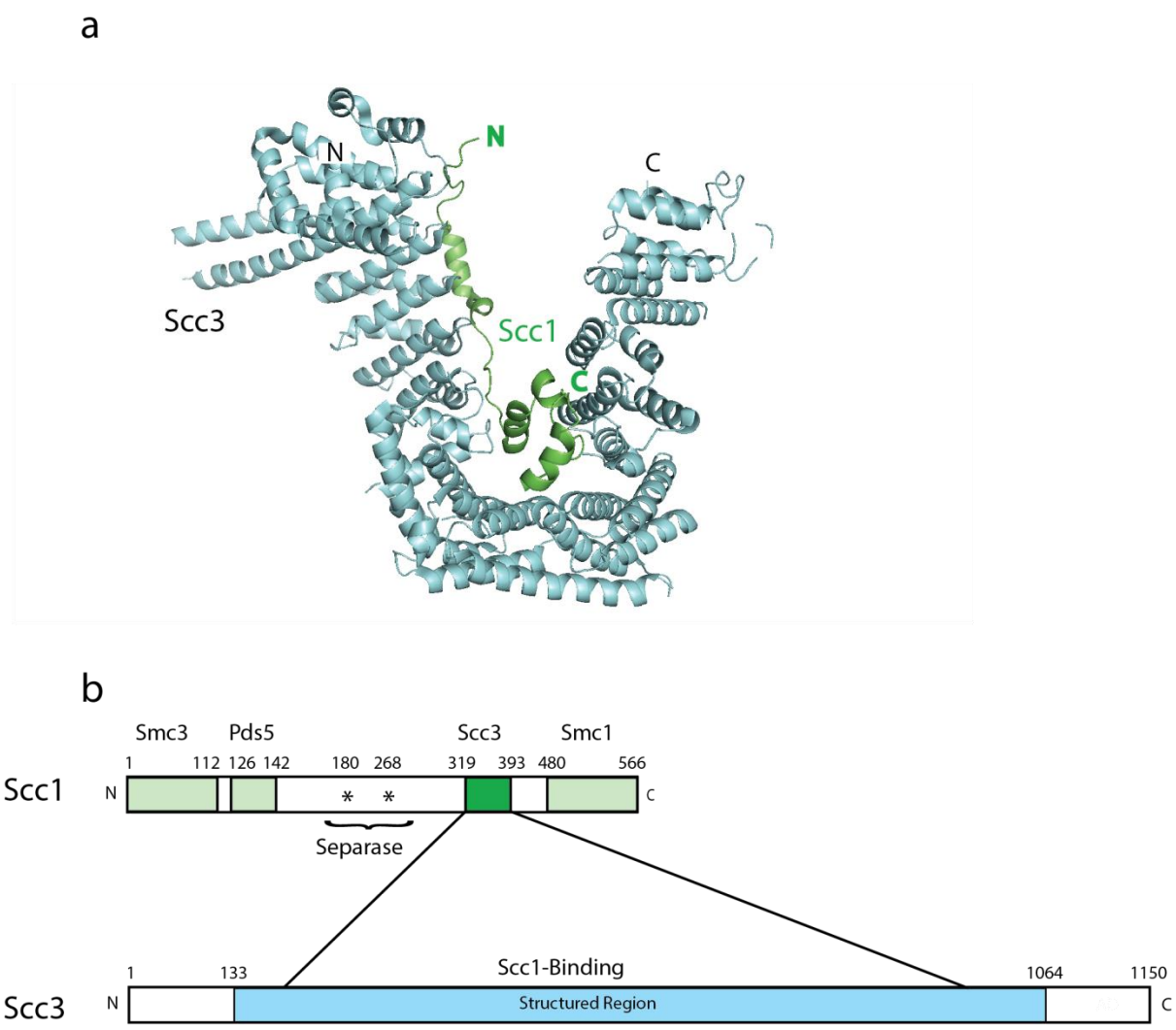

Figure 8 | Structure and domain organisation of Scc3-Scc1. (a) Structure of the human Scc3-Scc1 complex (aquamarine and green respectively; PDB 4PJW). (b) Domain organisation of yeast Scc1 and Scc3. Binding regions involved in the Scc3-Scc1 assembly are indicated.

Yeast Scc3 is an 1150 amino-acid protein, with a central alpha-helical HEAT-repeat domain bounded by regions of N- and C-terminal disorder. Scc3 was identified as a factor required for budding yeast viability (Kurlandzka et al., 1995, Kurlandzka et al., 1999), and was later shown to be a cohesin subunit, in yeast as well as in Xenopus, *C.elegans* and humans (Toth et al., 1999, Losada et al., 2000, Wang et al., 2003).

Telomere and centromere cohesion is differentially regulated by the Scc3 homologues SA1 and SA2, respectively, in mammalian cells (Canudas and Smith, 2009, Hara et al., 2014, Remeseiro et al., 2012a). Defective Scc3 leads to pathogenesis, as SA1 deficiency induces aneuploidy and tumourigenesis in mice, potentially due to impaired telomere replication and altered gene expression profiles, and inactivation of SA2 has been reported to be causative of aneuploidy in human cancer (Remeseiro et al., 2012b, Remeseiro et al., 2012a, Solomon et al., 2011).

The majority of the available surface area of Scc3 is engaged in binding an element of Scc1 C-terminal to the second Separase cleavage site, and it is this interaction which facilitates Scc3 recruitment to cohesin (Haering et al., 2002, Hara et al., 2014, Kulemzina et al., 2012, Roig et al., 2014, Zhang et al., 2013). Scc3 participates in the loading of cohesin, as well as release and maintenance of cohesion (Murayama and Uhlmann, 2014, Hu et al., 2011, Orgil et al., 2015, Chan et al., 2012, Chan et al., 2013, Roig et al., 2014). Structures of fungal and human analogues reveal an extended HEAT repeat conformation, which provides, in collaboration with Scc1, an interaction surface for the recruitment of cohesin regulators such as Sgo1 and Wapl, and thereby contributes to the regulation of centromeric cohesion (Kitajima et al., 2006, Shintomi and Hirano, 2009, Liu et al., 2013b, Nishiyama et al., 2013b, Hara et al., 2014, Hellmuth et al., 2014, Ouyang et al., 2013, Roig et al., 2014, Rowland et al., 2009, Chan et al., 2012).

1.4.3. Wapl

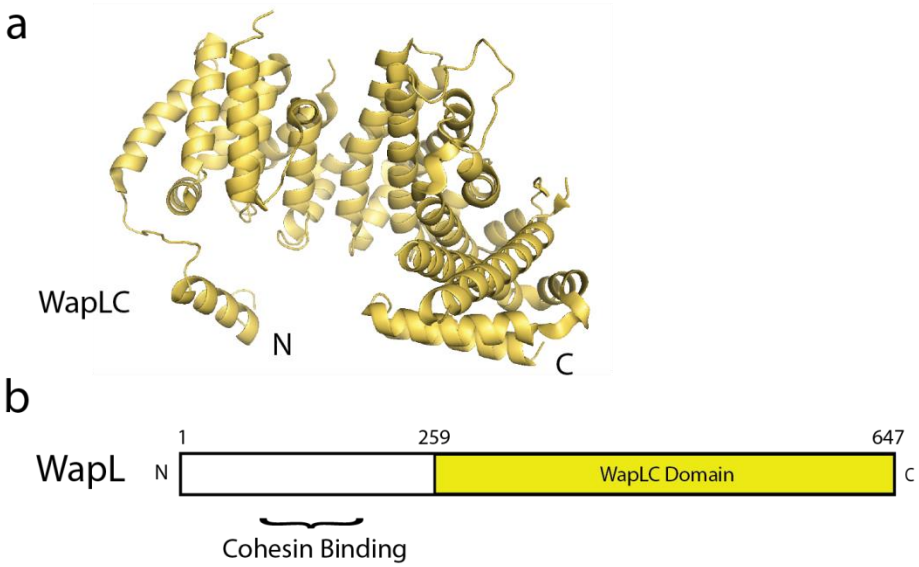

Figure 9 | Structure and domain organisation of Wapl. (a) Structure of the human WaplC domain (yellow; PDB 4K6J). (b) Domain organisation of yeast Wapl.

Wapl is generally considered to function as a key antagonist of cohesin and is thought to directly promote release of the complex from chromatin, in manner which can be counteracted in the cell by the acetylation of Smc3 and the recruitment of Sororin, and appears to be dependent on functional Pds5 and Scc3 (Gandhi et al., 2006, Kueng et al., 2006, Rowland et al., 2009, Sutani et al., 2009, Nishiyama et al., 2010, Chan et al., 2012, Haarhuis et al., 2013, Tedeschi et al., 2013, Lopez-Serra et al., 2013, Ouyang et al., 2013). Current evidence supports the notion that this release activity is exerted through Wapl-dependent opening of the Smc3-Scc1 interface of cohesin (Chan et al., 2012, Buheitel and Stemmann, 2013, Eichinger et al., 2013). Wapl associates with Cohesin substoichiometrically through cooperative, poorly defined interactions with Pds5, Scc1 and Scc3, and thus shuttles between cohesin complexes (Gandhi et al., 2006, Kueng et al., 2006, Shintomi and Hirano, 2009, Nishiyama et al., 2010, Chan et al., 2012, Kulemzina et al., 2012, Ouyang et al., 2013, Hara et al., 2014, Huis in 't Veld et al., 2014).

Yeast Wapl is a 647 amino-acid protein. The N-terminal region is predicted to be disordered, and has roles in mediating interactions with other components of cohesin (Shintomi and Hirano, 2009, Nishiyama et al., 2010, Ouyang et al., 2013, Hara et al., 2014, Gandhi et al., 2006). In contrast, the C-terminal region of Wapl, annotated here as the WaplC domain, is well-conserved between the Human and fungal proteins. The structures of human and of *Ashbya Gossypii*, a filamentous fungus, WaplC reveal a shared concave HEAT-repeat architecture (Chatterjee et al., 2013, Ouyang et al., 2013). The precise function of this domain is currently unknown, however mutation of conserved surface features, and outright deletion of WaplC, are sufficient to inhibit Wapl-mediated release (Sutani et al., 2009, Chan et al., 2012, Chatterjee et al., 2013, Ouyang et al., 2013).

1.4.4. Pds5

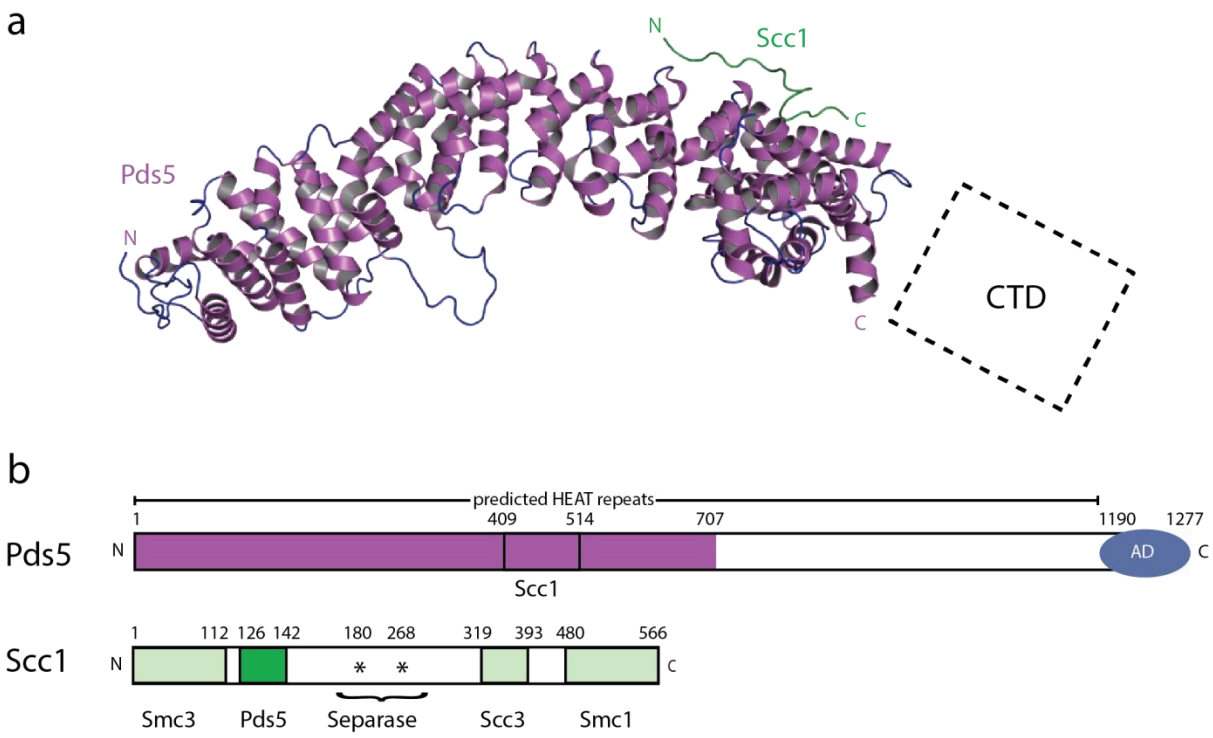

Figure 10 | Structure and domain organisation of Pds5-Scc1. (a) Structure of the yeast Pds5-Scc1 complex (violet and green respectively; this study). The C terminal 570 amino acids of Pds5 are absent from this structure (C-terminal domain; CTD). (b) Domain organisation of yeast Pds5 and Scc1. Binding regions involved in the Scc3-Scc1 assembly are indicated.

Yeast Pds5 is a 1,277 amino acid residue protein predicted to contain a HEAT repeat domain and a highly charged, intrinsically disordered C–terminal region. Initially identified in fungi, and was later shown to be conserved from budding yeast through to humans, where two isoforms, Pds5A and B, exist (Denison et al., 1993, Holt and May, 1996, Hartman et al., 2000, Panizza et al., 2000, Tanaka et al., 2001, Wang et al., 2003, Sumara et al., 2000). In metazoan cells, these isoforms have been found to both regulate cohesion at telomeres and chromosome arms, however Pds5B is thought to be the major contributor to centromeric cohesion (Carretero et al., 2013). Initial characterisation of the human equivalent revealed that it associated and dissociated from chromatin with dynamics similar to Cohesin, but that this interaction was salt

sensitive, as most Pds5 is depleted by high salt washes from Scc3 immunoprecipitated from Xenopus extracts (Sumara et al., 2000) . Yet, it is not apparent that Pds5 is depleted at physiological salt concentrations, so the relevance of this finding *in vivo* is unclear (Sumara et al., 2000). The discrepancy may arise from the finding that a substantial fraction of Pds5B, but not Pds5A dissociates under similar conditions, or alternatively from the choice of immunoprecipitation target, as the use of antibodies directed against specific Pds5 isoforms retain appreciable quantities of Scc1, a founding member of the trimeric Cohesin ring, even at high ionic strength (Gandhi et al., 2006). Recent evidence suggests that the interface between Scc1 and Pds5 may be discrete and principally hydrophobic in nature (Chan et al., 2013). Thus, as a result of contradictory experimental evidence, it is yet to be resolved whether Pds5 truly constitutes a core subunit of Cohesin.

Notably whilst the interaction of Pds5 with cohesin *in vitro* appears variable in nature, its association with cohesin *in vivo* is essential for the establishment and maintenance of cohesion. Moreover, the turnover of Pds5 in yeast and mammalian cells appears to correspond closely to that of cohesin, implying it is a stoichiometric, and fundamental, component of the complex (Chan et al., 2012, Sumara et al., 2000).

Of the factors that regulate cohesin, the structure and mechanisms of Pds5 function remain enigmatic. It not only cooperates with Wapl in mediating the release of cohesin from DNA, but is also implicated in establishing and maintaining cohesion by promoting Smc3 acetylation by Eco1 (Rowland et al., 2009, Unal et al., 2008, Ben-Shahar et al., 2008, Zhang et al., 2008, Hou and Zou, 2005, Minamino et al., 2015, Carretero et al., 2013). Pds5 is essential for the establishment of cohesion in yeast (Panizza et al., 2000, Hartman et al., 2000), and in mammals acetylation is disrupted in the absence of Pds5 (Carretero et al., 2013). Moreover knockout-mice that lack both Pds5 isoforms fail to complete embryonic development (Carretero et al., 2013). Cells from these mice exhibit aneuploidy and impaired function of the spindle assembly checkpoint. Whilst the nature of the interaction of Pds5 with cohesin *in vitro* remains elusive, it is essential for establishment of cohesion, and turnover of Pds5 in yeast and mammalian cells appears

to correspond to that of cohesin, implying it is a stoichiometric, and fundamental, component of the complex (Chan et al., 2012, Sumara et al., 2000).

Pds5 binds to Scc1 in close proximity to the Scc1–Smc3 interface, whose disengagement is thought to be required for dynamic release of cohesin from chromatin, therefore it is probable that Pds5 might fulfil its functions by regulating the opening and closure of this interface (Chan et al., 2013, Kulemzina et al., 2012, Shintomi and Hirano, 2009, Gause et al., 2010).

Mutations in the N-terminus of Pds5 are able to suppress *eco1-1* inactivation in yeast, possibly by neutralising a release-related activity in this domain, and result in a substantial increase in the residence time of Cohesin on DNA in Eco1 temperature sensitive mutants. In contrast with *eco1-1* suppressor mutations in Smc3 and Scc3, they do not induce cohesion defects (Rowland et al., 2009, Sutani et al., 2009, Chan et al., 2012). The release and establishment functions of Pds5 are hence potentially segregated into specific domains of the protein, and may be neutralised by the recruitment of Sororin, which stabilises cohesion in Metazoans (Liu et al., 2013b, Nishiyama et al., 2010, Lafont et al., 2010, Rankin et al., 2005). Whereas binding of Sororin to Cohesin relies entirely on Pds5, Wapl recruitment is only modestly reduced by the absence of Pds5, suggesting that their functional relationship may be more subtle than as target and binding scaffold respectively (Carretero et al., 2013).

Conversely, Pds5 may mediate acetylation, however, although there is some evidence that the human Esco1 isoform may have evolved the capacity to bind Pds5, direct recruitment of the acetyltransferase Eco1 by this protein does not seem to be a generally conserved feature (Carretero et al., 2013, Lafont et al., 2010, Vaur et al., 2012, Chan et al., 2013, Minamino et al., 2015).

Collectively, both such activities may require modulation of ATP hydrolysis by the Smc1–Smc3 head domains, the acetylation status of Smc3, and the recruitment of the release factor Wapl, or its inhibition by Sororin (Chan et al., 2013, Shintomi and Hirano, 2009).

Ultimately, detailed molecular characterisation of the transactions between Pds5 and cohesin at this interface will be essential to reveal the modes and mechanisms through which the fate of individual cohesin complexes, whether release or stable establishment of cohesion, is determined.

1.5. Scientific aims

At the inception of this thesis, structural information on the non-SMC subunits of cohesin was totally lacking, in addition there was (and still remains) a paucity of information regarding how Eco1 might establish cohesion, and how these factors might collaborate to promote different functional outcomes of the Cohesin complex. Therefore, I sought to address these questions throughout my thesis work.

1.5.1. Structural and biochemical characterisation of the Smc3-Smc1-Scc1 heterotrimer

Presumably to accommodate increased regulatory, mechanistic, and organismal complexity, Eukaryotic SMC complexes invoke an intrinsic asymmetry through the use of heterodimeric SMC proteins, in contrast to the homodimers of their prokaryotic equivalents. In order to address the structural and molecular basis for this evolutionary adaptation, I aimed to design and implement a strategy through which the cohesin heads could be assembled *in vitro* with their cognate Scc1 partner. If successful, this system would provide an invaluable tool in dissecting the molecular details of how energy produced through ATP hydrolysis might be transmitted to achieve different functional goals of the complex such as loading and release, and how these processes might be influenced by regulatory factors.

1.5.2. Eco1

Eco1 is an essential cohesion factor which is both tightly regulated, and also exhibits extremely high substrate specificity. Thus I aimed to characterise the basis of chromosomal targeting of Eco1, and the regulation of its acetyltransferase activity.

1.5.3. Defining cohesin release complexes

The diverse functional roles of cohesin and its sister complexes condensin and Smc5/6 are, at least in part, likely to be determined by the accessory factors with which they associate. SMC complexes have been generally described to act as topological linkers of DNA, however activities encompassing chromosomal targeting and the longevity of their association with chromatin is evidently regulated to a great extent through divergent HEAT repeat subunits. In recent years, a cohesin release activity, believed to be dependent on the interplay between Pds5, Scc3, and Wapl, was identified. Thus a major objective of this thesis was to investigate the molecular mechanisms through which these factors act to modulate the stability of cohesin on chromatin.

1.5.4. The structural basis of Pds5 function and recruitment to cohesin

Pds5 is a critical point of convergence for seemingly divergent functions of cohesin. In order to resolve the different roles ascribed to Pds5, I therefore sought to determine the structure of Pds5 in complex with Scc1 from the budding yeast *Saccharomyces cerevisiae* and investigated the nature of its transactions with cohesin at the Smc3–Scc1 interface.

Materials and Methods

Résumé en Français

Dans ce chapitre, sont décrits les matériels et méthodes employés dans cette étude. Les protocoles pour le clonage, l'expression et la purification des protéines recombinantes d'intérêt seront présentés. En outre, sont détaillé les méthodes employées pour la caractérisation ultérieure de ces protéines.

L'étude biochimique des assemblages macromoléculaires a été permise en utilisant une variété de techniques complémentaires telles que des « pulldowns », des expériences de retard sur gel (EMSA ou *electrophoretic mobility shift assay)* ainsi que des chromatographies d'exclusion stérique analytique (SEC pour size exclusion chromatography). L'identification de sous-domaines stables et de sous-ensembles de macromolécules d'intérêt a été accomplie grâce à une combinaison itérative de protéolyse limitée et d'outils bio-informatiques.

Enfin, la détermination de la structure macromoléculaire par SAXS et la cristallographie aux rayons X seront décrites, en particulier le processus de cristallisation des protéines, la collecte de données de diffraction, et les procédures de calcul utilisées pour la résolution de la structure.

2.1. Molecular cloning

For protein expression, constructs were isolated from yeast genomic DNA (Merck-Millipore), unless otherwise specified, by polymerase chain reaction (PCR), and inserted via restriction digestion, and ligation into the *E.Coli* expression vector of choice.

Human Pds5A and B were kindly provided by Jan-Michael Peters (IMP, Vienna) and Hongtao Yu (UT Southwestern, Dallas) respectively. Marko Kaksonnen (EMBL, Heidelberg) kindly provided *Ashbya Gossypii* genomic DNA.

Site-directed mutagenesis was performed with the QuikChange® Lightning kit (Agilent Technologies), essentially according to the manufacturers protocol.

2.2. Protein expression

2.2.1. Bacterial expression of native proteins

Protein expression was pursued in *E.Coli* BL21 (DE3, RIPL), and in BL21 (DE3) cells for individual proteins, and protein complexes respectively.

All native proteins were expressed in ZYP-5052 autoinduction media, according to the Studier protocol (Studier, 2005). Cells were cultured under agitation at 37°C, until an OD600 = 0.8 was obtained, and cultured overnight at the lower temperature of 18°C.

Cell harvesting was performed in a JLA-8.1 (Beckman) centrifuge, operated at 5000RPM for 20 minutes at 4°C. The resultant cell pellets were then washed, and resuspended in lysis buffer, prior to storage at -81°C or immediate purification.

2.2.2. Bacterial expression of selenomethionyl proteins

Expression of selenomethionine-labelled proteins was pursued in BL21 (DE3) cells, cultured in M9 minimal media supplemented with trace elements and vitamins.

Cells were cultured under agitation at 37°C, until an OD600 = 0.8 was reached. At the appropriate $OD=_{600}$, amino acids were added as solids to induce feedback inhibition of

methionine synthesis, and selenomethionine added to facilitate protein labelling; protein expression was induced by the addition of IPTG to a final concentration of 0.5M.

2.3. Protein purification

All cell lyses were performed under essentially similar conditions.

Cell pellets were resuspended in a lysis buffer appropriate to the protein under purification, supplemented with protease inhibitors (Roche), at a ratio of 10ml/g of bacteria. Lysis was then performed under high-pressure using a Microfluidizer (Microfluidics). Clarification of cell lysates was achieved by centrifugation (at an RPM of 14000, with a Beckman JLA-14 rotor) over a period of 45 minutes at 4°C. The resultant supernatant was then collected and the proteins within purified as befitted their associated affinity tag.

2.3.1. Immobilised metal-ion affinity chromatography

Exclusively his-tagged proteins were isolated by applying the appropriate supernatants to IMAC Sepharose Fast Flow 6 resin (GE Healthcare) charged with Co^{2+} and equilibrated in lysis buffer. The resin was subsequently washed with Lysis Buffer prior to elution in His Elution Buffer.

His-TEV tags, where required, were removed by incubation with his-tagged TEV protease (1:100w/w), and simultaneously dialysed into Cleavage Buffer in order to reduce the imidazole concentration of the sample. Dialysed protein mixtures were then passed over Co^{2+} resin to capture the protease, cleaved tags, and uncleaved protein prior to subsequent purification steps.

2.3.2. GST affinity chromatography

Constructs harbouring a GST tag were purified from lysed supernatants by applying them to Glutathione Sepharose 4 Fast Flow resin (GE Healthcare), equilibrated with lysis buffer. The resin was then washed in Lysis Buffer, and the proteins eluted in GST Elution Buffer.

Where appropriate, His-GST-TEV tags were removed as described for His-TEV proteins in section 2.3.1.

2.3.3. Anion exchange chromatography

Anion exchange was performed with a Mono Q^{TM} 5/50 GL column (GE Healthcare), in conjunction with an Äkta Purifier (GE Healthcare). Prior to application to the column, proteins were diluted to a final NaCl concentration of 100mM in Anion Exchange Buffer A. Gradient elution (from 10-100% Anion Exchange Buffer B) enabled separation of proteins from contaminants.

2.3.4. Size exclusion chromatography

Size exclusion chromatography was variably conducted, with HiLoad 16/60 Superdex 75 (or 200) grade columns (GE Healthcare), for preparative purposes, and a Superdex 200 Increase 10/300 GL for analytical purposes. Columns were connected to an Äkta Purifier, and the proteins collected by isocratic elution in SEC Buffer.

Purified proteins were concentrated, and aliquots flash frozen in liquid N_2 for storage at -80°C. The integrity, and purity, of protein samples was validated by SDS-PAGE, and mass spectrometry.

2.4. Crystallisation

Initial crystallisation trials were performed by the EMBL Grenoble HTX facility, with a standard setup of 576 conditions in 200nl drops (a 1:1 mixture of protein, at 20mg/ml, and well-solution) dispersed across 96-well sitting-drop plates, at 4°C.

2.4.1. Crystallisation of apo-Pds5T

Pds5-1-688, the first of 14 yeast Pds5 constructs tested, produced spherulites and low-quality crystals across a variety of conditions which it was not possible to optimise. Extensive further refinement of the construct resulted in Pds5T (1-701), the truncation used for final x-ray crystallography experiments, in the context of determination of both the apo- and Scc1-bound structure.

Unliganded Pds5T first crystallised in 0.1M MES pH 6, and 1.6M Ammonium Sulphate. Crystals from which data was collected arose in 1.5M Lithium Sulphate, 0.1M MES pH 6.5, grown at 4°C using the hanging-drop vapour-diffusion method, and were cryoprotected in a solution containing 2M Lithium Sulphate, and 0.1M MES pH 6.5.

Despite extensive attempts at optimisation, including osmotic dehydration, streak-seeding, microseeding, screening of cryo-conditions, additive screening, crystallisation of selenomethionine-labelled protein, trimming of the N-terminus, *in situ* proteolysis, on-beam annealing, and random-matrix microseeding, to identify new crystallisation conditions, Apo-Pds5T crystals did not yield diffraction to a resolution greater than 6Å.

2.4.2. Crystallisation of Pds5T-Scc1

Upon refinement of the length of the Scc1 moiety, the Pds5T-Scc1 complex first crystallised in 0.1M MES pH 6.5, 15% MPD.

2.5. Structure determination

All protein models have no Ramachandran outliers, good stereochemical parameters, and low crystallographic R_{work}/R_{free}, indicating a good agreement with the diffraction data (Appendix Table 1).

2.5.1 X-ray data collection and processing

Diffraction data for Apo-Pds5T were collected at beamline ID23–2 of the ESRF, at 100°K at an X–ray wavelength of 0.99987Å. Data collection strategies for Apo-Pds5T were determined by the initial characterisation of two diffraction images captured over 1 degree of rotation (Monaco et al., 2013), and were adhered to with minor modification.

Diffraction data for native and selenomethionine–derivatised Pds5T–Scc1 were collected at 100°K at an X–ray wavelength of 0.965Å at beamline ID30A–1/MASSIF–1 of the European Synchrotron Radiation Facility, with a Pilatus 6M–F detector. Data collection strategies for native and SeMet Pds5T-Scc1 were calculated and implemented automatically using MXpressE and MXpressE SAD respectively (Svensson et al., 2015).To ensure good redundancy for SeMet Pds5T-Scc1, images were collected by default over 360 degrees of rotation.

Data were subsequently processed using XDS (Kabsch, 2010), and scaled with AIMLESS (Winn et al., 2011).

2.5.2. Heavy atom phasing

Heavy atom parameter refinement and SAD phase calculations were performed with SHARP using anomalous signal from 12 Selenomethionine sites. The electron density map was improved with solvent flattening using PARROT. An initial model was then built at a resolution of 3.4Å, using BUCCANEER and Coot, as implemented in PHENIX, and served as a search model for molecular replacement in a higher resolution native dataset.

For the Scc1^{L128M} validation dataset, the data were phased directly using the final Pds5T-Scc1 model as an input for molecular replacement. SeMet residues were then visualised by the generation of an anomalous difference map using PHENIX, using the Pds5T-Scc1^{L128M} model produced by molecular replacement for the calculation of structure factors. Subsequent visualisation of the resultant map in Coot showed clear anomalous signal at the expected L128M position, thus validating the register and orientation of the Scc1 chain.

2.5.3. Molecular replacement and refinement of Pds5T-Scc1

A final model for the Pds5–Scc1 complex was produced by iterative rounds of manual model building and refinement using Coot and PHENIX (Emsley and Cowtan, 2004, Adams et al., 2010). The final Pds5-Scc1 complex model, containing residues 3–697 of Pds5 and 126–142 of Scc1 was refined to a resolution of 2.9 Å with an R_{work} and an R_{free} of 26.5% and 29.8%, respectively. No electron density was observed for residues 610–623 in Pds5. The register of Scc1 was verified by an anomalous difference map generated from diffraction data collected from a selenomethione–labeled Scc1^{L128M} mutant. Analysis of the refined structure in MolProbity showed that there no residues in disallowed regions of the Ramachandran plot. The MolProbity all atom clash score was 5.77, placing the structure in the 100th (best) percentile of structures (N=97) refined at comparable resolution.

2.5.4. Molecular replacement and dynamic elastic network refinement of apo-Pds5T

The structure of apo Pds5T was determined by molecular replacement with Pds5T 3–697, at a resolution of 5.7 Å in space group I422. The initial model was used as both a starting and reference model for subsequent Deformable Elastic Network (DEN) refinement using CNS over a grid–enabled web–server hosted by SBGrid (Schroder et al., 2010, O'Donovan et al., 2012). The refinement protocol was similar to that previously published (Brunger et al., 2012) with the following non–default setting: only a single overall anisotropic B–factor refinement was carried out per chain. DEN restraints and non–crystallographic symmetry (NCS) restraints were maintained throughout the refinement procedure. Seven different temperatures (from 0 to 3000K) were tested in the slow–cooling simulated annealing scheme. Of the resulting models, the one with the lowest R_{free} value (31.1%) was selected for subsequent analysis.

2.5.5 Small angle X-ray scattering

X–ray scattering data were collected using an inline HPLC setup, at the Bio–SAXS beamline (BM29) of the European Synchrotron Radiation Facility (Pernot et al., 2013). Inline size-exclusion chromatography was performed at a temperature of 10°C using a Superdex 200 Increase 10/300 GL column equilibrated in SEC buffer. Data were collected with a photon–counting Pilatus 1M detector at a sample–detector distance of 2.86 m, a wavelength of λ = 0.991 Å and an exposure time of 1 second/frame. A momentum transfer range of 0.008 to 0.47 $Å^{-1}$ was covered ($q = 4\pi \sin\theta/\lambda$, where θ is the scattering angle and λ the X–ray wavelength). Data were collected across the elution peak, buffer scattering was subtracted and frames from 1380–1410 showing constant a radius of gyration (R_g) were merged for further analysis. From the idealized scattering curves, the radius of gyration was obtained using the Guinier approximation in Primus (Petoukhov et al., 2012). The maximum particle dimensions, D_{max}, distance distribution function, p(r), and Porod Volume, Vp, were computed from the entire scattering patterns using GNOM. The program CORAL from the ATSAS suite

(Petoukhov et al., 2012) was to model the Smc3-NScc1-Pds5T ternary complex, using the Smc3–Scc1 (4UX3) and Pds5–Scc1 complex as input files. The Smc3–Scc1 and Pds5–Scc1 complexes were treated as rigid bodies, missing segments from Smc3 (amino acid residues 1223–1236), Scc1 (amino acid residues 1–24; linker 113–127; 143–165) and Pds5 (amino acid residues 1–4; 693–672) were modeled as dummy atoms. The final model conforms well to the scattering data, with a χ^2=1.27.

2.6. Bioinformatic methods

2.6.1 Protein secondary structure prediction

The majority of protein secondary structure predictions were performed with the PSIPRED protein sequence analysis workbench (Buchan et al., 2013). The PSIPRED v3.3 and DISOPRED3 &DISOPRED2 options were selected by default.

The HHPred server at Tübingen was also used to compare and validate predictions for HEAT repeat packing of Pds5 when designing constructs (Soding et al., 2005).

2.6.2. Proteolytic peptide fragmentation prediction

The intact masses of protein fragments generated by limited proteolysis were submitted to the FindPept tool (Gattiker et al., 2002). In order to unambiguously assign their N- and C-terminal boundaries, the resultant predictions of cleavage fragments were collated with protein termini identified in acid hydrolysis experiments, alongside secondary structure prediction and sequence conservation as evaluated by multiple sequence alignments.

2.6.3. Multiple sequence alignments

Collections of orthologous proteins were assembled with BLAST, and assembled and visualised using the JalView plugin on the EMBL-EBI ClustalOmega webserver (Sievers and Higgins, 2014).

2.7. Protein biochemistry

2.7.1. Limited proteolysis

The Proti-AceTM and Proti-AceTM 2 kits (Hampton Research) were used initially to identify suitable proteases, defined as those which cleave but do not result in the total degradation of the target of interest after 30 minutes of incubation at a 1:100 protein: protease ratio, according to the manufacturer's protocol.

Limited proteolysis experiments were designed such that proteins of interest were digested, in SEC Buffer, at several ratios of protein against an appropriate protease (1:100, 1:500, and 1:1000), with samples being taken, and boiled in SDS-loading buffer to inactivate the protease, at a series of time points ranging from 5 minutes to 4 hours.

Reactions were universally setup with 20µg of input protein, in a final volume of 100µl. Incubations were always performed on ice to ensure a consistent reaction temperature. For samples which were subsequently size excluded to isolate co-migrating complexes, reactions were performed with 100µg of input protein, incubated against protease at a 1:100 ratio for 30 minutes, prior to loading on a Superdex 200 10/300 GL column.

Samples were then analysed by SDS-PAGE, and the N- and C- termini of cleavage products of interest sequenced by acid hydrolysis. Results from acid hydrolysis sequencing were then collated with masses obtained from mass spectrometry of in-solution limited proteolysis samples in order to definitively determine protein domain boundaries.

2.7.2. Analytical size-exclusion chromatography

Proteins were incubated individually, or in combination, at a concentration of 30 µM in SEC buffer, a final volume of 100 µl for two hours at 4 °C, with gentle agitation. Following this incubation period, the sample was loaded onto a Superdex 200 Increase 10/300 GL, or Superdex 200 10/300 GL column equilibrated in SEC buffer, and subjected to size–exclusion chromatography. Fractions were subsequently analysed by SDS–PAGE.

2.7.3. *In Vitro* pulldowns

Pds5T variants, wild–type and mutants, were isolated as described. NScc1 (wild–type and Scc1$^{V137G–L138G}$) was purified via a C–terminal 6×His tag, in complex with the Smc3Hd. All preparations were subject to anion exchange and size-exclusion chromatography as described. Proteins were mixed to a final concentration of 2.5µM each in binding buffer (300 mM NaCl, 20 mM HEPES pH 7.5, 30 mM Imidazole, 5 % Glycerol and 0.5 mM TCEP), at a final volume of 150 µl, with 25 µl of Co^{2+}–IMAC beads per reaction, and incubated at 4 °C for two hours with gentle agitation. Following this incubation, an input sample was taken, the beads washed four times with binding buffer, and a bound sample taken. Samples were run on SDS–PAGE and the results visualized with Coomassie blue staining. GST–Wapl and Pds5 pulldowns were performed under identical conditions, albeit using Glutathione Sepharose 4B resin (GE Healthcare), and without imidazole in the binding buffer.

Wapl-FLAG pulldowns were also performed as above, in the absence of reducing agent, with Anti-FLAG agarose resin.

2.7.4. Acetylation assays

Acetylation reactions were incubated, at various durations, at 30°C in a buffer containing 25mM Tris-HCl pH 7.5, 100mM, 5% glycerol, 10µM aceyl-CoA, and 50nM acetyltransferase. Where appropriate, reactions were additionally supplemented with 50 µM ATP, 1mM $MgCl_2$, and 150nM substrate protein.

2.7.5. Wapl-ternary complex pulldowns

The ternary Smc3hd-NScc1-Pds5 complex was mixed, at a final concentration of 2.5µM, at a 1:1, 1:2 and 1:4 molar ratio with GST-WaplFl in binding buffer (150 mM NaCl, 20 mM HEPES pH 7.5, 5 % Glycerol and 0.5 mM TCEP), at a final volume of 150 µl, with 25µl of GST Sepharose beads per reaction, and incubated at 4 °C overnight, with rotation on a vertically oriented carousel. Subsequent procedures for washing and analysis were identical to those described for the *in vitro* pulldowns.

2.7.6. Electrophoretic mobility shift assays

Electrophoretic mobility shift assays were designed such that a fixed concentration was mixed with a concentration series of protein. The initial protein concentration was set at 50µM, and serially diluted against a premix containing 10µM ADAR DNA (kindly provided by Srinivasan Rengachari of the Panne Group). Protein and DNA mixtures were incubated in a buffer containing 20mM Hepes pH 7.5, 150mM NaCl, 1mM DTT and 5% glycerol, for 30 minutes at room temperature. Protein-DNA complexes were resolved by electrophoresis on 6% native polyacrylamide gels, at 90V over a period of 45 minutes. Gels were then stained with ethidium bromide to evaluate DNA migration.

2.8. Yeast methods

All yeast work was performed by the Häring Laboratory at EMBL Heidelberg. Methods are included here for completeness.

2.8.1. Yeast strain generation and validation

Wild–type or mutant variants of the *PDS5* and *SCC1* genes, under their endogenous promoter sequences, were integrated into the *URA3* or *TRP1* loci of diploid *PDS5/Δpds5* or *SCC1/Δscc1* strains respectively. Gene integration was confirmed by PCR, and the presence of the correct mutation(s) confirmed by DNA sequencing. Expression of integrated Pds5 and Scc1 was tested by western blotting against their respective C–terminal PK_6 and HA_6 epitope tags. Genotypes are listed in Appendix Table 2.

2.8.2. Tetrad dissection

Diploid cells were sporulated and 12 tetrads of two independently obtained strains for each mutant dissected on YEP plus 2% glucose (YEPD) plates and imaged after 48 h at 30°C. Genotypes of resultant haploids were assigned by marker analysis.

2.8.3. Protein co-immunoprecipitation

Wild–type or mutant Pds5 proteins fused to a C–terminal PK_6 tag were expressed from an ectopic copy, under the *PDS5* promoter, in strains expressing endogenous Scc1 fused to a C–terminal HA_6 tag. Whole cell extracts from asynchronous cell cultures were

prepared by glass bead lysis as described(Cuylen et al., 2011) and Scc1–HA_6 immunoprecipitated with anti–HA antibody (12CA5). Precipitation of Scc1–HA_6 and co–precipitation of Pds5–PK_6 were analysed by western blotting against HA (12CA5) and PK (anti–V5; AbD Serotec) tags.

2.8.4. Split dot cohesion assay

To test for cohesion defects, wild–type or mutant Pds5 proteins fused to a C–terminal PK_6 tag were expressed from an ectopic copy under control of the *PDS5* promoter in a *pds5–101* strain, which had *CDC20* under control of the *GAL1* promoter and tetracycline operator sequences, integrated at the *URA3* marker close to centromere of chromosome V, labelled by the expression of tetracycline repressor-GFP fusion proteins. Yeast cells grown in YEP plus 2% raffinose and 2% galactose (YEPRG) at 25°C to OD_{600} = 0.4–0.5 were collected by filtration and re–suspended in YEPD at 25°C to repress Cdc20 expression and arrest cells in metaphase with intact spindles. After 2.5 hours in YEPD, cultures were shifted to 35°C to inactivate Pds5–101 and aliquots of cells were taken at the indicated time points for immediate imaging GFP maker ‘spots’ in a DeltaVision Spectris Restoration microscope (Applied Precision) with a 60× oil immersion objective.

Results

Résumé en Français

Dans ce chapitre, sont décrits les résultats obtenus au cours de la thèse. Ces résultats sont séparés en plusieurs sections thématiques. La première section décrit la logique de conception et les tentatives avortées d'isolation du complexe ternaire stable SMC1-Smc3-Scc1. La seconde se concentre sur la caractérisation des activités d'acétyltransférase et de liaison à l'ADN de la cohésine acétyltransférase Eco1. L'isolement et la caractérisation des sous-unités non-SMC de cohésine sont décrits dans plusieurs sections. Alors qu'un sous-complexe Pds5-NScc1 a pu être identifié, aucune preuve n'a pu être apportée pour soutenir l'idée que Pds5, Scc3 et Wapl pourraient interagir. Grâce à la protéolyse limitée, la spectroscopie de masse et la bio-informatique, Pds5 et un complexe comprenant Pds5-Scc1 ont été cristallisées. Les cristaux contenant Pds5 et Scc1 ont diffractés à une résolution maximale de 2,9Å. Ainsi, grâce à la collaboration avec le laboratoire de Haering à l'EMBL Heidelberg, nous avons pu interroger en détail la base structurelle et biologique de l'assemblage entre Pds5-Scc1 et la cohésine. En résumé, les résultats présentés ici établissent que l'interface Pds5-Scc1, décrite dans la structure, est essentielle pour le recrutement de Pds5 à la cohésine et est, en outre, essentielle pour la cohésion de chromatides sœurs. Ceci fournis des preuves substantielles indiquant que Pds5 est une sous-unité stœchiométrique de la cohésine. La structure révèle aussi l'existence d'éléments conservés à la surface de Pds5 qui pourraient participer à la régulation dynamique de capture de la chromatine par la cohésine.

3.1. Assembling a heterotrimeric cohesin head complex

The heterotrimeric cohesin head complex, composed of the Smc3hd, Smc1hd and Scc1 has been confirmed, more specifically the NScc1/Smc3hd interface, to constitute a key focal point in the entrapment and release of DNA by cohesin, in Yeast, Fly and Humans. At this interface reside the functional ABC ATPase heads of Smc3 and Smc1, which are bridged by interactions with the N-terminal and C-terminal domains of Scc1 respectively. It is at this exit gate where interactions with the Releasin complex are thought to execute reversible release of cohesin from DNA. Notably, this releasing activity can be counteracted by acetylation of Smc3hd by Eco1 (Ben-Shahar et al., 2008, Chan et al., 2012, Rowland et al., 2009). This modification apparently uniquely facilitates stable closure of the exit gate and stablishes robust sister chromatid cohesion.

At current SMC head dimer structures are restricted to bacterial homodimers, thus there remains a need for structural characterisation of the eukaryotic system to understand the biological relevance of heterodimeric SMC rings. As revealed by past research, there is an obvious asymmetry to the cohesin head module, both enzymatically and architecturally (in terms of their association with Scc1).

Structural characterisation of the eukaryotic cohesin head complex would afford considerable insight into how Pds5-Wapl might execute DNA release and why this activity is so substantially antagonised by Smc3hd acetylation.

Therefore, to understand the structural and biochemical basis of the differential functions attributed to the Smc3hd-Smc1hd-Scc1 complex, I designed and pursued a fusion protein strategy to isolate and enforce such an assembly *in vitro*.

3.1.1. Mutual entrapment of SMC heads by an Scc1 domain-swap,

The stable dimerisation of native Smc1 & Smc3 is dependent on the association of their hinge domains (Haering et al., 2002). Thus, any attempt to isolate a Smc3hd-Smc1hd-Scc1heterotrimer as a more discrete assembly would naturally require that this function of the hinge should somehow be recapitulated. One approach could involve the use of a

so-called ‘bonsai’ construct in which the coiled-coils separating the head and hinge domains would be substantially truncated, as has proven particularly successful in characterising the kinetochore protein Ndc80 (Ciferri et al., 2008, Alushin et al., 2010). However, it was our preference to attempt to establish a more discrete system which would limit the requirement for construct optimisation to the ATPase heads, and Scc1.

To this end, I designed domain-swap constructs, in which each Smc head was tethered to the Scc1 partner of the opposing head, as depicted in figure 11 a-d.; in this system, the physical linkage between Scc1 and the Smc heads would facilitate co-purification the entire ternary assembly. Given that Smc-Scc1 assemblies are functionally asymmetric (Buheitel and Stemmann, 2013, Chan et al., 2012, Eichinger et al., 2013, Gruber et al., 2006, Rowland et al., 2009, Arumugam et al., 2006), I operated on the assumption that they would also be structurally asymmetric, which has now been demonstrated (Gligoris et al., 2014, Haering et al., 2004). Therefore, for the approximation of domain boundaries, and of linker lengths between the Smc and Scc1 proteins, I firstly modelled a hypothetical Smc3hd-Smc1hd-Scc1 assembly (figure11. a) based on available structures. In this model, Smc1-CScc1 is depicted as in the reported crystal structure (1W1W), with Smc3-NScc1 modelled on the Smc1hd and the NScpA chain from prokaryotic Condensin (3ZGX) respectively. As NScc1 interacts with the coiled-coil domain of Smc3, I extended the coiled-coils to include 4 heptad pairs.

The Smc3hd was fused C-terminally to the N-terminus of CScc1 (figure11b) through a short glycine-serine linker of 10 amino acids (aa), which would accommodate the hypothetical distance between these domains (figure11a) Similarly, NScc1 was fused C-terminally via a considerably longer linker of 30aa to the N-terminus of the Smc1hd (figure11c). Given the almost ludicrously extended linker, the Smc1hd was, as described in section 3.1.2., also cloned and expressed without such a fusion, lest the fusion protein should prove insoluble.

These constructs were assembled using overlap extension PCR and inserted into the two open reading frames of a modified pET DUET-1 vector harbouring a GST-TEV tag in the first ORF.

The final intended product of this endeavour is displayed in cartoon form in figure11d.

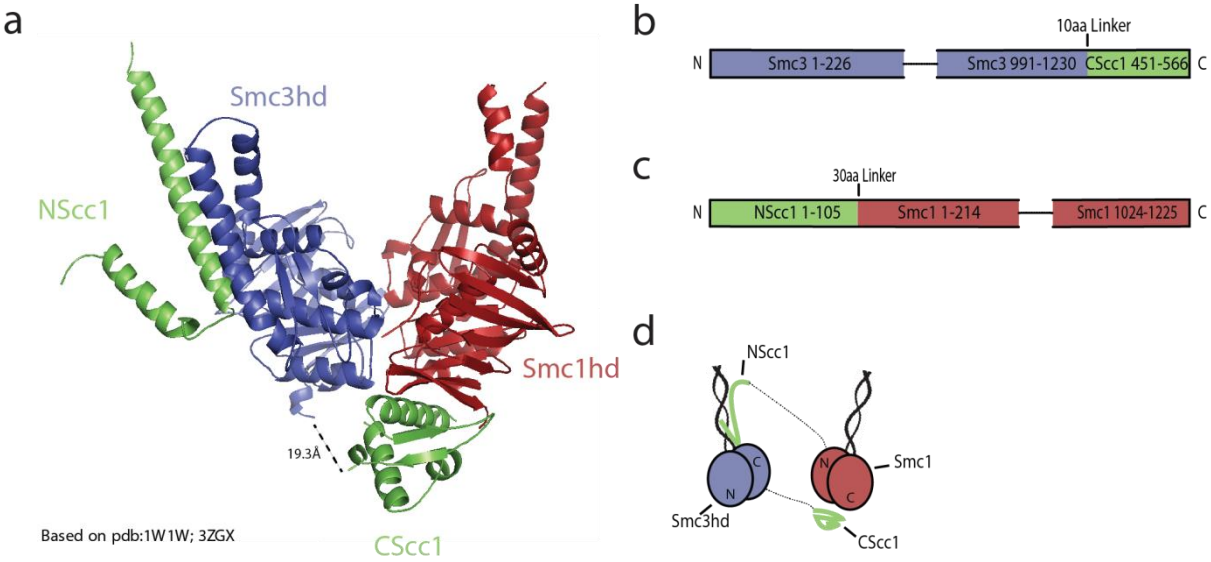

Figure 11 | Strategy design for the isolation of a Smc3hd-Smc1hd-Scc1 complex. (a) A model of the Smc3hd (blue), the Smc1hd (red), and the N- and C-terminal domains of Scc1 (green). (b) Sequence boundaries for the fusion of Smc3 to CScc1. (c) Sequence boundaries for the fusion of Smc1 to NScc1. (d) Schematic representation of the assembled Smc3hd-Smc1hd-Scc1 complex.

3.1.2. Solubility and initial purification of a Smc3hd-Smc1hd-Scc1 complex

The fusion constructs of Smc3-CScc1 and NScc1-Smc1, or Smc1 alone, described in the previous section were cloned together into a single pET-DUET vector with an N-terminal 6xHistidine tag and an N-terminal GST-TEV tag respectively (figure 12.a). A purification strategy (figure 12. b) was devised such that bacterial supernatants containing the recombinant proteins would first be exposed to Co^{2+}-charged IMAC sepharose resin, thus isolating 6xHis-Smc3-CScc1 in complex with GST-NScc1-Smc1 or GST-Smc1, along with any free 6xHis-Smc3-CScc1, whilst excluding excess GST-fusion proteins. To remove free 6xHis-Smc3-CScc1, protein would then be eluted from the IMAC resin with imidazole, and passed over GST sepharose. Complexes captured by GST should therefore constitute a homogeneous ternary species of Smc3-Scc1-Smc1. These assemblies would then be eluted by TEV-mediated cleavage of GST tags, and a final size-exclusion step would be pursued (not depicted).

However, unfortunately it soon became obvious that these fusion proteins were, at best, very poorly soluble. In initial purifications (figure 12. c and d), the strongest bands corresponding to the expected molecular weights appeared to reside in the pellet fraction, indicating that the proteins were confined to inclusion bodies. Western blotting against the 6xHis and GST tags confirmed that this was the case. As neither protein had been previously expressed in bacteria, the cloning and expression was repeated using insect cells, but produced identical results, thus indicating that the fusion strategy pursued herein may be intrinsically unfeasible irrespective of expression system. This aspect of the thesis was considered unlikely to be conducive to success, and was therefore discontinued.

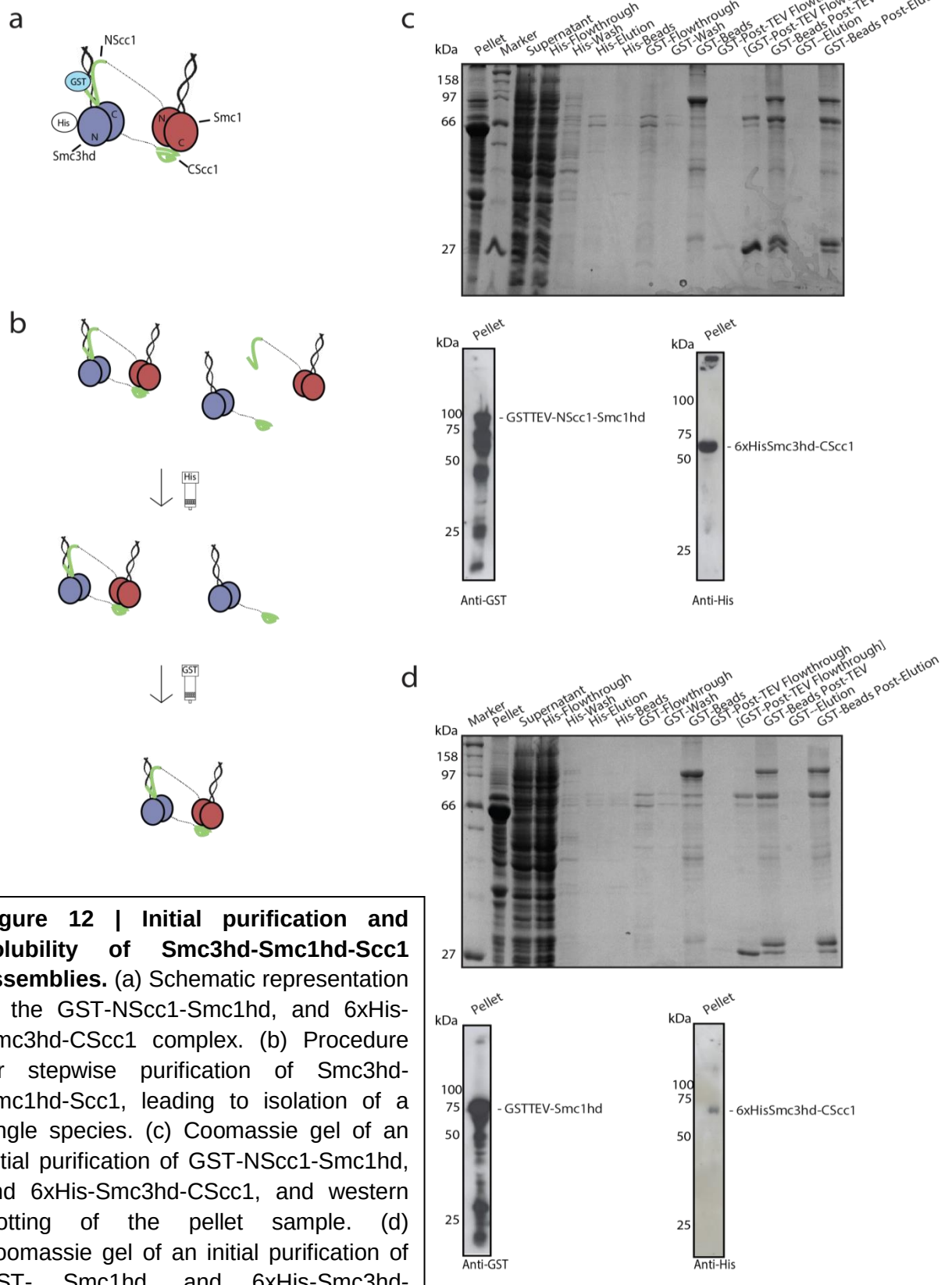

Figure 12 | Initial purification and solubility of Smc3hd-Smc1hd-Scc1 assemblies. (a) Schematic representation of the GST-NScc1-Smc1hd, and 6xHis-Smc3hd-CScc1 complex. (b) Procedure for stepwise purification of Smc3hd-Smc1hd-Scc1, leading to isolation of a single species. (c) Coomassie gel of an initial purification of GST-NScc1-Smc1hd, and 6xHis-Smc3hd-CScc1, and western blotting of the pellet sample. (d) Coomassie gel of an initial purification of GST- Smc1hd, and 6xHis-Smc3hd-CScc1, and western blotting of the pellet sample.

3.2. Eco1, the cohesin acetyltransferase

The cohesin Acetyltransferase, Eco1, is thought to establish stable cohesion by acetylating two adjacent residues on the Smc3hd, which reside in close proximity to its nucleotide binding domain (Ben-Shahar et al., 2008, Unal et al., 2008, Zhang et al., 2008, Rowland et al., 2009, Gligoris et al., 2014). This modification exponentially enhances the stability of cohesin on DNA, increasing its residence time on chromatin from ~20 minutes to over 6 hours (Chan et al., 2012, Peters and Nishiyama, 2012, Buheitel and Stemmann, 2013, Eichinger et al., 2013).

Eco1 acts during S-phase, presumably in order to couple cohesion to sister chromatid synthesis, and is composed of two principle functional domains: a C2H2 Zinc Finger and a GCN5 family histone acetyltransferase (HAT) domain (Ivanov et al., 2002). I therefore, in collaboration with a trainee, Siyi Zhang, under my supervision, sought to characterise the relationship between these functional domains *in vitro.*

3.2.1. Eco1 is an active acetyltransferase *in vitro*

As anticipated, recombinant GST-Eco1 isolated from bacteria is an active acetyltransferase (figure 13a). It becomes autoacetylated within 30 mins (which was the earliest time-point recorded) in a manner that is neither stimulated by nor inhibited by the inclusion of a 32bp DNA sequence. Furthermore, the activity of Eco1 *in vitro* is dependent on the integrity of its zinc finger, as mutation of two of the zinc-coordinating cysteines results in a total loss of function (figure 13b).

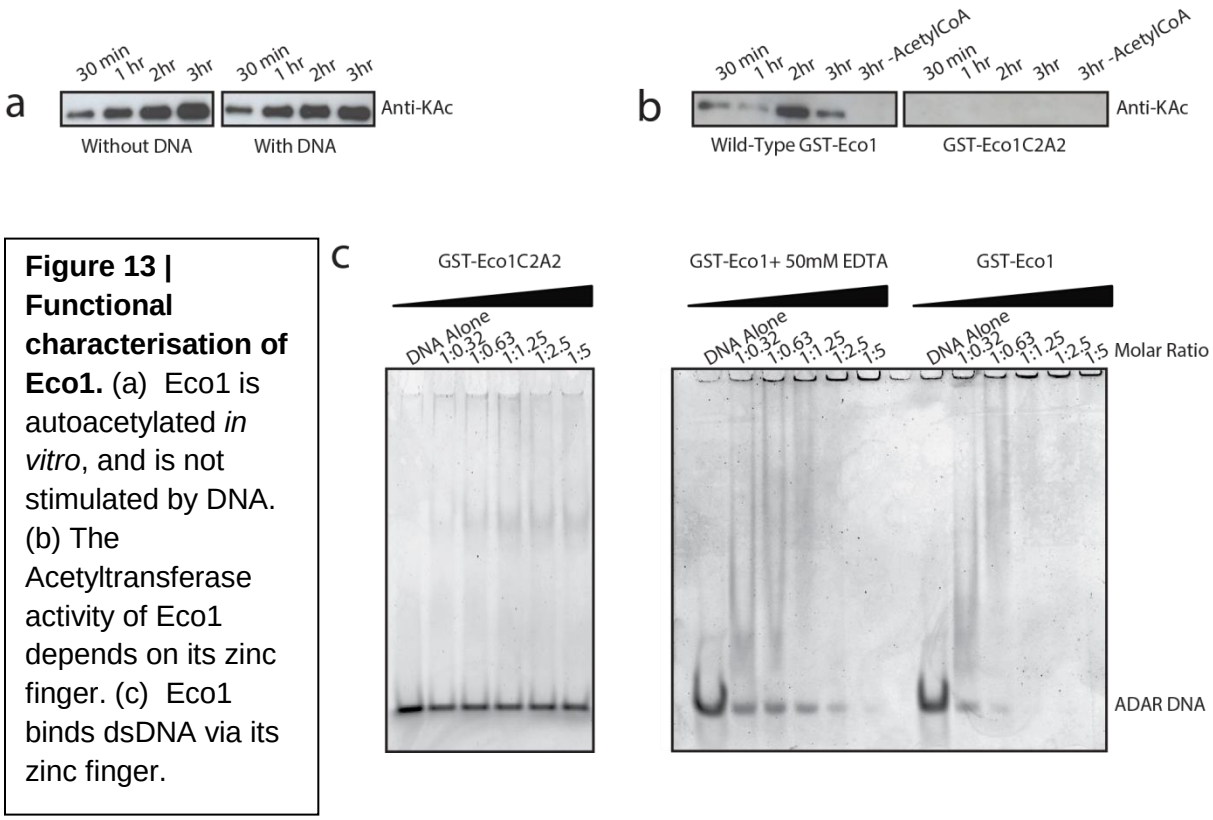

Figure 13 | Functional characterisation of Eco1. (a) Eco1 is autoacetylated *in vitro*, and is not stimulated by DNA. (b) The Acetyltransferase activity of Eco1 depends on its zinc finger. (c) Eco1 binds dsDNA via its zinc finger.

3.2.2. Eco1 binds dsDNA in a manner dependent on its zinc finger

As zinc finger domains are frequently involved in the engagement of DNA, we decided to test whether the Eco1 zf binds to dsDNA. To do so, we employed a 32bp ADAR DNA sequence, a reagent already available in our lab, and we found that the mixture of Eco1 and DNA at various ratios results in a substantial shift, commencing even at a substoichiometric ratio of 1:0.32 of protein:DNA. As the shift in DNA does not result in discrete species, we would speculate that Eco1 binds DNA in a manner that is not sequence-specific. Thus, Eco1 presumably interacts with the phosphate backbone, rather than the sugar bases. Furthermore, we discovered that the addition of EDTA, which chelates divalent cations such as zinc, and the mutation of two of the zinc finger cysteines to alanine results in perturbation and abolition of DNA binding respectively. We therefore conclude that Eco1 engages DNA in a manner dependent on its zinc finger. With this information comes the implication that Eco1 may interact with chromatin

independently of recruitment factors such as PCNA, as was previously suggested (Moldovan et al., 2006).

3.3. Characterisation of the non-SMC cohesin subunits

3.3.1. Isolation of full-length Scc3, Pds5, and Wapl

To initiate structural and biochemical studies of the non-SMC HEAT repeat subunits of cohesin, I cloned genes encoding the full-length proteins into the pETM11 vector, enabling their expression and purification in *E.Coli,* via N-terminal HisTEV tags. Purifying full-length, intact protein proved to be quite challenging, as they all behaved in a rather polydisperse manner (figure 14 a-c), however I was able to isolate sufficiently pure material for subsequent experiments. Pds5 and Wapl resulting from these purifications migrate on SDS-PAGE at the expected positions for full-length material (figure 14. d), whereas Scc3 purifications yielded both full-length protein, and an apparently stoichiometric additional band at ~70kDa (figure 14. e), possibly indicating degradation. Later optimisation of the Wapl purification resulted in essentially homogenous preparations of this protein, which elute at a volume suggestive of dimerisation or polydispersity (figure 22a).

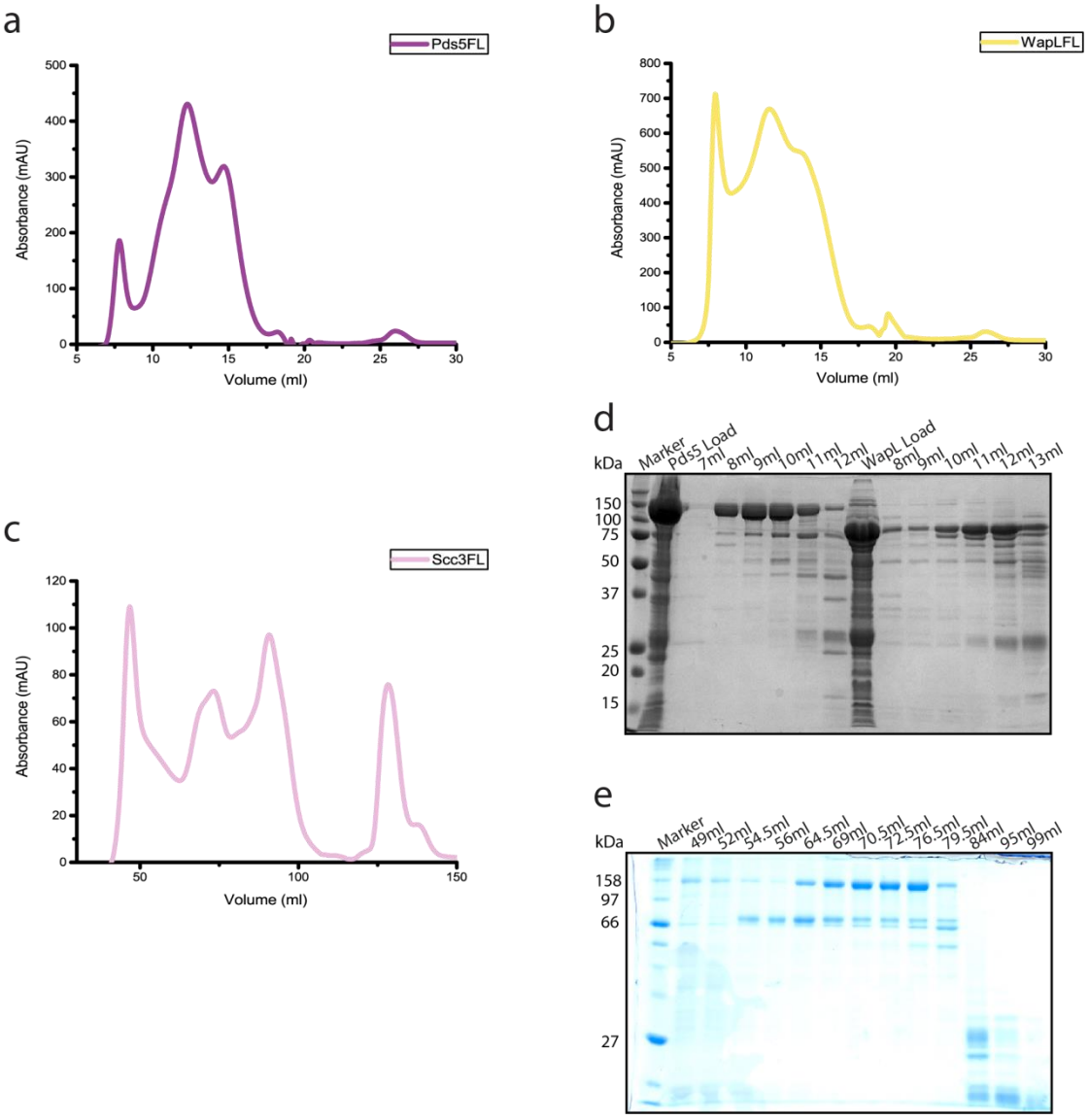

Figure 14 | Full-length non-Smc subunit purification. (a) S200 10/300 GL gel filtration profile of Pds5FL. (b) S200 10/300 GL gel filtration profile of WaplFL (c) S200 15/60 gel filtration profile of Scc3FL. (d) SDS-PAGE of Pds5FL and WaplFL gel filtration fractions. (e) SDS-PAGE of Scc3FL gel filtration fractions.

3.3.2. Prediction and crystallisation of subdomains in Pds5, Scc2, and Scc3

In parallel with efforts to isolate full-length versions of the non-Smc HEAT repeat subunits, I designed and sought to purify potential truncation constructs. To do so, I used structural bioinformatics to predict potential globular domains (construct boundaries are detailed in the appendix). In most cases, solubility assays revealed that

these constructs were insoluble (figure 15a-b), in contrast to the full-length proteins, indicating that the boundaries chosen must somehow have caused structural destabilisation. However, removal of regions of predicted N- and C- terminal disorder from Scc3 resulted in the purification of a monodisperse, crystallisable truncation construct (figure 15c). Testing revealed that these crystals did not diffract. Shortly thereafter we learned that a competing lab had already obtained a structure of Scc3, and thus I did not seek to optimise these crystals further.

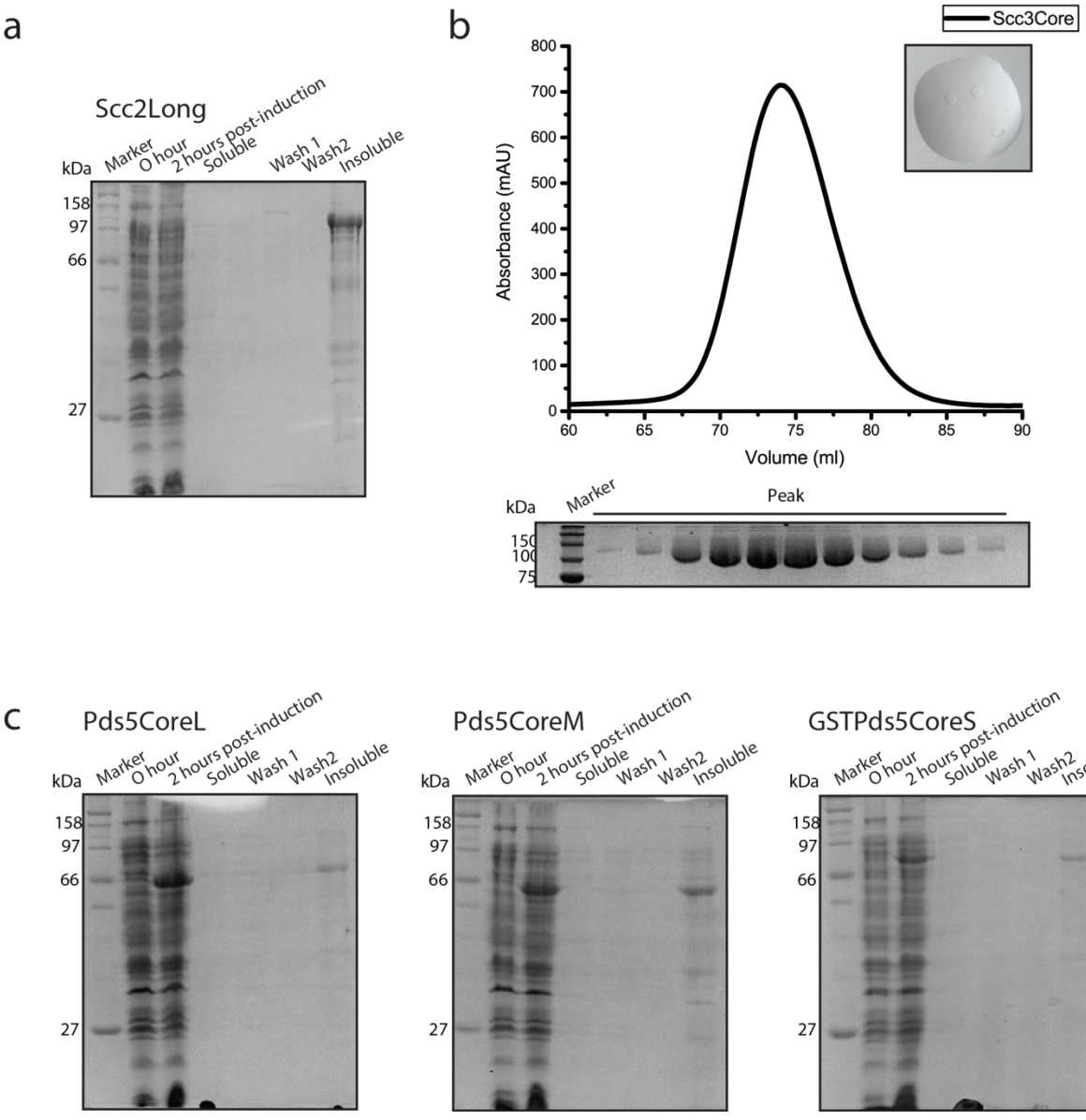

Figure 15 | Non-Smc subunit truncation solubility, purification and crystallisation of Scc3 (a) Scc2Long is principally found in the insoluble fraction (b) The Scc3 core truncation elutes as a single species from gel filtration, and is crystallisable (c) Solubility assays of Pds5 truncations reveal they are insoluble

3.3.3. Identification of a stable Pds5 truncation

Limited proteolysis is a powerful biochemical technique that facilitates the identification of stable, protease-resistant subdomains within proteins of interest. The full-length Pds5 isolated in figure15d was of sufficient quality to perform limited proteolysis, and so I performed such an assay using a 1:500 dilution of trypsin, collecting samples at a series of predetermined time points as shown in figure 16a. The sample was principally degraded into two prominent bands, annotated as 'Upper Band' and 'Lower Band' (figure 16a), and so the SDS-PAGE gel on which these samples had been run was submitted to the EMBL Proteomics Core Facility (PCF) in Heidelberg for boundary identification. Bands of interest were then cut out of the gel for further analysis by acid-hydrolysis, a mass spectrometry technique in which protein samples are exposed to hydrochloric acid to catalyse hydrolysis of the peptide bonds between amino-acids. This produces a series of peptides, which can then be measured by mass-spectrometry, and can thus be evaluated for sequence assignment of the domain boundaries of the protein sample under investigation. I was thus able to obtain putative domain boundaries for the selected fragments, which showed that the protein was substantially C-terminally truncated by trypsin (figure16b). It is important to note that these boundaries are not necessarily definitive, as the technique is limited also by which peptides are suitable for analysis by the MALDI instrument; however they were sufficient to provide an approximate region of the protein to truncate. A small selection of C-terminal peptides were also detected, yet were not considered further for two reasons. Firstly, they are very distant in the sequence from other peptides. Secondly, they were poorly represented, with few such peptides being detected by the instrument. Hence these peptides were disregarded and considered to represent unlikely intermediates of the original limited proteolysis experiment.

In order to determine the domain boundaries unambiguously, I repeated the assay and submitted in solution samples for analysis of the 'intact' degradation products and these also provided evidence that the truncation product encompassed the N-terminal ~700 or so amino acids of the protein.

a

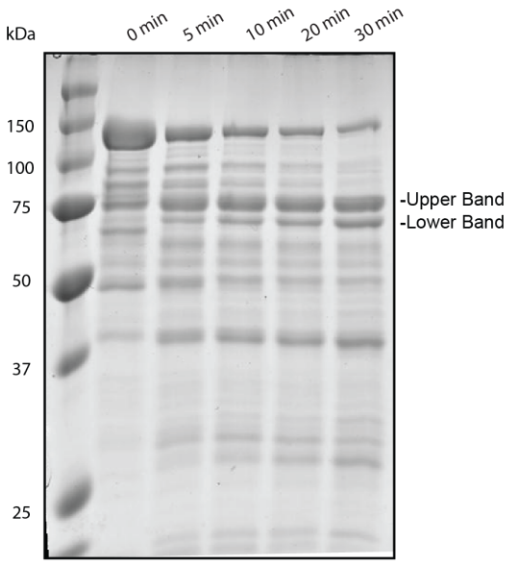

b

Upper Band

```
1    MAKGAVTKLK FNSPIISTSD QLISTNELLD RLKALHEELA SLDQDNTDLT
51   GLDKYRDALV SRKLLKHKDV GIRAFTACCL SDILRLYAPD APYTDAQLTD
101  IFKLVLSQFE QLGDQENGYH IQQTYLITKL LEYRSIVLLA DLPSSNNLLI
151  ELFHIFYDPN KSFPARLFNV IGGILGEVIS EFDSVPLEVL RLIFNKFLTY
201  NPNEIPEGLN VTSDCGYEVS LILCDTYSNR MSRHLTKYYS EIIHEATNDD
251  NNSRLLTVVV KLHKLVLRLW ETVPELINAV IGFIYHELSS ENELFRKEAT
301  KLIGQILTSY SDLNFVSTHS DTFKAWISKI ADISPDVRVE WTESIPQIIA
351  TREDISKELN QALAKTFIDS DPRVRRTSVM IFNKVPVTEI WKNITNKAIY
401  TSLLHLAREK HKEVRELCIN TMAKFYSNSL NEIERTYQNK EIWEIIDTIP
451  STLYNLYYIN DLNINEQVDS VIFEYLLPFE PDNDKRVHRL LTVLSHFDKK
501  AFTSFFAFNA RQIKISFAIS KYIDFSKFLN NQESMSSSQG PIVMNKYNQT
551  LQWLASGLSD STKAIDALET IKQFNDERIF YLLNACVTND IPFLTFKNCY
601  NELVSKLQTP GLFKKYNIST GASIMPRDIA KVIQILLFRA SPIIYNVSNI
651  SVLLNLSNNS DAKQLDLKRR ILDDISKVNP TLFKDQIRTL KTIIKDLDDP
701  DAEKNDNLSL EEALKTLYKA SKTLKDQVDF DDTFFFTKLY DFAVESKPEI
751  TKYATKLIAL SPKAEETLKK IKIRILPLDL QKDKYFTSHI IVLMEIFKKF
801  PHVLNDDSTD IISYLIKEVL LSNQVVGDSK KEIDWVEDSL LSDTKYSAIG
851  NKVFTLKLFT NKLRSIAPDV PRDELAESFT EKTMKLFFYL IASGGELISE
901  FNKEFYPTPS NYQTKLRCVA GIQVLKLARI SNLNNFIKPS DIIKLINLVE
951  DESLPVRKTF LEQLKDYVAN ELISIKFLPL VFFTAYEPDV ELKTTTKIWI
1001 NFTFGLKSFK KGTIFERALP RLIHAIAHHP DIVGGLDSEG DAYLNALTTA
1051 IDYLLFYFDS IAAQENFSLL YYLSERVKNY QDKLVEDEID EEEGPQKEEA
1101 PKKHRPYGQK MYIIGELSQM ILLNLKEKKN WQHSAYPGKL NLPSDLFKPF
1151 ATVQEAQLSF KTYIPESLTE KIQNNIKAKI GRILHTSQTQ RQRLQKRLLA
1201 HENNESQKKK KKVHHARSQA DDEEGDGDRE SDSDDDSYSP SNKNETKKGH
1251 ENIVMKKLRV RKEVDYKDDE DDDIEMT
```

Lower Band

```
1    MAKGAVTKLK FNSPIISTSD QLISTNELLD RLKALHEELA SLDQDNTDLT
51   GLDKYRDALV SRKLLKHKDV GIRAFTACCL SDILRLYAPD APYTDAQLTD
101  IFKLVLSQFE QLGDQENGYH IQQTYLITKL LEYRSIVLLA DLPSSNNLLI
151  ELFHIFYDPN KSFPARLFNV IGGILGEVIS EFDSVPLEVL RLIFNKFLTY
201  NPNEIPEGLN VTSDCGYEVS LILCDTYSNR MSRHLTKYYS EIIHEATNDD
251  NNSRLLTVVV KLHKLVLRLW ETVPELINAV IGFIYHELSS ENELFRKEAT
301  KLIGQILTSY SDLNFVSTHS DTFKAWISKI ADISPDVRVE WTESIPQIIA
351  TREDISKELN QALAKTFIDS DPRVRRTSVM IFNKVPVTEI WKNITNKAIY
401  TSLLHLAREK HKEVRELCIN TMAKFYSNSL NEIERTYQNK EIWEIIDTIP
451  STLYNLYYIN DLNINEQVDS VIFEYLLPFE PDNDKRVHRL LTVLSHFDKK
501  AFTSFFAFNA RQIKISFAIS KYIDFSKFLN NQESMSSSQG PIVMNKYNQT
551  LQWLASGLSD STKAIDALET IKQFNDERIF YLLNACVTND IPFLTFKNCY
601  NELVSKLQTP GLFKKYNIST GASIMPRDIA KVIQILLFRA SPIIYNVSNI
651  SVLLNLSNNS DAKQLDLKRR ILDDISKVNP TLFKDQIRTL KTIIKDLDDP
701  DAEKNDNLSL EEALKTLYKA SKTLKDQVDF DDTFFFTKLY DFAVESKPEI
751  TKYATKLIAL SPKAEETLKK IKIRILPLDL QKDKYFTSHI IVLMEIFKKF
801  PHVLNDDSTD IISYLIKEVL LSNQVVGDSK KEIDWVEDSL LSDTKYSAIG
851  NKVFTLKLFT NKLRSIAPDV PRDELAESFT EKTMKLFFYL IASGGELISE
901  FNKEFYPTPS NYQTKLRCVA GIQVLKLARI SNLNNFIKPS DIIKLINLVE
951  DESLPVRKTF LEQLKDYVAN ELISIKFLPL VFFTAYEPDV ELKTTTKIWI
1001 NFTFGLKSFK KGTIFERALP RLIHAIAHHP DIVGGLDSEG DAYLNALTTA
1051 IDYLLFYFDS IAAQENFSLL YYLSERVKNY QDKLVEDEID EEEGPQKEEA
1101 PKKHRPYGQK MYIIGELSQM ILLNLKEKKN WQHSAYPGKL NLPSDLFKPF
1151 ATVQEAQLSF KTYIPESLTE KIQNNIKAKI GRILHTSQTQ RQRLQKRLLA
1201 HENNESQKKK KKVHHARSQA DDEEGDGDRE SDSDDDSYSP SNKNETKKGH
1251 ENIVMKKLRV RKEVDYKDDE DDDIEMT
```

Figure 16 | Identification of a stable domain in Pds5 by limited proteolysis (a) SDS-PAGE gel of a limited proteolysis experiment with Pds5. Protected bands of interest are annotated (b) Peptides identified by acid hydrolysis (in red) of the upper and lower bands identified in overlaid on the full-length Pds5 protein sequence.

3.3.4. Refinement and crystallisation of a stable Pds5 truncation

Mass spectrometry results from section 3.3.3. facilitated the approximate determination of the C-terminal boundary of a protease resistant fragment of Pds5. I therefore designed and purified an initial series of three truncations (T1-3) within this region (figure 17a-b). These truncations behave as well-ordered, globular entities, and thus I sought to crystallise them. One of these truncations (T1) produced poor quality, needle-like crystals, and another (T3) produced spherulites. UV screening and diffraction imaging demonstrated that the needles were indeed protein crystals. Further additive screening and seeding experiments did not yield diffraction grade crystals.

Sequence analysis of Pds5 predicts that it consists of an elongated α-helical repeat protein (Panizza et al., 2000). More specifically it is expected to comprise many HEAT repeats, a structural fold whose basic repeating unit is composed of two anti-parallel α-helices, which typically combine to form higher-order assemblies whose gradual involution determines the overall shape of the molecule. As these paired helices typically form discrete bundles stabilised by a conserved, hydrophobic core, it is possible that the presence of a 'stray' C-terminal α-helix lacking its partner could introduce instability which might be refractory to crystallisation, even if the protein appears well-behaved in solution.

As we lacked conclusive information on where these pairs might terminate, I designed two constructs to test the register of these repeats: one which truncates a predicted α-helix (T4), and a second which extends the protein by a single α-helix (T5). Please note that henceforth, truncation T5 will be referred to as Pds5T. The former, T4, despite being a relatively moderate further truncation, substantially destabilises the protein, whereas the latter, Pds5T, was purified to homogeneity and yields high-quality crystals which are manually reproducible. However, at best, these crystals diffract to a minimum Bragg spacing of 5.8Å.

Despite extensive attempts, I was unable to improve the diffraction of the apo-Pds5T crystals. Strategies included techniques aimed toward improving diffraction quality, such as on-beam annealing, additive screening, and screening of a selenomethionine-

substituted derivative protein. This was ultimately of no consequence, neither improving nor worsening diffraction resolution.

Chemical methods were also employed, including reductive methylation, in which the ε-amino group of lysines are alkylated in order to modify protein hydropathy, solubility and pI; thereby potentially promoting alternate crystal forms. In addition, various concentrations of yttrium chloride were screened, the trivalent yttrium cation of which can facilitate stable intermolecular interactions to enable crystallisation . However, both of these methods lead to marked precipitation.

I additionally pursued the purification of modest further truncation of the Pds5T N and C terminal amino acids in an attempt to change crystal packing by influencing potential crystallisation contacts. However the influence such truncations had on crystallisation was to totally abolish it.

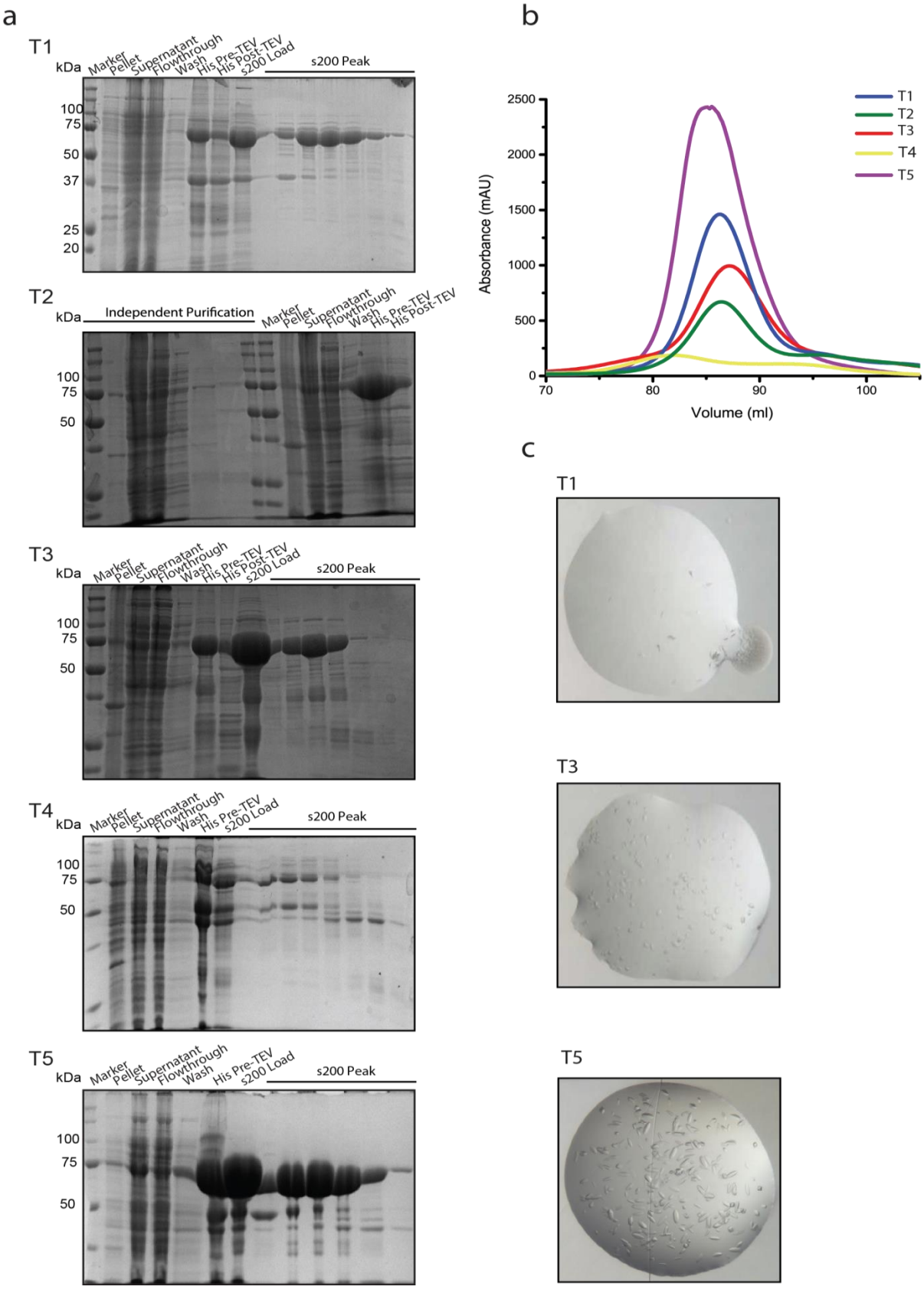
a
T1
kDa
Marker
Pellet
Supernatant
Flowthrough
Wash
His Pre-TEV
His Post-TEV
s200 Load
s200 Peak
100
75
50
37
25
20
T2
kDa
Independent Purification
Marker
Pellet
Supernatant
Flowthrough
Wash
His Pre-TEV
His Post-TEV
100
75
50
T3
kDa
Marker
Pellet
Supernatant
Flowthrough
Wash
His Pre-TEV
His Post-TEV
s200 Load
s200 Peak
100
75
50
T4
kDa
Marker
Pellet
Supernatant
Flowthrough
Wash
His Pre-TEV
s200 Load
s200 Peak
100
75
50
T5
kDa
Marker
Pellet
Supernatant
Flowthrough
Wash
His Pre-TEV
s200 Load
s200 Peak
100
75
50
b
Absorbance (mAU)
2500
2000
1500
1000
500
0
70
80
90
100
Volume (ml)
T1
T2
T3
T4
T5
c
T1
T3
T5

Figure 17 | Purification and crystallisation of Pds5 truncations (a) SDS-PAGE gels of a series of 5 Pds5 truncations (b) Gel filtration traces at a wavelength of 280nm of the same truncations, corresponding to s200 Peak' samples in 'a' (c) Crystallisation of constructs T1, T3 and T5.

3.3.5. Screening orthologues

Another approach frequently employed when difficulties are encountered in the course of seeking to structurally characterise macromolecules is the isolation of similar constructs of orthologous proteins. I was successful in obtaining truncations of Pds5 from *Ashbya Gossypii* (AgPds5T), a filamentous fungus, and Human Pds5B (hPds5T). AgPds5T was very well expressed in *E.Coli* and migrated essentially as a monomer in solution, whereas hPds5T was fairly poorly expressed and appeared to be moderately truncated (figure 18a-b). Both proteins were submitted for crystallisation screens, but neither yielded crystals. AgPds5T did produce spherulites (not shown), thus it is possible that further refinement of the C-terminal α-helices, as with yPds5T, may have been similarly successful in improving the propensity of the sample to crystallise. As yPds5T-Scc1 crystals, described later in the text, were obtained in parallel with this objective and diffracted to 2.9Å after refinement of the crystallisation conditions, I did not seek to further optimise the Pds5 orthologue constructs.

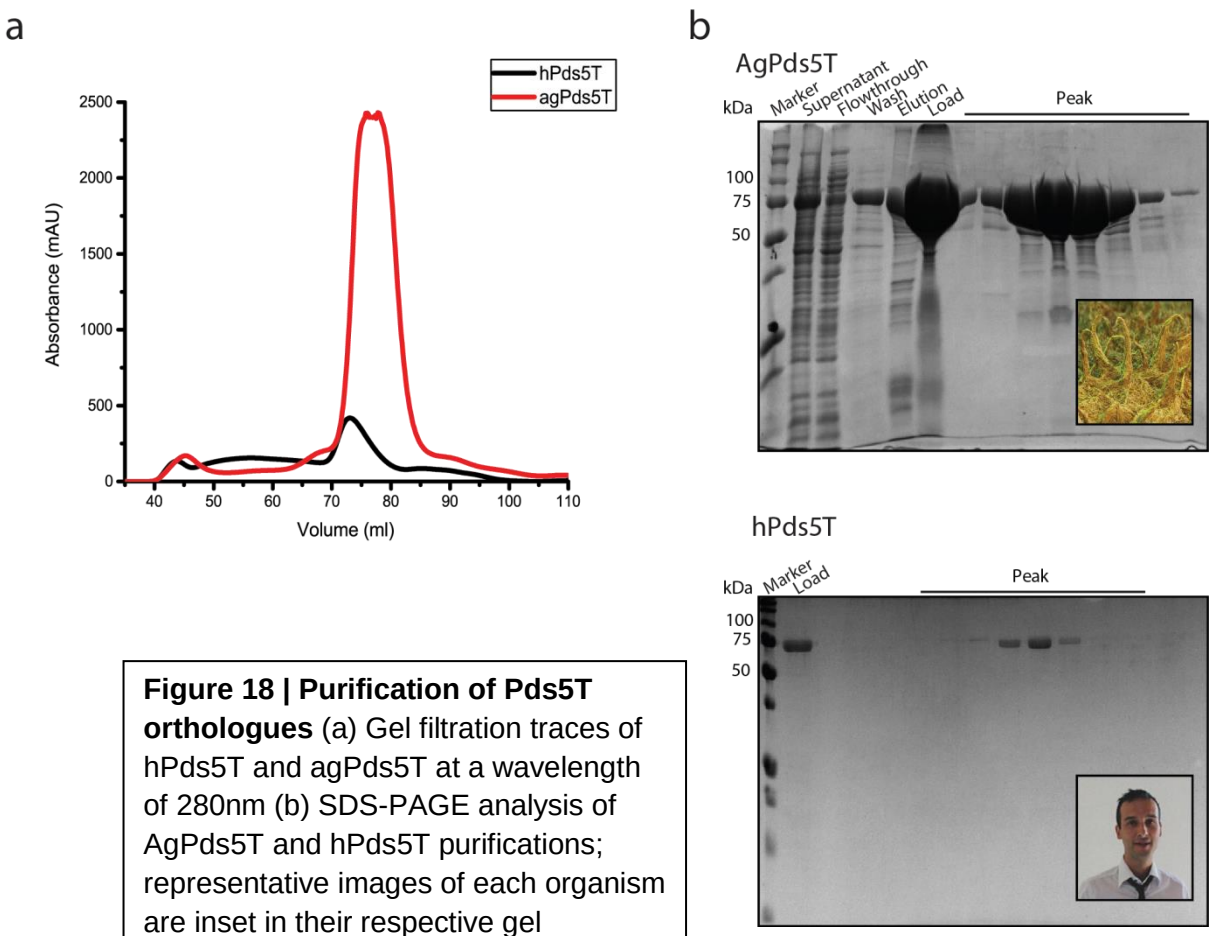

Figure 18 | Purification of Pds5T orthologues (a) Gel filtration traces of hPds5T and agPds5T at a wavelength of 280nm (b) SDS-PAGE analysis of AgPds5T and hPds5T purifications; representative images of each organism are inset in their respective gel

3.3.6. Electrophoretic mobility shift assays

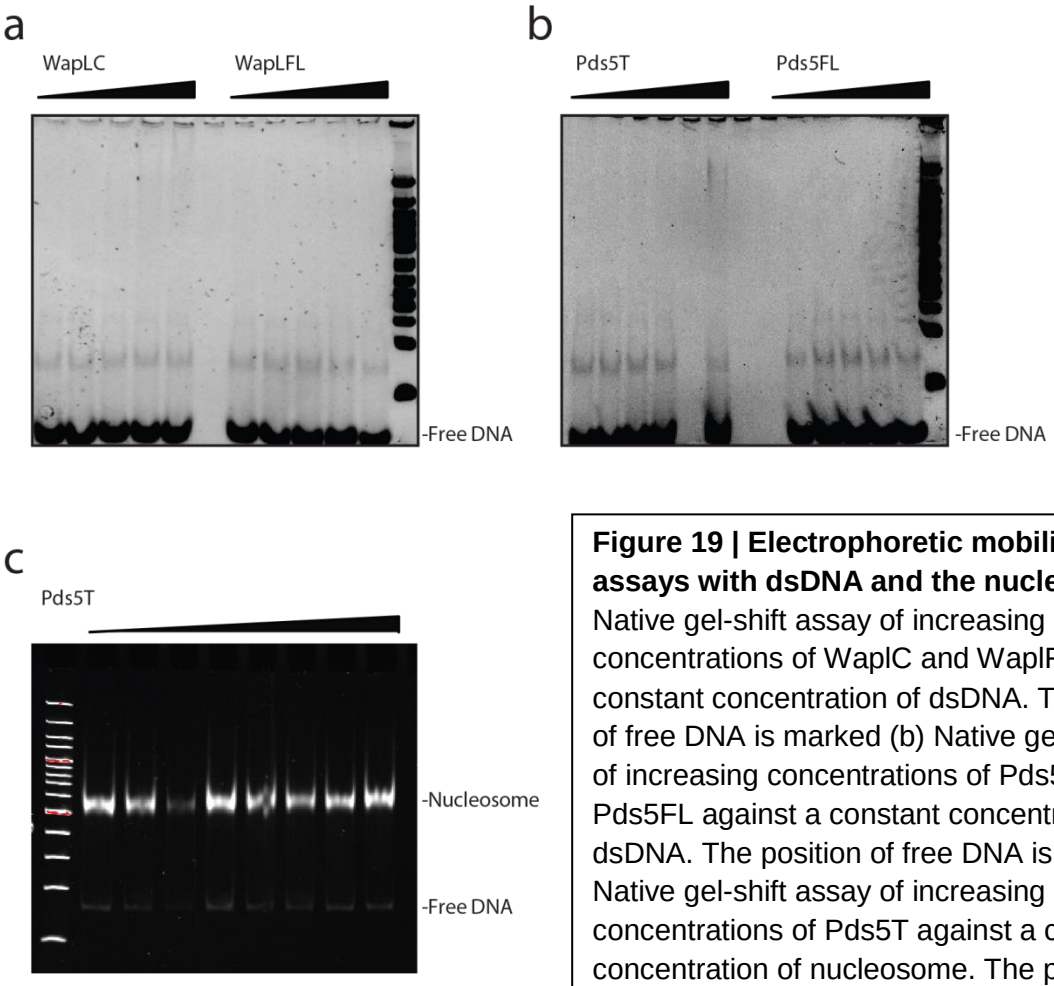

Figure 19 | Electrophoretic mobility shift assays with dsDNA and the nucleosome (a) Native gel-shift assay of increasing concentrations of WaplC and WaplFL against a constant concentration of dsDNA. The position of free DNA is marked (b) Native gel-shift assay of increasing concentrations of Pds5T and Pds5FL against a constant concentration of dsDNA. The position of free DNA is marked (c) Native gel-shift assay of increasing concentrations of Pds5T against a constant concentration of nucleosome. The positions of free DNA, and of the nucleosome, is marked

As cohesin is involved in chromatin transactions, electrophoretic mobility shift assays were performed to assess DNA binding of the Pds5 and Wapl subunits by titrating the full-length and indicated truncation constructs against a random 32bp dsDNA. Reasoning that Pds5 might interact with chromatin, either as a sensor for when the cohesin complex has engaged sister chromatids, or as an event that might further stabilise the association of cohesin with chromatin, Pds5T was also tested against the nucleosome. However, no interaction could be observed for Wapl or Pds5 constructs using either substrate (figure 19). In contrast to the Scc2-Scc4 loading complex, and the

analogous HEAT repeat proteins of condensin, engagement of DNA, and of chromatin by Pds5, does not appear to be a feature of Wapl and Pds5.

3.3.7. Pulldown assays

The nature of the association of Wapl with Pds5 remains ambiguous, with prior experiments in the literature reporting alternatively that they may form a direct binary complex in vitro and in vivo, or that such interactions depend on additional factors, such as Scc1 (Rowland et al., 2009, Shintomi et al., 2009, Nishiyama et al., 2010, Chan et al., 2012, Kulemzina et al., 2012, Ouyang et al., 2013). Therefore, to further characterise these putative assemblies *in vitro*, I isolated a series of GST-Wapl constructs encompassing the full-length protein (WaplFL), as well as the N- and C-terminal regions, WaplN ($Wapl^{1-249}$) and WaplC ($Wapl^{250-647}$) respectively, which would allow simultaneous dissection of domain requirements for any interactions observed. Similarly, given the proposition that Wapl may interact with the Smc3 head to achieve its release function, I also performed pulldowns to investigate the nature of their association in solution (Chatterjee et al., 2013). I found no evidence of any association between full-length Pds5 and GST-WaplFL, despite employing buffer conditions similar to those previously published (figure 20a). Correspondingly, there was no retention of Pds5 or Pds5T by the aforementioned subdomains of Wapl (figure 20a). In contrast to a report suggesting that Wapl might interact with the Smc3 ATPase head through its WaplC domain, I also could not reproduce this interaction (figure 20b).

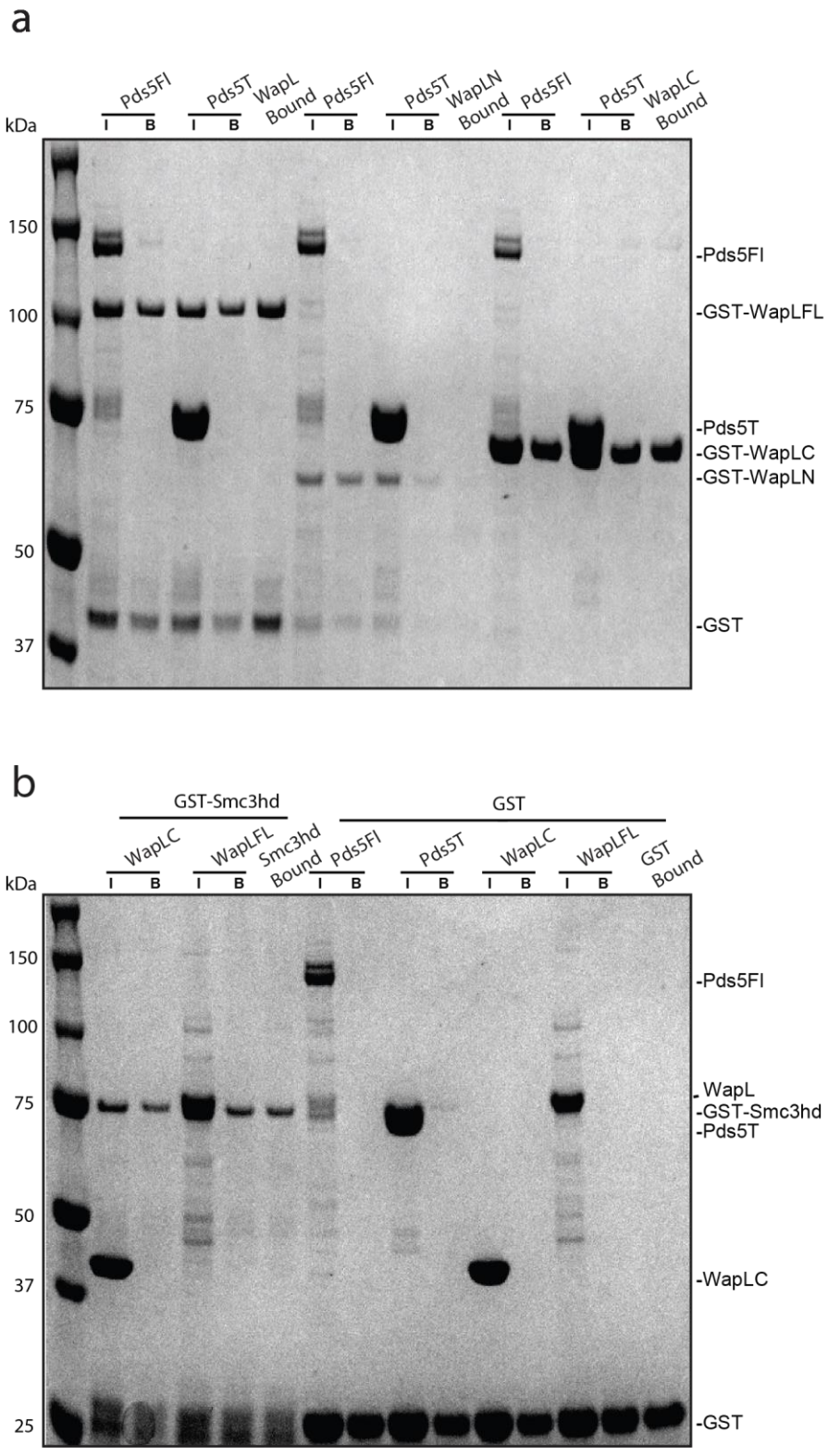

Figure 20 | GST pulldowns of Wapl, Pds5 and Smc3 (a) Pulldowns of Pds5, and Pds5T against GST-Wapl(lanes 2-6), aGST-WaplN (lanes 7-11), and GST-WaplC (lanes 12-15). I: Input, B: Bound (b) Pulldowns of WaplC and WaplFL against GST-Smc3hd (lanes 2-6), and GST-binding controls (lanes 7—15).

3.3.8. Analytical size exclusion

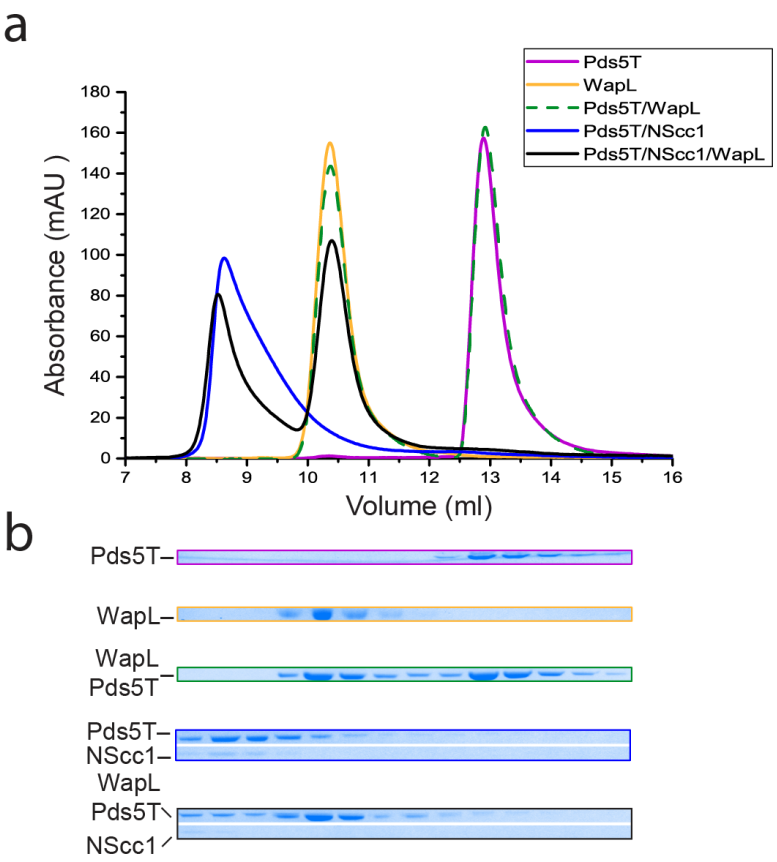

Figure 21 | Analytical size-exclusion of Pds5, Wapl, and Scc1. (a) Size-exclusion chromatography profiles for Pds5T, Wapl, Pds5T-Wapl, Pds5T-NScc1 and Pds5T-NScc1-Wapl preparations are shown. (b) Fractions from each run were analysed by SDS-PAGE. Coomassie stained are shown below. Gels were cropped to show the relevant sections.

The N-terminal segment of Scc1, upstream of a proximal Separase cleavage site, was previously shown to be required for the recruitment of Pds5 to cohesin (Kulemzina et al., 2012, Chan et al., 2013). Furthermore, it was recently shown that the mutation of highly conserved hydrophobic residues in this domain of Scc1 perturb the recruitment of Pds5 to cohesin in vivo, emphasising the relevance of this interaction (Chan et al., 2013)

To investigate the nature of this association, I designed an NScc1 construct which extends from the predicted, and now published, Smc3 binding region through a domain required for Pds5 binding, terminating shortly before the N-terminal Separase cleavage site (Haering et al., 2002, Chan et al., 2013, Burmann et al., 2013. Gligoris et al., 2014). Initial purification of a Pds5T-NScc1$^{1-168}$ yielded a pure complex which migrates close to the exclusion volume of a 24ml s200 column (figure 21 a, b).

To explore the nature of the putative Pds5, Scc1, and Wapl sub-assemblies described in the literature, I subjected these proteins to analytical size-exclusion under buffer conditions essentially identical to those reported previously. The gel-filtration traces from these experiments did not support the existence of a ternary assembly between these proteins, nor of binary Pds5-Wapl complexes, as no appreciable changes in the elution profiles of these proteins are detected upon mixing (figure 21a, b), consistent with the pulldown experiments from figure 20a.

3.3.9. Identification of a Pds5T-Scc1 subcomplex

In parallel with efforts to improve apo-Pds5T crystal diffraction, I sought to isolate liganded forms of Pds5. Following limited proteolysis and mass-spectroscopy, the Scc1 construct was refined to a 5kDa Pds5-binding domain.

a

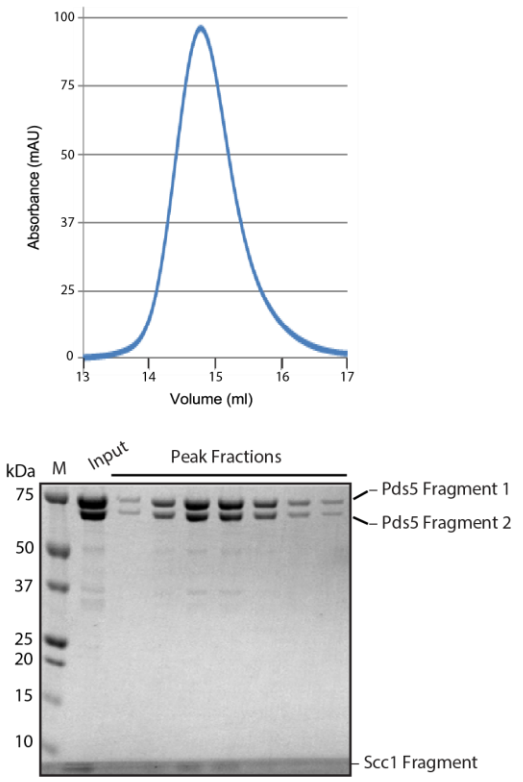

b

Pds5 Fragment 1

```
1   GAMAKGAVTK LKFNSPIIST SDQLISTNEL LDRLKALHEE LASLDQDNTD
51  LTGLDKYRDA LVSRKLLKHK DVGIRAFTAC CLSDILRLYA PDAPYTDAQL
101 TDIFKLVLSQ FEQLGDQENG YHIQQTYLIT KLLEYRSIVL LADLPSSNNL
151 LIELFHIFYD PNKSFPARLF NVIGGILGEV ISEFDSVPLE VLRLIFNKFL
201 TYNPNEIPEG LNVTSDCGYE VSLILCDTYS NRMSRHLTKY YSEIIHEATN
251 DDNNSRLLTV VVKLHKLVLR LWETVPELIN AVIGFIYHEL SSENELFRKE
301 ATKLIGQILT SYSDLNFVST HSDTFKAWIS KIADISPDVR VEWTESIPQI
351 IATREDISKE LNQALAKTFI DSDPRVRRTS VMIFNKVPVT EIWKNITNKA
401 IYTSLLHLAR EKHKEVRELC INTMAKFYSN SLNEIERTYQ NKEIWEIIDT
451 IPSTLYNLYY INDLNINEQV DSVIFEYLLP FEPDNDKRVH RLLTVLSHFD
501 KKAFTSFFAF NARQIKISFA ISKYIDFSKF LNNQESMSSS QGPIVMNKYN
551 QTLQWLASGL SDSTKAIDAL ETIKQFNDER IFYLLNACVT NDIPFLTFKN
601 CYNELVSKLQ TPGLFKKYNI STGASIMPRD IAKVIQILLF RASPIIYNVS
651 NISVLLNLSN NSDAKQLDLK RRILDDISKV NPTLFKDQIR TLKTIIKDLD
701 DPD
```

Pds5 Fragment 2

```
1   GAMAKGAVTK LKFNSPIIST SDQLISTNEL LDRLKALHEE LASLDQDNTD
51  LTGLDKYRDA LVSRKLLKHK DVGIRAFTAC CLSDILRLYA PDAPYTDAQL
101 TDIFKLVLSQ FEQLGDQENG YHIQQTYLIT KLLEYRSIVL LADLPSSNNL
151 LIELFHIFYD PNKSFPARLF NVIGGILGEV ISEFDSVPLE VLRLIFNKFL
201 TYNPNEIPEG LNVTSDCGYE VSLILCDTYS NRMSRHLTKY YSEIIHEATN
251 DDNNSRLLTV VVKLHKLVLR LWETVPELIN AVIGFIYHEL SSENELFRKE
301 ATKLIGQILT SYSDLNFVST HSDTFKAWIS KIADISPDVR VEWTESIPQI
351 IATREDISKE LNQALAKTFI DSDPRVRRTS VMIFNKVPVT EIWKNITNKA
401 IYTSLLHLAR EKHKEVRELC INTMAKFYSN SLNEIERTYQ NKEIWEIIDT
451 IPSTLYNLYY INDLNINEQV DSVIFEYLLP FEPDNDKRVH RLLTVLSHFD
501 KKAFTSFFAF NARQIKISFA ISKYIDFSKF LNNQESMSSS QGPIVMNKYN
551 QTLQWLASGL SDSTKAIDAL ETIKQFNDER IFYLLNACVT NDIPFLTFKN
601 CYNELVSKLQ TPGLFKKYNI STGASIMPRD IAKVIQILLF RASPIIYNVS
651 NISVLLNLSN NSDAKQLDLK RRILDDISKV NPTLFKDQIR TLKTIIKDLD
701 DPD
```

c

Observed Mass (Da)	Fragment Identity
79392	Pds5T
70685	Pds5 1-616
5065	Scc1 116-159

Figure 22 | Defining a Pds5T-Scc1 subcomplex by limited proteolysis (a) Size-exclusion and SDS-PAGE analysis of a proteolysed Scc1-Pds5 complex (b) Peptides identified by acid hydrolysis (in red) of Pds5 fragments overlaid on the Pds5T protein sequence (c) Masses observed in MS analysis of the size-exclusion peak from (a) and the corresponding domain assignments of fragments in Scc1 and Pds5

For this objective, I subjected the Pds5T-PScc1M complex to limited proteolysis by chymotrypsin and passed this material over a size-exclusion column, in order to isolate potential co-migrating subdomains of each protein. The result was a single peak (figure 23a) which contained two bands corresponding to Pds5, Pds5T and $Pds5^{1-616}$, as shown by acid hydrolysis and intact MS (figure 22b, c), and a series of small peptides which run below the 10kDa protein marker. Given their small size, I hypothesised that these fragments probably corresponded to peptides which co-migrated with the larger proteins at this position due to complex formation; however they proved to be prohibitively small for analysis by acid hydrolysis. Thus, during analysis of intact masses from MS, we isolated these smaller masses and subjected them to on-machine fragmentation and further MS (MS/MS) to ascertain their identity. Of these fragments, de novo amino-acid sequencing of fragments resulting from MS/MS of a 5065Da peptide indicated the presence of a co-eluting subdomain of Scc1 (Joanna Kirkpatrick, personal communication). Collation of this mass with predicted chymotryptic cleavage sites resulted in the unambiguous assignment of the fragment as $Scc1^{116-159}$. Co-expression of this Scc1 construct with the Pds5 crystallisation construct allowed me to isolate a binary complex which crystallises robustly. To exclude the possibility that the initial $NScc1^{1-168}$ construct design might have led to the omission of key residues in elements of Scc1 further toward the C terminus, I repeated the limited proteolysis experiment using Pds5T-Scc1 complexes with C-terminal extensions, the furthest tested being $NScc1^{1-251}$, which terminates shortly in advance of the second Separase cleavage site, and obtained similar results (not shown).

As I was also presented with a novel construct of Pds5, I cloned and attempted to purify this protein, however it displayed poor expression and solubility, similar to T4. During the course of the MS/MS experiments, peptides corresponding to the region of Pds5 between the Pds5T and $Pds5^{1-616}$ were also detected, and so deletion of these intervening amino acids most likely results in structural destabilisation of the protein.

3.4. The structural basis of Pds5 recruitment to cohesin

The following chapter describes work which was undertaken as a collaborative effort. In vivo characterisation of the Pds5T-Scc1 structure we obtained was performed by Marc Kschonsak, Jutta Metz, and Christian Häring. The results are included here to highlight the biological significance of the biochemical and biophysical characterisation I undertook during my thesis work.

3.4.1. Structure of the Pds5T-Scc1 complex

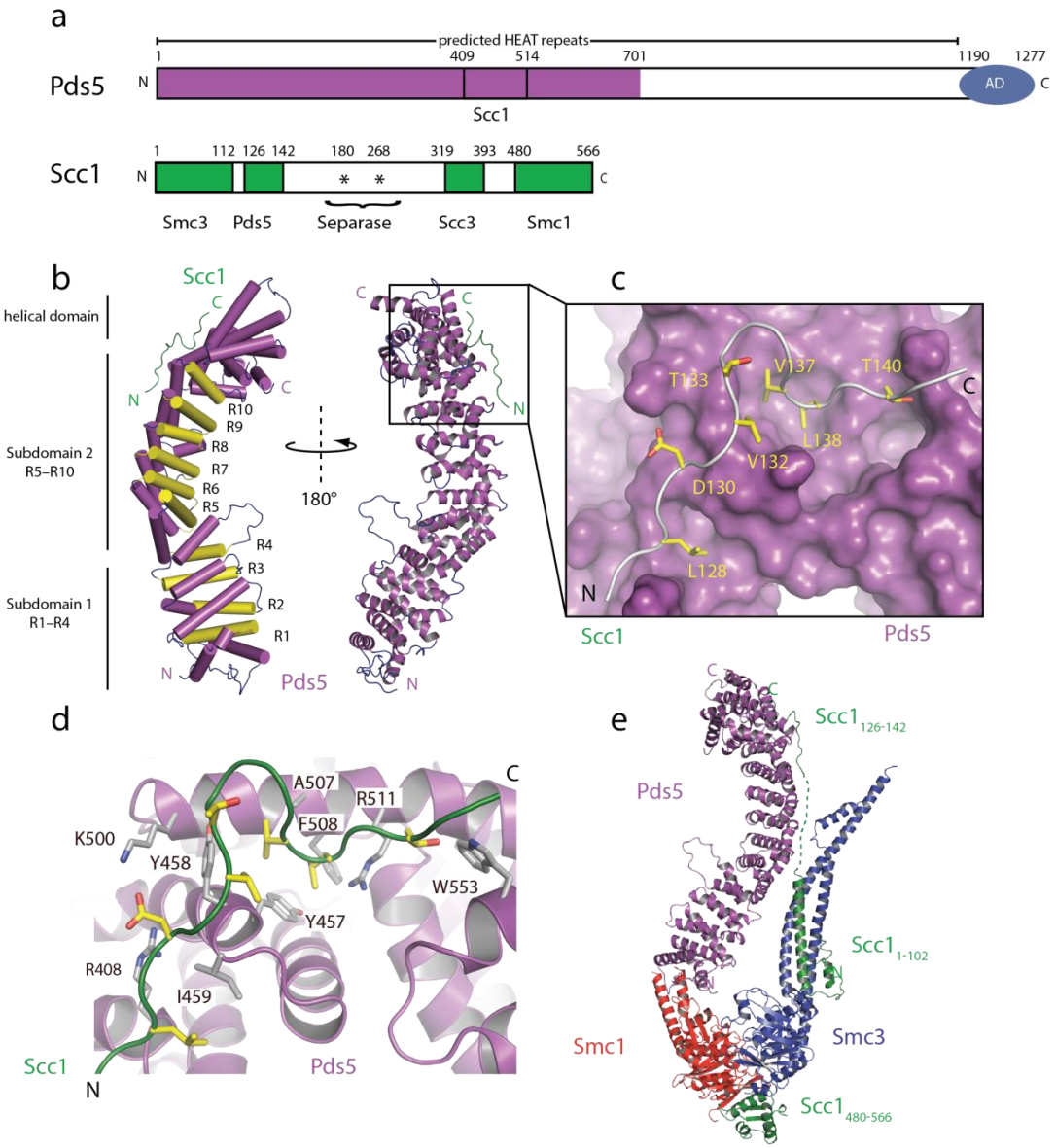

Figure 23 | Structure of the Pds5-Scc1 complex. (a) Domain architecture of Pds5 and Scc1. Regions involved in complex formation are indicated. (b) A ribbon view of Pds5 structure with the HEAT repeats R1–R10 labelled. Pds5 is shown in magenta and Scc1 in green. (c) Surface rendered view of the Pds5–Scc1 interface. Select Scc1 residues are indicated (d) View of interactions between Pds5 and Scc1. Select Pds5 residues are labeled. Nitrogen and oxygen atoms are shown in blue and red, respectively. Scc1 backbone atoms are coloured in green and sidechain carbon atoms in yellow. Pds5 sidechain carbon atoms are in grey. (e) Hypothetical model of the quaternary Smc1-Smc3-Scc1-Pds5, (coloured red, blue, green, and magenta respectively) complex containing available structural data (PDB codes 1W1W, 4UX3, this study). A flexible linker comprising amino acid residues 103–125 of Scc1 (dotted green line) separates Pds5 from the N–terminal fragment (1–102) of Scc1 bound to the Smc3Hd.

Budding yeast Pds5 is a 1,277 amino acid residue protein predicted to contain a HEAT (Huntington, EF3, PP2A, TOR1) repeat domain and a highly charged C-terminal region (Figure 23a). Scc1 is a 566 amino acid residue protein that contains binding sites for the cohesin Smc3 and Smc1 subunits in its conserved N- and C-terminal domains. Two Separase cleavage sites are located in the center of the protein and are flanked by Pds5 and Scc3 binding sites. To derive further insight into the function of Pds5 and the molecular basis of its interaction with Scc1, I employed limited proteolysis to identify a crystallisable Pds5-Scc1 cohesin subcomplex, as described in section 3.5.

a

Sample	Observed Mass (Da)	Expected Mass (Da)
Pds5T	80649.12	80647.57
Pds5T-Scc1	80647.81	80647.57
	5019.64	5019.60

b

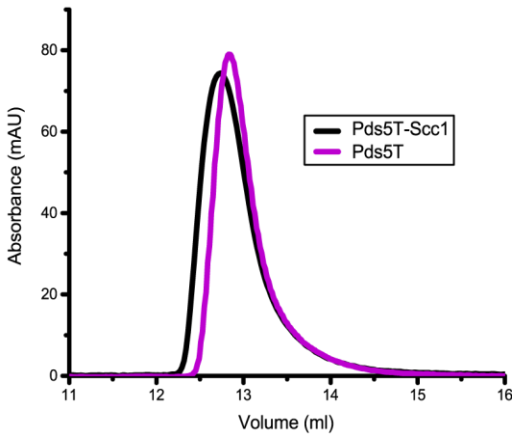

Figure 24 | Biochemical analysis of Pds5T and Pds5T-Scc1. (a) Proteolytic fragments of Pds5 and Scc1 were cloned expressed and co-purified. Mass spectroscopy shows the integrity

of the expressed constructs. (b) Size exclusion chromatography of Pds5T and of the Pds5T-Scc1 complex.

Mass spectrometry revealed that an N-terminal fragment of Pds5 (Pds5T; residues 1-701) is sufficient for complex formation with a fragment of Scc1 (residues 116-159) (figure 22; figure 24a). Expression of these proteins in Escherichia coli facilitated the purification and crystallisation of Pds5T in isolation, and of the Pds5T–Scc1 complex (Figure 24b). While crystals obtained of Pds5T in isolation only diffracted to a minimum Bragg spacing of 6.0 Å, the Pds5T–Scc1 complex diffracted to 2.9 Å. Diffraction data collected from selenomethionine–substituted derivatives of these crystals enabled the determination of initial phases by single wavelength anomalous diffraction (SAD) and the generation of an incomplete model, built into a 3.4 Å resolution map. This model was then employed in phasing the higher resolution data by molecular replacement and to build a final model containing residues 3–610 and 623–697 of Pds5 and residues 126–142 of Scc1 (Table 1, appendix).

As predicted from the amino acid sequence, Pds5T consists of tandem HEAT repeats (designated R1–10) which together form a superhelical array. A segment containing an extended loop interrupts the solenoid, such that HEAT repeats R4 and R5 are apposed in a perpendicular fashion. Thus, the HEAT repeats are segregated into two major subdomains: R1–R4 and R5–R10 (Figure 23b). Towards the C terminus, the solenoid is interrupted by a 6 α-helix platform that serves as a scaffold for Scc1 binding. Residues 126–142 of Scc1 form an extended coil that binds along the outer surface of Pds5T, such that its C–terminal end progresses toward the C terminus of Pds5 and terminates along the 6 α-helix scaffold, perpendicular to the main axis of Pds5 (Figure 23b). To validate the register and binding orientation of Scc1, we mutated residue L128 in our Scc1 construct to methionine and produced crystals of selenomethionine–substituted Pds5T–Scc1. An anomalous difference map revealed an additional peak at the expected position and therefore unambiguously confirmed the binding register (Figure

25a). Calculation of an |Fo|−|Fc| omit map generates positive density for the Scc1 chain (Figure 25b).

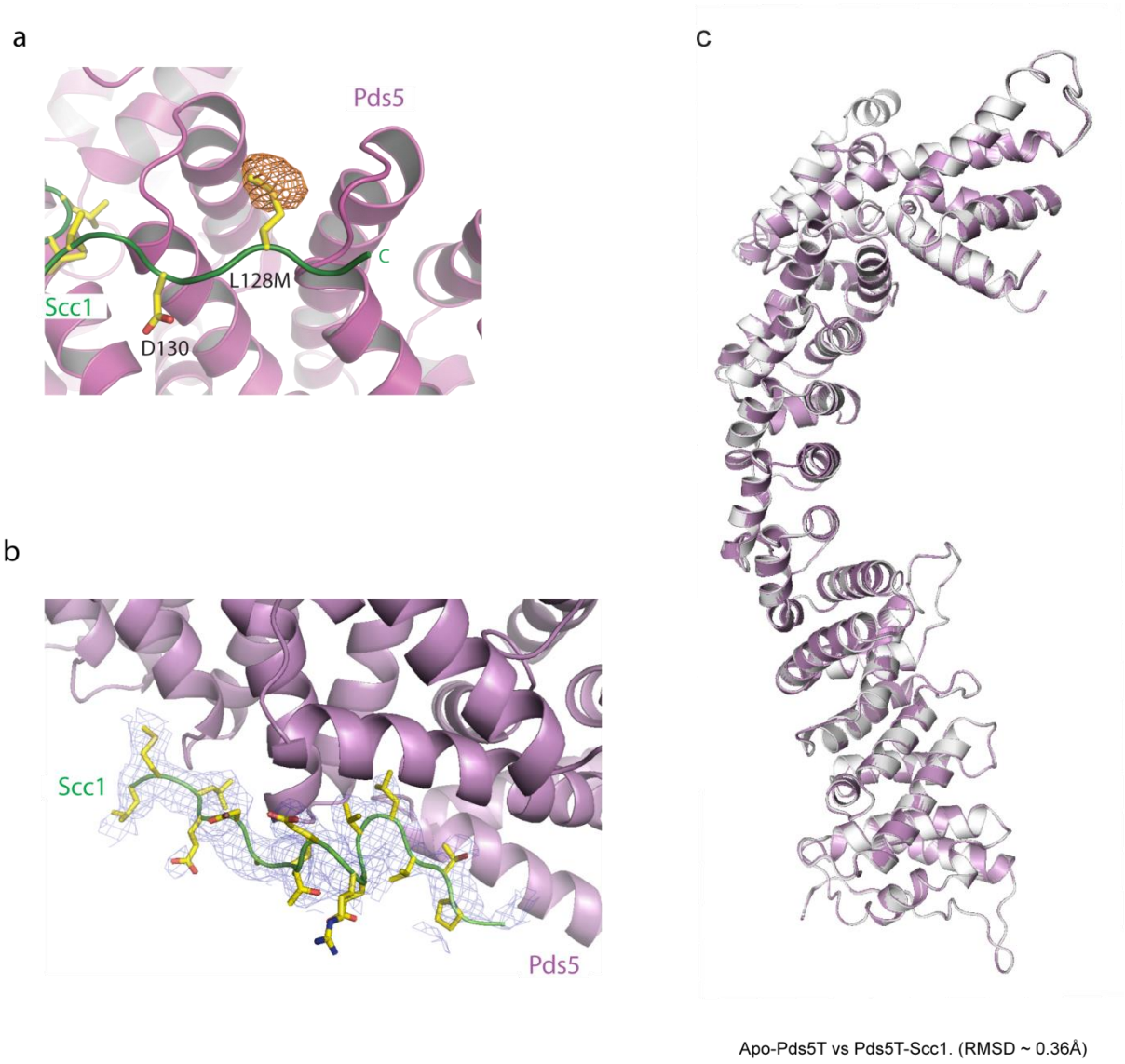

Figure 25 | Validation of the Scc1 register and structural analysis of Pds5 (a) Anomalous difference map of a selenomethionine–substituted crystal containing the mutation Scc1^{L128M}. (b) Electron density for Scc1 from an |Fo|−|Fc| omit map contoured to1.5σ (shown as a blue mesh) (c) Structural superimposition of apo (grey) and Scc1-bound Pds5T (violet).

The extended conformation of Scc1 depends on its contacts with the surrounding Pds5T and so this domain is likely to be unstructured in the absence of its partner. In contrast, Pds5T does not undergo major conformational changes upon binding to Scc1:

our 5.8 Å crystal structure of Pds5T in isolation retains an identical conformation to that observed for the Pds5T–Scc1 complex, despite a different crystal packing environment (Cα root mean square deviation = 0.36 $Å^2$; Figure 25c). Engagement of this domain of Scc1 positions Pds5 in close proximity to the Smc1–Smc3 head complex (Figure 23e), as the Smc3 and Pds5 binding regions of Scc1, Scc11-102 and Scc1126-142 respectively, are separated by only 24 amino-acids. Such close positioning of Pds5 to the Smc1–Smc3 head complex may potentially of be consequence in regulating the closure of the Scc1–Smc3 interface (Chan et al., 2012, Buheitel and Stemmann, 2013, Eichinger et al., 2013, Gligoris et al., 2014, Huis in 't Veld et al., 2014).

Scc1 interacts with Pds5 predominantly through a tridentate projection of hydrophobic residues into three cognate hydrophobic pockets, the first two of which sit astride a salt bridge formed between conserved residues on both proteins. These interfaces are additionally interspersed by and reinforced with electrostatic interactions. The first hydrophobic pocket, including $Pds5^{I459}$, accommodates $Scc1^{L128}$ (Figure 23c). Backbone contacts of $Pds5^{R408}$ further stabilise this interaction (Figure 23d). Further toward the C terminus, Pds5R408 together with Pds5K500 participate in electrostatic interactions with Scc1D130. The second hydrophobic pocket is the most substantial and robustly anchors Pds5 to Scc1. Additional contacts occur between Scc1V132 and Pds5Y458. Electrostatic interactions between Scc1T133 and Scc1E136 curve the peptide and loop the intervening sequence, such that residues Scc1V137 and Scc1L138 project deeply into the hydrophobic pocket lined by Pds5Y457, Pds5Y458 and Pds5I459. The third hydrophobic pocket, delimited by Pds5I515 and abutted by Pds5W553, accommodates Scc1T140 (Figure 23d).

3.4.2. Conservation of the Pds5-Scc1 interface

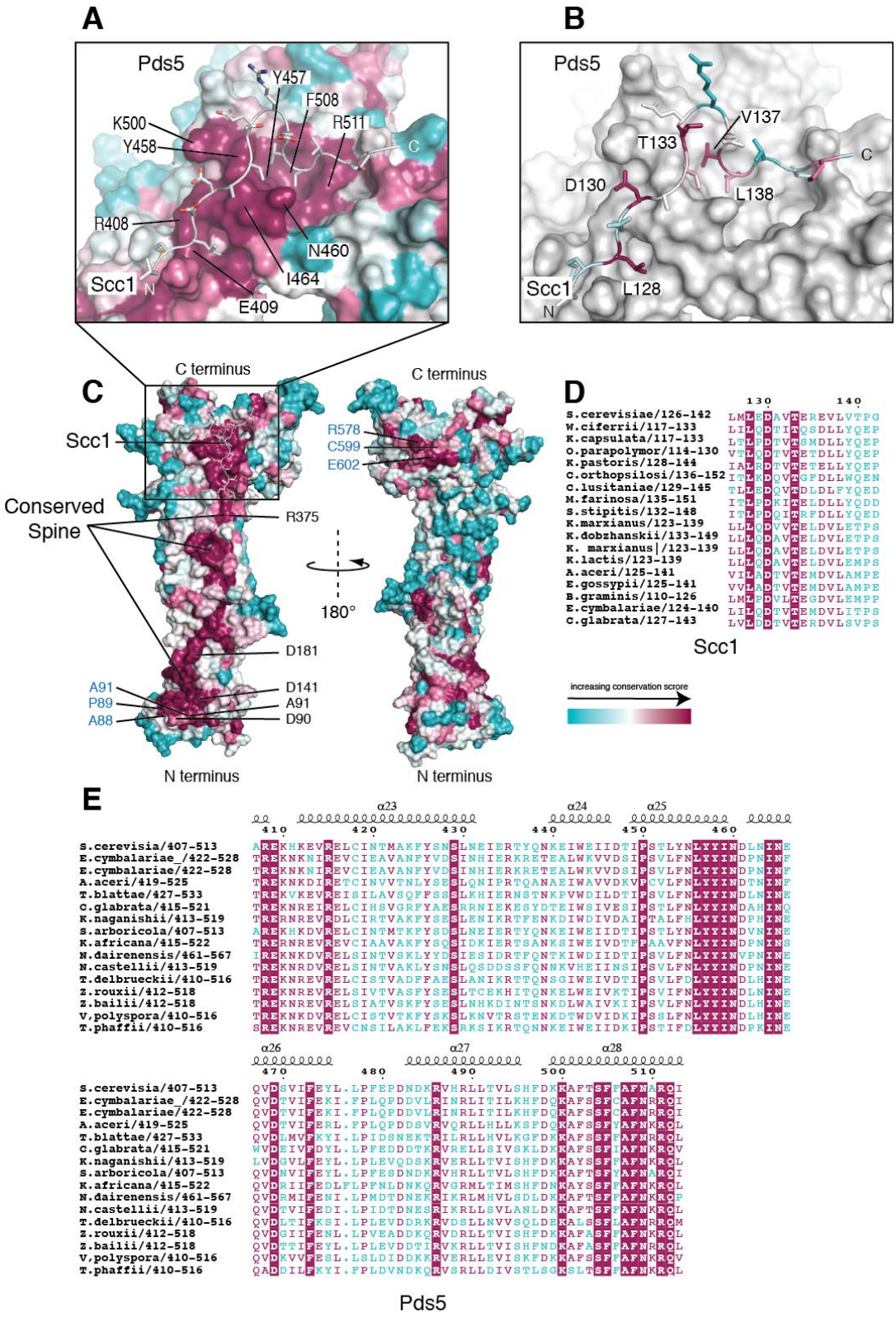

Figure 26 | Surface conservation of Pds5 and Scc1. (a) The region of Pds5 around the Scc1 binding interface is shown and coloured according to sequence conservation. Highly conserved residues of Pds5 are indicated. (b) Sequence conservation of Scc1 is mapped onto the structure and Pds5 is shown in grey. Scc1 residues are shown as sticks and highly conserved Scc1 residues are indicated. (c) Surface residue conservation of Pds5 (left) including a 180° rotation (right). The conserved Scc1 binding site on Pds5 is part of a larger conserved spine that flows from the N terminus of Pds5. Residues in the conserved spine that were analysed are indicated in black. Previously published surface-located *eco1-1* suppressor mutants are shown in blue (d) Alignment of Scc1 amino acid sequences. (e) Alignment of Pds5 amino acid sequences.

To investigate conserved surface features, which may themselves correspond to conserved functional elements, sequence alignments for Pds5T and Scc1 were compiled and amino acid conservation mapped onto the structure. Amino acid residues of Pds5T buried in the heterodimerisation interface are usually conserved, whilst conservation of residues not engaged in the interface is divergent (Figure 26a, c, e). Similarly, Scc1 residues facing the interface are also well conserved (Figure 26b, d). In particular, the chemical properties of residues in the second hydrophobic pocket are highly conserved in divergent eukaryotes, ranging from yeasts to humans (Figure 27).

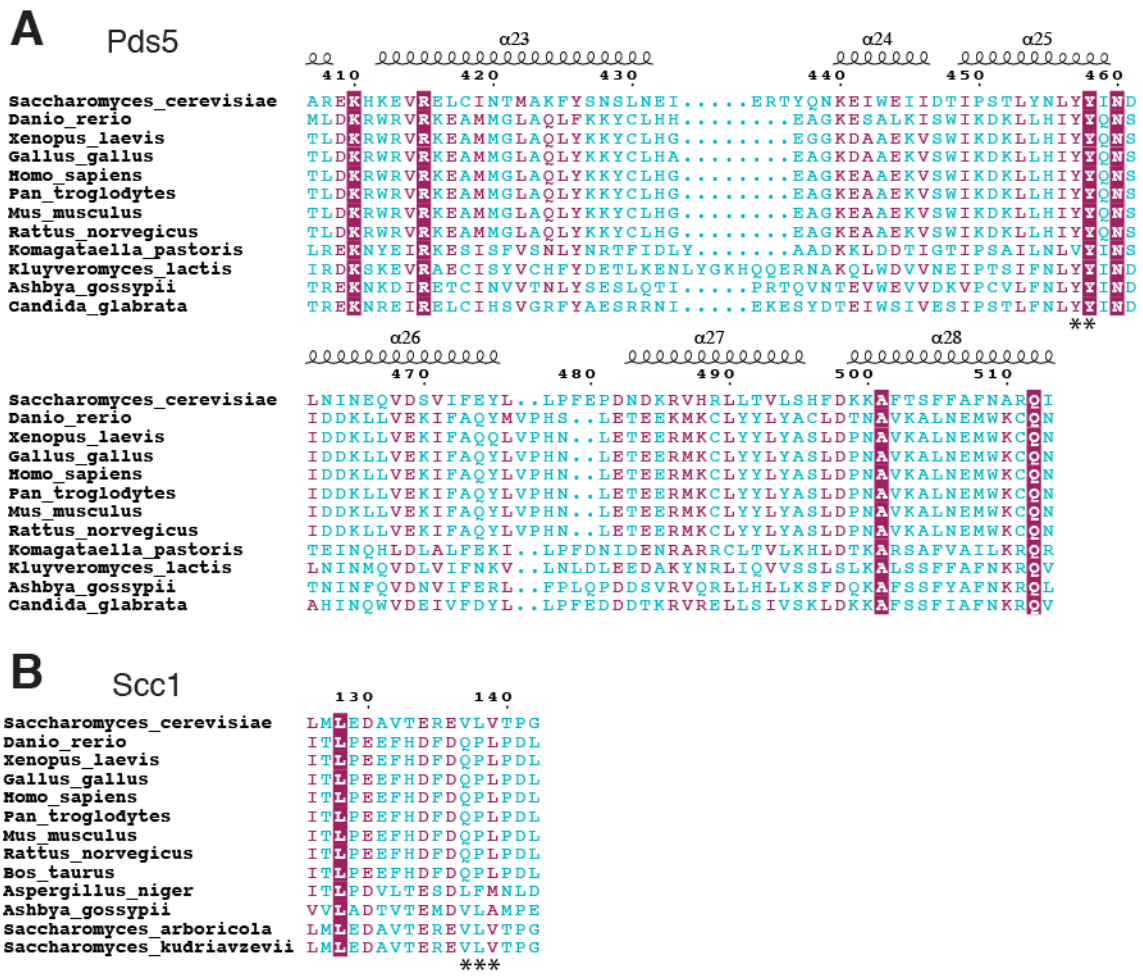

Figure 27 | Sequence conservation of Pds5 and Scc1. (a) Sequence conservation of Pds5 across eukaryotes. Residues in the second hydrophobic pocket are indicated with an *. (b) Sequence conservation of Scc1. Residues important for Pds5 binding are indicated with an *. Conserved residues are shown in violet. Secondary structure is displayed above the corresponding primary sequence.

Thus, it is likely that the same interface is also relevant for Pds5 and Scc1 function in organisms whose genomes encode orthologous proteins. Furthermore, the conserved Scc1 binding site on Pds5 is part of a larger conserved surface spine that extends towards the N terminus of Pds5 (Figure 26c), which suggests that this region of Pds5 might also be required for other aspects of cohesin function.

3.4.3. Analysis of the Pds5-Scc1 interface

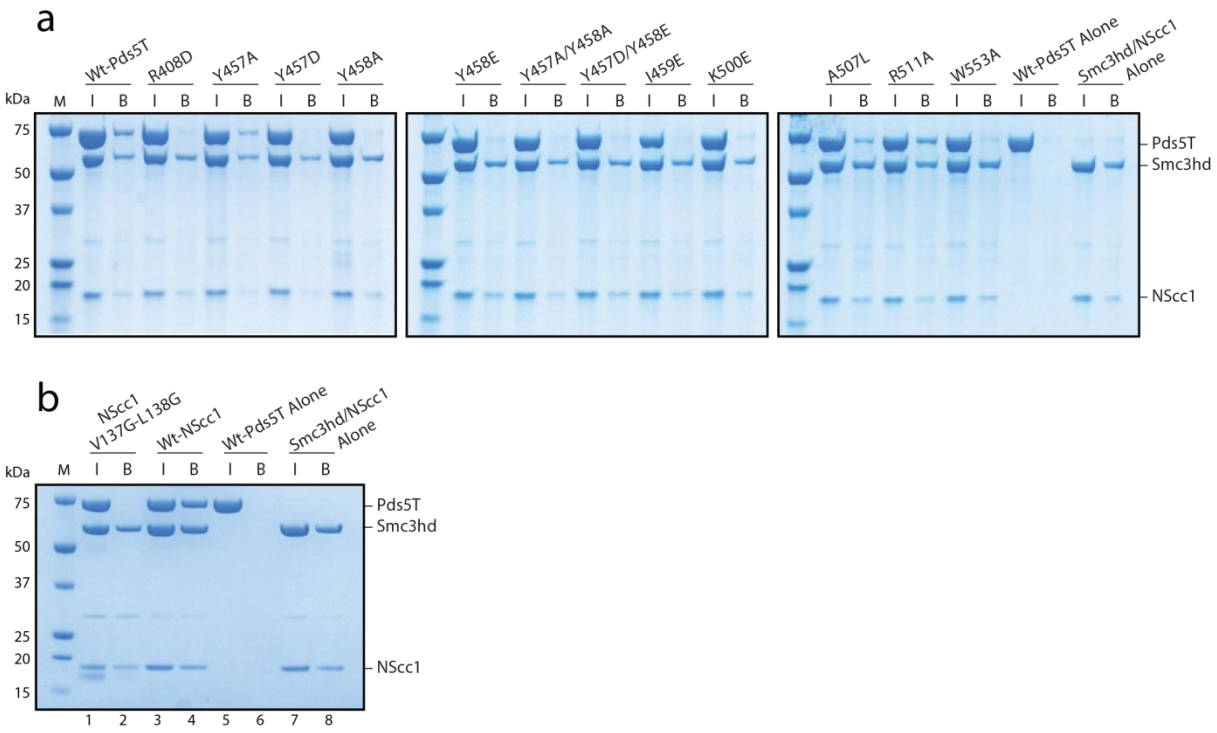

Figure 28 | Interaction of Pds5T with Smc3hd-NScc1. (a) His-tagged Smc3hd-NScc1 was used to pulldown the indicated Pds5T mutants. (b) The Smc3hd-NScc1$^{V137G/L138G}$ mutant (lanes 1, 2) or Smc3hd-NScc1 wild-type (lanes 3, 4) was used to pulldown wild-type Pds5T. Controls for Pds5T are shown in lanes 5, 6 and for Smc3Hd-NScc1 in lanes 7, 8. M: Marker; I: Input; B: Bound.

Purification of the Pds5-binding domain of Scc1 in isolation proved intractable, thus to establish the relevance of the assembly described in our structure, we performed pulldown assays of Pds5T against a binary complex of the Smc3 head (Smc3Hd) and an N–terminal region of Scc1 encompassing binding sites for both of the larger proteins (NScc1; amino acid residues 1–159; C-terminal 6×Histidine tag). We found that the mutation of conserved residues in the Scc1 binding domain of Pds5, including Pds5^{R408D}, Pds5^{Y457D}, Pds5^{Y458A}, Pds5^{Y458E}, Pds5$^{Y457A/Y458A}$, Pds5$^{Y458D/Y458E}$ and Pds5^{I459E}, greatly reduced binding to the Smc3Hd–NScc1 complex (Figure 28a). Other mutations in the interface, including Pds5^{K500E}, Pds5^{A507L} and Pds5^{W533A}, reduced but

did not fully abolish binding. Whereas the Pds5^{Y457A} and Pds5^{R511A} mutants exhibit essentially wild–type binding.

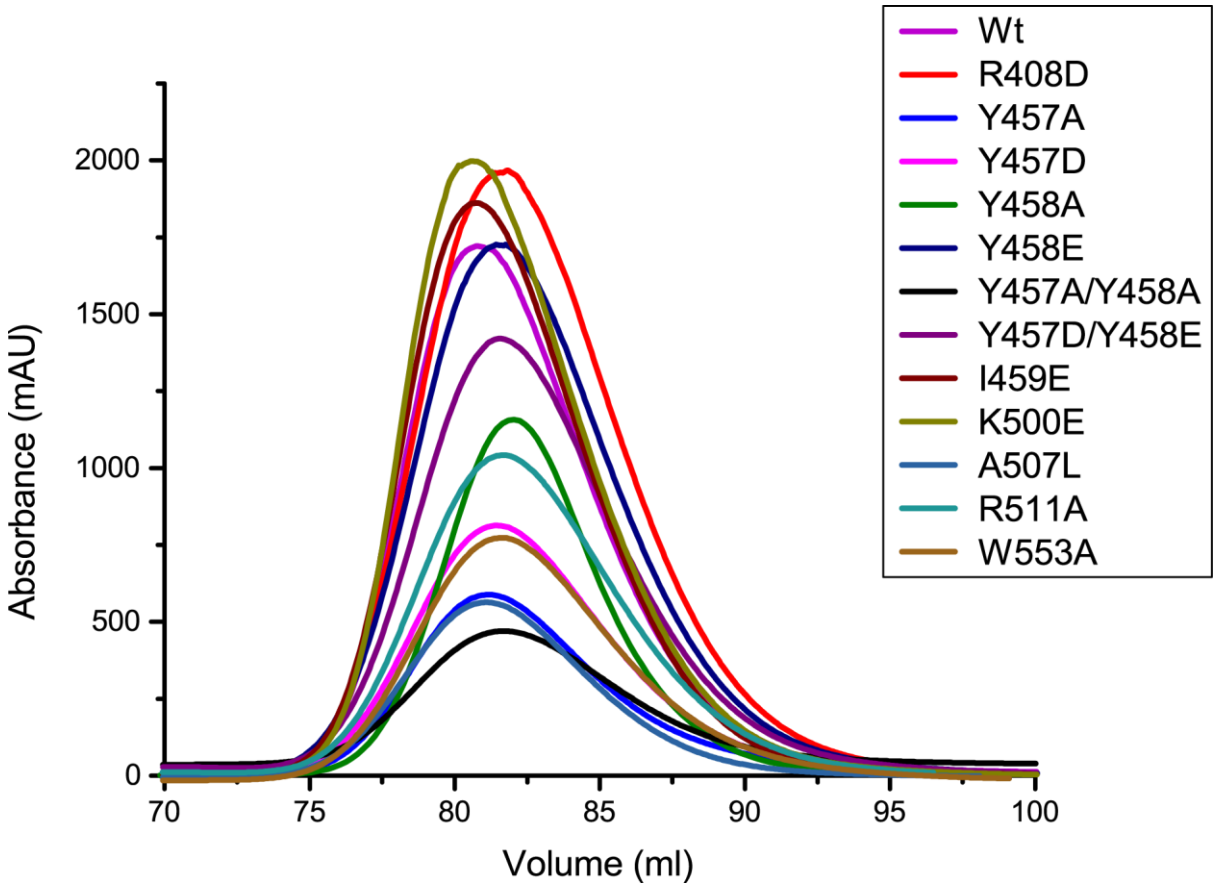

Figure 29 | Size exclusion chromatography of Pds5 mutants. Mutations are located on the surface and do not impact the structural integrity of Pds5T. Gel filtration traces are coloured and annotated according to Pds5 variant.

All mutations analysed are located on the surface of Pds5T and do not interfere with protein stability, as judged by size exclusion chromatography (Figure 29). Any impact of these mutations on Scc1 binding is therefore attributable to the perturbation of specific interactions, rather than to any consequent destabilisation of protein folding. Consistent with a previous *in vivo* study (Chan et al., 2013), simultaneous mutation of Scc1$^{V137G/L138G}$ abolished binding of Pds5T (Figure 28b), confirming that the integrity of this hydrophobic interaction is pivotal to their association.

To test whether the newly revealed Pds5–Scc1 interface is essential for cohesin function, we firstly investigated whether mutant versions of Pds5 or Scc1 that perturb the Pds5–Scc1 interaction have any impact on cell viability.

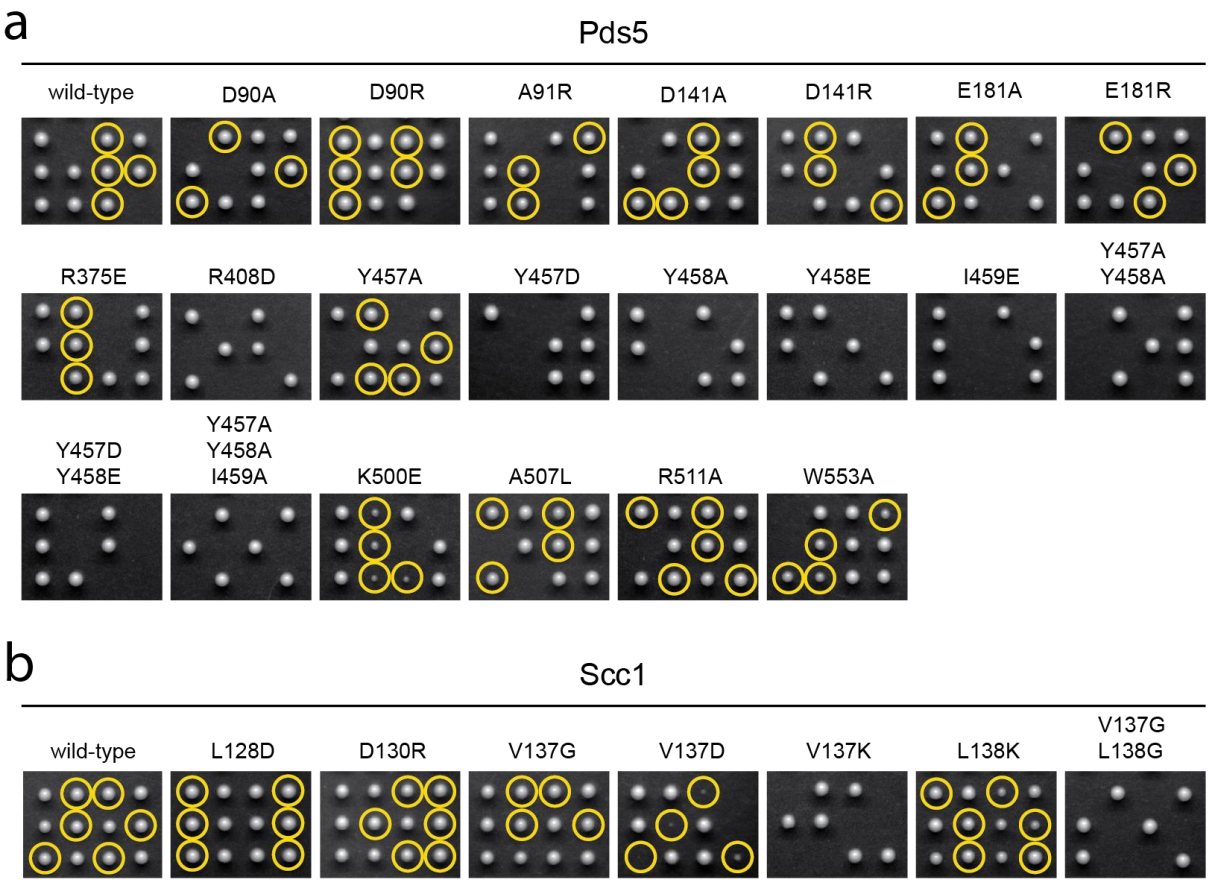

Figure 30 | Complementation analyses of Pds5 and Scc1 mutants. (a) Diploid PDS5/Δpds5 yeast cells expressing an ectopic copy of wild–type or mutant Pds5–PK6 were sporulated, tetrad–dissected, and analysed after 48h at 30°C. Three representative tetrads are shown for each mutant. Cells containing the ectopic copy of Pds5 over Δpds5 are circled. (b) Analysis of wild-type or mutant Scc1-HA_6 as in (a). Due to genetic linkage between the *TRP1* locus, where the ectopic copy of Scc1 integrates, and the endogenous *SCC1* locus, only cells that integrated the ectopic copy of Scc1 on the *Δscc1* chromosome were analysed.

In concordance with the pulldown experiments, mutations in Pds5 that disrupted binding of Pds5T to Smc3Hd–NScc1, including $Pds5^{R408D}$, $Pds5^{Y457D}$, $Pds5^{Y458A}$, $Pds5^{Y458E}$,

Pds5$^{Y458A/Y458A}$, Pds5$^{Y458D/Y458E}$,Pds5^{I459E} (Figure 28a), and the triple mutant Pds5$^{Y458A/Y458A/I495A}$, failed to complement deletion of the essential *PDS5* gene, and resulted in cell death (Figure 30a). Mutations that reduced binding of Pds5T to Smc3Hd–NScc1, including Pds5^{K500E} and Pds5^{W533A} (Figure 28a), confer an impairment in cell growth that is approximately proportionate to the weakening of binding strength observed *in vitro* (Figure 30a).

A lower resolution Pds5T-Scc1 structure features an extension of Scc1 not present in the electron density of the original crystal which reveals that Pds5^{W533} also interacts with Scc1^{L143}, and may provide further explanation for the severity of phenotypes observed for this mutant (Figure 31).

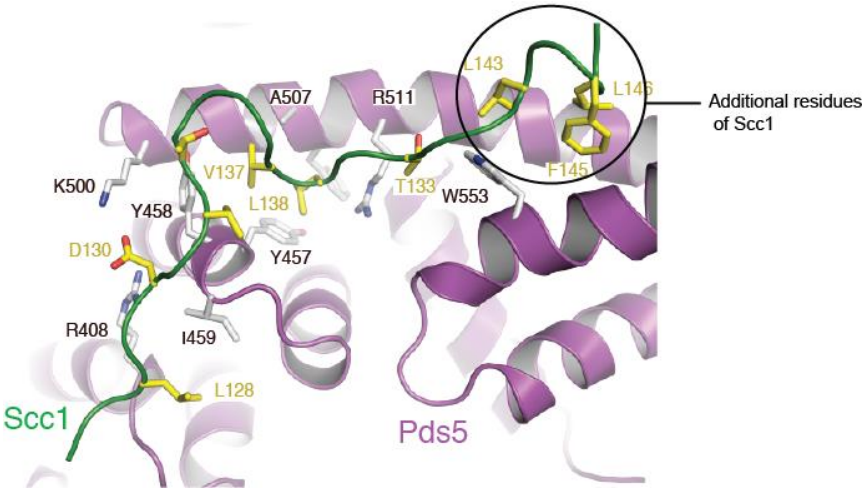

Figure 31 | Structure of Pds5T with extended Scc1. Structure of Pds5T–Scc1 at 3.7 Å reveals a further 4 C–terminal Pds5-interacting residues of Scc1.

Finally, mutations that had little to no discernable influence on the interaction of Pds5T with Smc3Hd–Scc1 *in vitro*, including Pds5^{Y457A}, Pds5^{A507L} and Pds5^{R511A} (Figures 28a and 30a), did not notably alter cell growth.

Conversely, as anticipated, mutations in Scc1 that interfere with Pds5 binding, including Scc1^{V137K} and Scc1$^{V137G/L138G}$ (Figure 30b)(Chan et al., 2013), failed to complement deletion of the essential *SCC1* gene while the individual mutation of these two residues to Scc1^{V137D} and Scc1^{L138K} conferred a considerable reduction in cell growth (Figure 30b). In contrast, neither a single Scc1^{V137G} mutation nor the individual mutation of

neighboring residues, Scc1^{L128D} and Scc1^{D130R}, had any observable impact on cell growth. As all mutant proteins were expressed at equivalent levels to their wild–type counterparts, these results are not a consequence of aberrant protein expression, but instead are specifically attributable to the loss of critical Pds5 and Scc1 functionality (Figure 32).

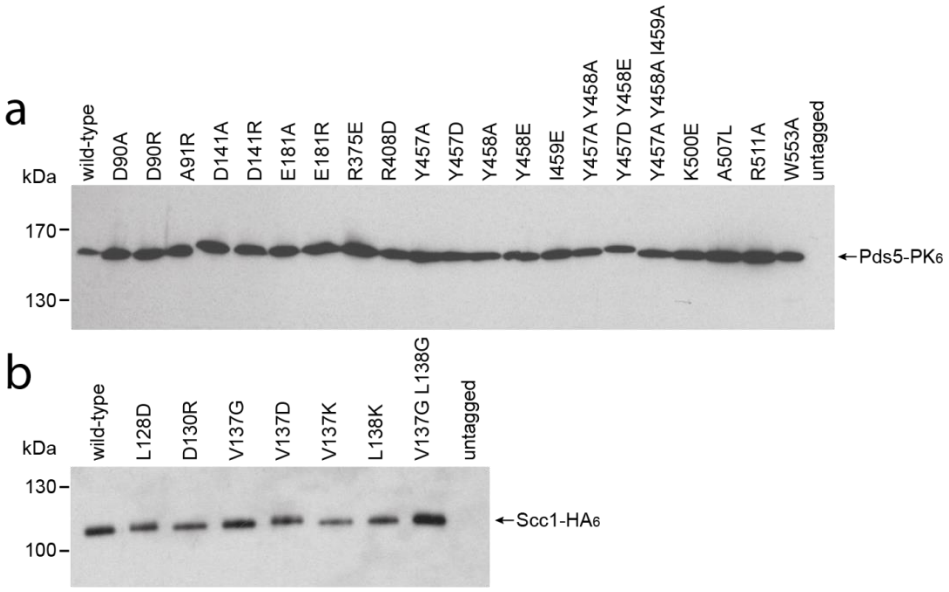

Figure 32 | Expression controls for Pds5 and Scc1 in Yeast. (a) Western blotting of yeast cell extracts (strains C4307-C4328) against the C-terminal PK6 epitope showed that Pds5 mutants were expressed at levels comparable to wild-type Pds5. (b) Western blotting of yeast cell extracts (strains C4329-C4336) against the C-terminal HA6 epitope confirmed that Scc1 mutants were expressed at levels comparable to wild-type Scc1.

We conclude that, as diminished binding affinity observed *in vitro* directly correlates with reduced cell growth, the Pds5–Scc1 interface identified in our crystal structure is a necessary requirement for cohesin function *in vivo*.

To assess the functional importance of the conserved surface spine (Figure 26c), we mutated a series of residues along its length (Pds5$^{D90A\ or\ R}$, Pds5^{A91R}, Pds5^{D141R}, Pds5^{E181R} and Pds5^{R375E}, as shown in Figure 26c). However, despite their high conservation, individual mutations within this spine have no apparent effect on cell growth (Figure 30a).

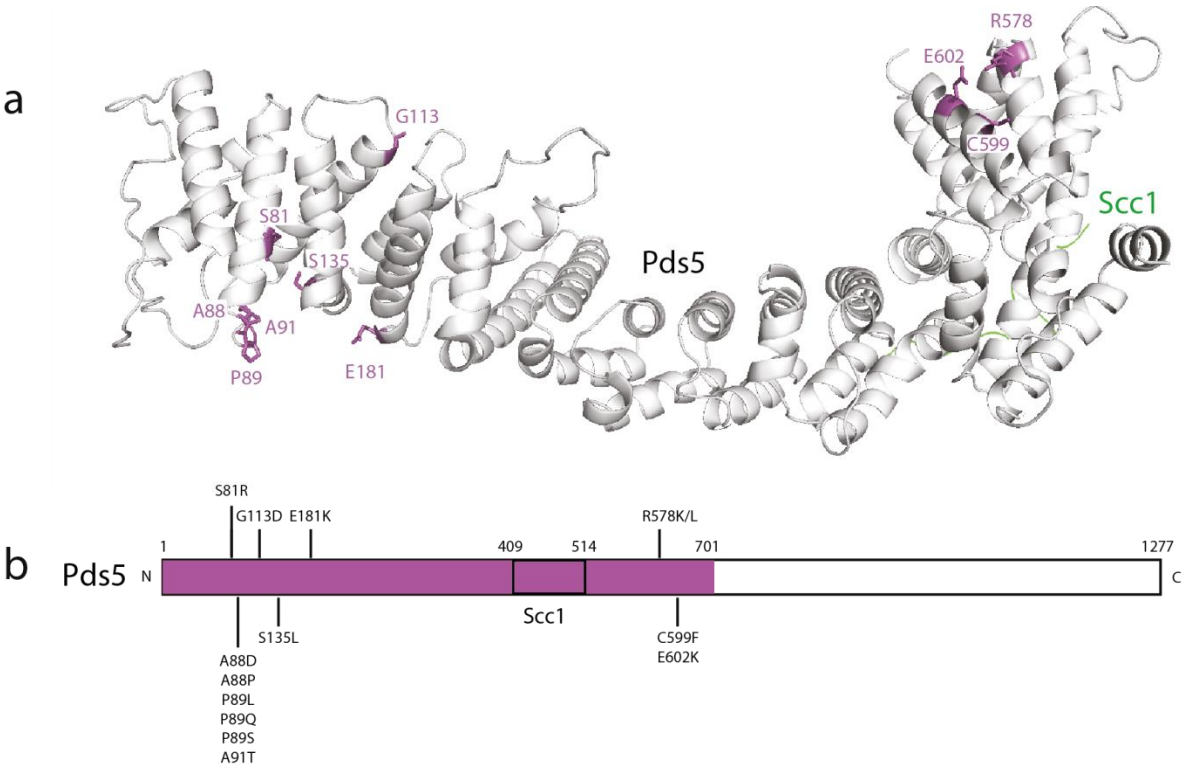

Figure 33 | *Eco1-1* suppressor mutants. (a) *Eco1-1* suppressor mutants mapped onto the Pds5T structure. (b) *Eco1-1* suppressor mutations mapped onto the Pds5 sequence.

Previous reports identified a series of mutations in the N–terminal region of Pds5 which suppress inactivation of the temperature sensitive *eco1-1* allele in yeast (Rowland et al., 2009, Sutani et al., 2009). Of the surface–exposed suppressor mutations the majority, encapsulating Pds5$^{A88D\ or\ P}$, Pds5$^{P89S\ or\ Q\ or\ L}$ and Pds5^{A91T} cluster around the highly conserved Pds5^{D90}, suggesting that the surrounding negatively charged patch might function predominantly in the control of Pds5–mediated cohesin release activity (Figure 33). In contrast, other reported suppressor mutations such as Pds5^{S81R}, Pds5^{G113D} and Pds5^{S135L}, are likely to disrupt stable packing of local HEAT-repeats, as they affect buried residues. Suppressor mutations have also been reported in residues Pds5^{R578}, Pds5^{C599} and Pds5^{E602} (Rowland et al., 2009, Sutani et al., 2009). As Pds5^{R578} forms a salt–bridge with Pds5^{E602} to stabilize association of two α- helices, it is probable that mutation of these residues would also lead to local structural perturbation of Pds5. The mechanistic basis for how such mutations might rescue inactivation of the temperature

sensitive *eco1-1* allele remains unclear, however the observation that a large fraction of suppressor mutants are situated within or close to the conserved surface of Pds5 suggests that these elements of Pds5 might somehow function in regulating cohesin release.

3.4.4. Pds5-Scc1 interface mutants are defective in sister chromatid cohesion

As Pds5 is an essential component of the cohesin complex, we expected that disruption of the Pds5–Scc1 interaction would result defective sister chromatid cohesion. Hence, we first investigated whether mutations in Pds5 that disrupt the interaction with Scc1 *in vitro* also do so within the context of the native yeast cohesin complex.

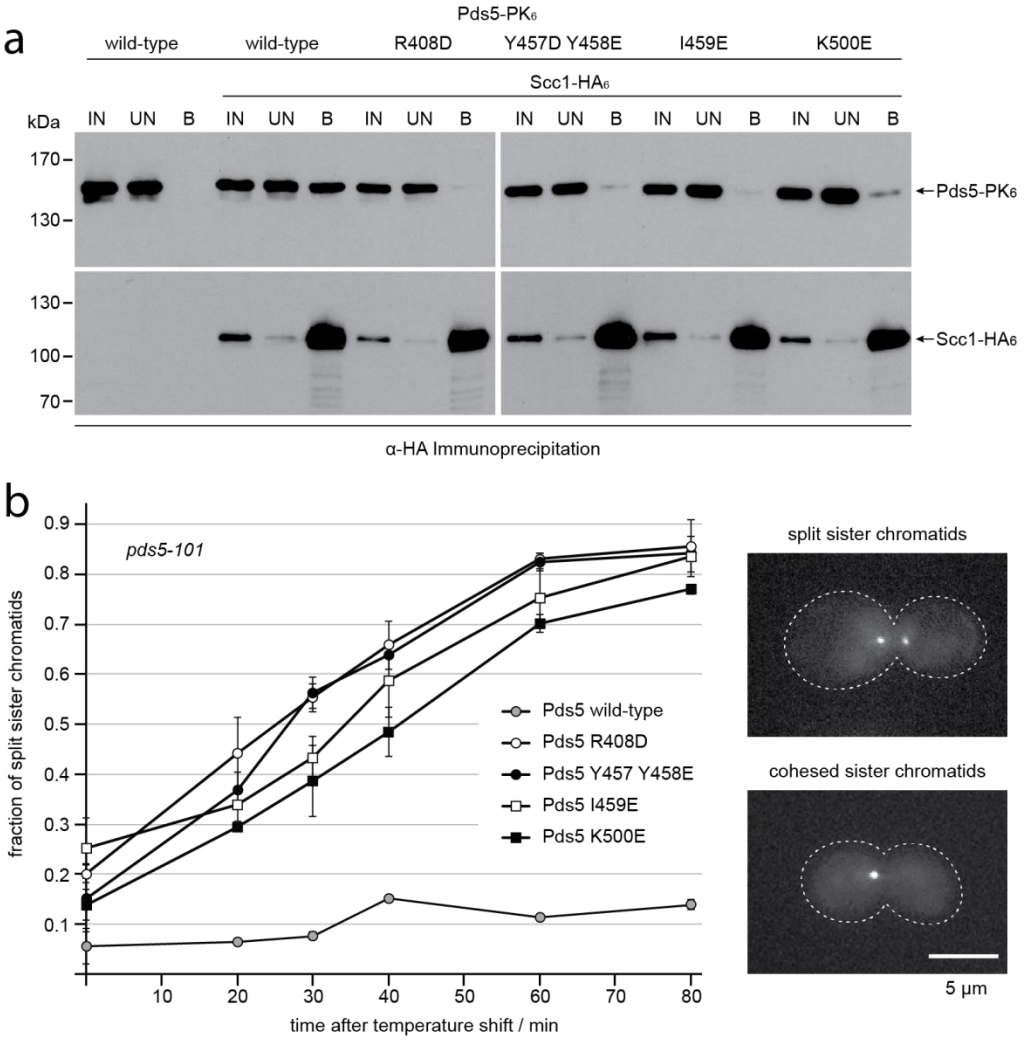

Figure 34 | Cohesin binding mutants of Pds5 fail to maintain sister chromatid cohesion. (a) Co-immunoprecipitation of Scc1–HA_6 from whole cell extracts of asynchronous yeast cultures expressing ectopic copies of the indicated Pds5–PK_6 variants (wild-type, and mutants) IN (input), UN (unbound) and B (bound, 17× relative to input for Pds5, 42.5× for Scc1) fractions. (b) Sister chromatid cohesion was assayed in cells expressing wild–type or mutant Pds5–PK6 in a pds5–101 temperature–sensitive background. Cells were arrested in metaphase by Cdc20 depletion, shifted to the restrictive temperature and released. The fraction of cells with split sister chromatids at time points after shifting to the restrictive temperature was determined for >100 cells per time point and strain. Mean values (±max/min) of two independent repeats per mutant are plotted.

Co–immunoprecipitation of Pds5 mutants that affect the salt–bridge ($Pds5^{R408D}$, $Pds5^{K500E}$) and hydrophobic interactions ($Pds5^{Y457D/Y458E}$, $Pds5^{I459E}$) with HA–tagged Scc1 produced phenotypes consistent with the *in vitro* pull–down assays (Figure 34a). Whereas $Pds5^{R408D}$, $Pds5^{Y457D,458E}$ and $Pds5^{I459}$ abolished any appreciable association of Pds5 with cohesin in this assay, $Pds5^{K500E}$ retained a modest capacity to bind cohesin. As disruption of single residues in the Pds5-Scc1 interface appears to be sufficient to abolish Pds5 recruitment in the context of the yeast holocomplex *in vivo* and in the context of the Smc3Hd-NScc1 complex *in vitro,* we are led to conclude that robust interactions between Pds5 and cohesin appear to be exclusively mediated through the Pds5-Scc1 interface described in our structure. Our experiments therefore suggest that this interface is necessary and sufficient for Pds5 recruitment to cohesin

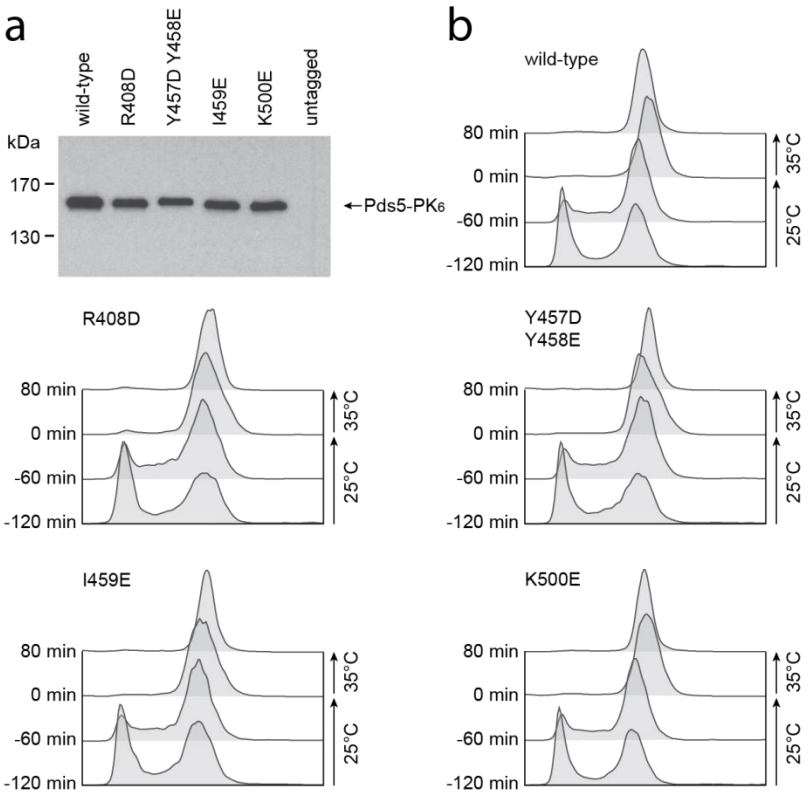

Figure 35 | Pds5 expression and cell cycle arrest. (a) Western blotting of whole cell extracts against a C-terminal PK6 tag showed comparable expression levels between of wild–type and mutant Pds5 proteins (strains C4381-C4385). (b) FACScan analysis of DNA content of yeast cells (as in (a)) that were arrested by Cdc20 depletion at the permissive temperature of 25°C, and released from arrest at the restrictive temperature of 35°C. Indicated time points are relative to the time of release (t = 0).

In order to investigate the influence of Pds5 mutations on sister chromatid cohesion, we expressed Pds5 variants, including the wild–type and interface mutants, from an ectopic copy in a *pds5–101* temperature–sensitive strain and evaluated the competence of these cells to maintain cohesion (Figure 34a) (Panizza et al., 2000). It is important to note that this strain expresses tetracycline repressor–GFP fusions which bind to multiple tandem *tet* operators inserted in the *URA3* locus (Michaelis et al., 1997) and enable visualisation of inter-sister distances close to the centromere. Thus levels of sister chromatid cohesion in these cells can be monitored by wide-field microscopy. We arrested cells containing wild–type or interface mutant Pds5 in metaphase by depletion

of Cdc20, which otherwise permits cell cycle progression by activating the anaphase promoting complex (Figures 34b & 35b) and then inactivated *pds5-101* by shifting cells to the restrictive temperature(Panizza et al., 2000). Whereas cells expressing ectopic copies of wild–type Pds5 retained sister chromatid cohesion, cells that expressed any of the mutant Pds5 versions rapidly lost cohesion, as was apparent by the appearance of 'split' GFP spots (Figure 34b). Notably, loss of cohesion was slightly less severe for the $Pds5^{K500E}$ mutant, which maintains residual viability and binding to Scc1, compared to $Pds5^{R408D}$, $Pds5^{Y457D/Y458E}$ and $Pds5^{I459E}$, which fail entirely to bind Scc1. These phenotypes are clearly attributable to the mutation of specific Pds5 residues, as expression levels of wild–type and mutant Pds5 do not detectably differ (Figure 35a). Collectively, these data demonstrate that the inviability of Pds5–Scc1 interface mutants arises from the inability of the mutant Pds5 proteins to interact with cohesin, and their consequent failure to functionally contribute to sister chromatid cohesion. We therefore conclude that the interface described in the Pds5–Scc1 crystal structure is fundamental to Pds5 recruitment to cohesin *in vivo* and is thus essential for the correct execution of sister chromatid cohesion.

3.4.5. A structural model of the Pds5-Smc3-Scc1 complex

Multiple roles have been ascribed to Pds5 in the regulation of the cohesin complex. In addition to promoting cohesion, Pds5 also participates in the removal of cohesin from chromatin, apparently by interacting with the dissociation factor Wapl (Losada et al., 2005, Kueng et al., 2006, Rowland et al., 2009, Shintomi and Hirano, 2009, Sutani et al., 2009, Nishiyama et al., 2010, Chan et al., 2012). Acetylation of $Smc3^{K112/K113}$ by Eco1 is a key determinant of sister chromatid cohesion, and is thought to interfere with this cohesin release function of Pds5 (Rowland et al., 2009, Chan et al., 2012). Our structure shows that Pds5 binds in close proximity to the Smc3-Scc1 interface (Figure 24e), therefore it is possible that Pds5 might somehow monitor the acetylation status of cohesin and regulate opening or closure of the ring by directly engaging the Smc3–Scc1 interface (Chan et al., 2012).

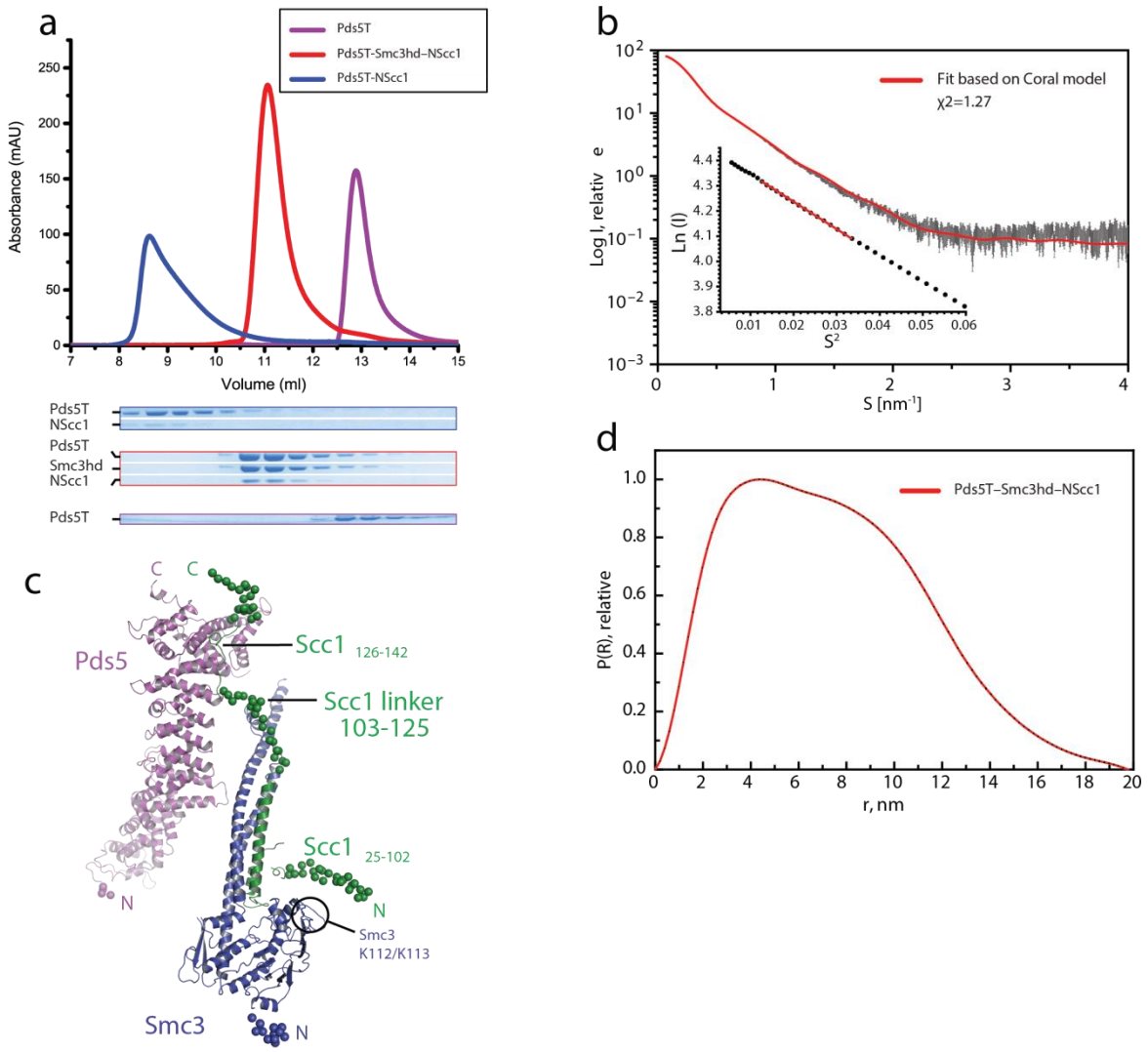

Figure 36 | SAXS analysis of the Pds5T-Smc3hd-NScc1 complex. (a) Size–exclusion chromatography profiles for Pds5T, Pds5T–NScc1 and the Pds5T– Smc3Hd–NScc1 complex. Fractions from each run were analysed by SDS–PAGE. Coomassie stained bands corresponding to each protein are indicated. Gels were cropped to show the relevant sections. (b) Experimental SAXS profile (log intensities calculated as a function of momentum transfer) for the Pds5T– Smc3Hd–NScc1 complex is shown (black) and the fitted curve (red) obtained using CORAL. The Guinier region is inset. Points 10–25 were used for analysis and showed an s*Rg = 1.06 (values < 1.3 indicate good quality data). (c) Structural model of the Pds5T– Smc3Hd–NScc1 complex generated from SAXS data. Pds5 (magenta), Smc3 (blue), Scc1 (green). Unstructured amino acid residues are displayed as dummy atoms. The region of Smc3

containing the residues K112/K113 acetylated by Eco1 are highlighted. (d) Distance distribution function.

To investigate this possibility, we isolated a ternary complex comprised of Pds5T–Smc3Hd–NScc1 (Figure 36a), and sought to characterize this assembly in solution by small angle X–ray scattering (SAXS; Figure 36b-d).

To reduce confounding inter–particle interference and aggregation effects, we collected scattering data using an in–line size exclusion chromatography system (Pernot et al., 2013). The scattering profile showed no aggregation and a linear Guinier range, indicative of well–behaved, monodisperse sample (Figure 36b and inset). From these data, we obtained a radius of gyration (R_g) of 56 ± 0.5Å. The distance distribution function p(r) displayed a skewed shape characteristic for elongated particles with a maximum diameter (D_{max}) of 198 ± 10Å (Figure 37d). As structural models for almost the entire complex except the Scc1$^{103–125}$ linker were available, we evaluated the scattering curves by rigid body modeling using the atomic models for Smc3Hd–Scc1$^{1–102}$ and Pds5T–Scc1$^{126–142}$ and modeled the missing amino acid residues, including the Scc1$^{103–125}$ linker, using Coral (Petoukhov et al., 2012). The resultant model of the ternary complex conforms very well (χ^2= 1.27) to the SAXS data (Figure 37b) While we cannot exclude that other missing parts of the proteins engage in direct interactions, the model suggests at least a limited degree of conformational flexibility. In agreement with biochemical and cell biological analyses demonstrating that Pds5 is recruited to cohesin exclusively through Scc1, these data reveal that the conserved surface of Pds5T does not stably engage the Smc3Hd domain (Figure 36c).

Discussion

Résumé en français

La structure de Pds5 avec une résolution quasi atomique, dans un complexe avec son partenaire de liaison Scc1, sera d'une grande importance pour révéler les événements moléculaires qui se produisent lors de l'entrée de l'ADN et la sortie des anneaux de cohésine. Bien que les mécanismes exacts de l'ouverture du portail restent flous, nos expériences avec des préparations de protéines, structurellement et biophysiquement bien caractérisés, excluent la proposition que Pds5 recrute simplement Wapl pour dégager l'interface Smc3-Scc1. Nous avons identifié des éléments conservés sur la surface de Pds5 qui sont en corrélation étroite avec les positions des mutants suppresseurs qui sont sensés empêcher l'ouverture des anneaux de cohésine en l'absence de l'acétylation de Smc3. Ces caractéristiques pourraient donc permettre à Pds5 de coopérer avec d'autres facteurs. Ainsi, cette nouvelle structure offre un jalon important pour la poursuite de la dissection du rôle que Pds5 pourrait jouer dans la fonction avec la cohésine. En résumé, ce travail donne un aperçu détaillé structurellement dans la fonction Pds5 ainsi que Scc1 et établit un cadre pour étudier plus précisément les détails moléculaires dans la façon dont Pds5 coopère avec d'autres facteurs pour exécuter la régulation dynamique de l'ouverture du cercle de cohésine. La structure de Pds5-Scc1, ainsi que des structures précédemment publiées d'autres sous-unités de cohésine, permettra maintenant de progresser dans la compréhension des questions mécanistes qui peuvent être abordées. Cela se traduira, à terme, par un modèle moléculaire détaillée de la fonction et la régulation de la famille des cohésines.

At the inception of this thesis, structural and biochemical information pertaining to the cohesin complex and its regulation was extremely limited. However, the field has advanced at an impressive pace. All three heterotypic interfaces of the core cohesin ring have now been described in molecular detail, and are strongly in support of the notion that this complex functions as a large ring to entrap DNA. Concurrent cell biological evidence arose to implicate the opening and closure of the Smc3-Scc1 interface as being central to the regulation of dynamic and cohesive populations of cohesin.

In parallel, the structures of Scc3 bound to Scc1, and of the WaplC domain in isolation have advanced our understanding of how the stability of cohesin on chromatin might be regulated by revealing the nature of their conserved functional surfaces. Finally, the partial structure of the Scc2-Scc4 loader complex has lent insight into how cohesin is targeted to chromatin.

Thus the work presented in this thesis consequently completes this complement of, at least partial, structural information corresponding to regulators of cohesin.

Pds5 is a highly conserved regulator of cohesin function that has multiple roles in sister chromatid cohesion. Paradoxically, Pds5 not only participates in the establishment and maintenance of cohesion, but also collaborates with Wapl and Scc3 to promote the release of cohesin from chromatin in (Panizza et al., 2000, Hartman et al., 2000, Vaur et al., 2012). To advance our understanding of the multiple functions associated with Pds5, we have determined the structure of Pds5 in complex with a fragment of Scc1. Our structure comprises a large N–terminal fragment of Pds5, including regions that have been previously shown to be critical for Pds5 function (Sutani et al., 2009, Rowland et al., 2009) and a segment of Scc1 that is required for the interaction of Pds5 with cohesin (Chan et al., 2013). Through a series of biochemical and *in vivo* experiments, we found that the disruption of key features of the Pds5–Scc1 interface revealed by the structure abolishes Pds5 recruitment to cohesin. We further establish that the minimal Pds5–Scc1 interface is necessary and sufficient for the interaction between the two proteins, and is critical for sister chromatid cohesion, as its disruption

cannot be rescued by other components of the cohesin apparatus.

4.1. A Conserved Interaction Surface Mediates Pds5 Recruitment to Cohesin

Whereas the requirement for Pds5 in sister chromatid cohesion is well established, it has remained controversial in which stages of the cohesin cycle it participates. Early experiments pointed towards a model in which Pds5 is uniquely required for maintenance of cohesion, but not its establishment (Hartman et al., 2000, Stead et al., 2003). Initial observations suggested that the interaction of Pds5 with human cohesin is salt sensitive, thus it was proposed that Pds5 might therefore constitute a transiently bound regulatory factor, rather than a *bona fide* cohesin subunit (Sumara et al., 2000, Losada et al., 2005, Kueng et al., 2006, Gandhi et al., 2006) However, it was recently reported that Pds5 both promotes Smc3 acetylation and antagonizes its deacetylation, and thereby contributes to the establishment and maintenance of cohesion (Chan et al., 2013, Vaur et al., 2012).

Furthermore, as the simultaneous deletion of both Pds5 isoforms in mice is lethal, it is highly likely that Pds5 function is also essential in vertebrates (Carretero et al., 2013). Therefore, there is an increasing body of evidence to suggest that, from yeast to humans, Pds5, like the other cohesin core components, is essential to both establishment and maintenance of cohesion (Panizza et al., 2000, Hartman et al., 2000, Losada et al., 2005, Vaur et al., 2012, Carretero et al., 2013).

We observed a strong correlation between the strength of the Pds5–Scc1 interaction, cell viability and sister chromatid cohesion. Mutations such as $Pds5^{K500E}$ and $Pds5^{W533A}$, which reduced but did not fully abolish binding, led to considerably reduced cell growth. Whilst our cohesion assay specifically addresses maintenance, but not establishment, of cohesion, the direct correlation between binding strength, cell viability and sister chromatid cohesion reported in this study, leads us to propose that Pds5 is an integral cohesin subunit. As the Pds5–Scc1 complex investigated herein remains associated under stringent conditions, we conclude that Pds5, in all probability, is continuously and stoichiometrically bound to the cohesin complex throughout the cell cycle. We therefore

suggest that Pds5, like Scc3, should be considered a core subunit of the cohesin complex rather than a mere regulator of its function.

The Pds5–Scc1 interface is highly conserved across diverse eukaryotes. We would suggest therefore that the mechanism of recruitment we describe here is a general and necessary feature of cohesin function in all organisms containing Pds5. Differences in phenotypes observed upon disruption of Pds5 in *Schizosaccharomyces pombe* might reflect divergent modes of cohesion establishment and maintenance in this organism, as experimentally extended arrest of such cells in G2/M induces sister chromatid separation and cell death (Tanaka et al., 2001, Vaur et al., 2012).

4.2. Role of Pds5 in Regulating the Smc3-Scc1 Interface

Not only does Pds5 contribute to the establishment and maintenance of cohesion, conversely, Pds5 also controls the release of cohesin from chromatin in collaboration with Wapl and Scc3 (Sutani et al., 2009, Rowland et al., 2009, Gandhi et al., 2006, Shintomi and Hirano, 2009, Chan et al., 2013). As Pds5 binds in close proximity to the Smc3Hd, one might envision that it could control Smc3 acetylation, and thus the stable closure of the cohesin ring, by binding directly to the region surrounding Smc3$^{K112/113}$.

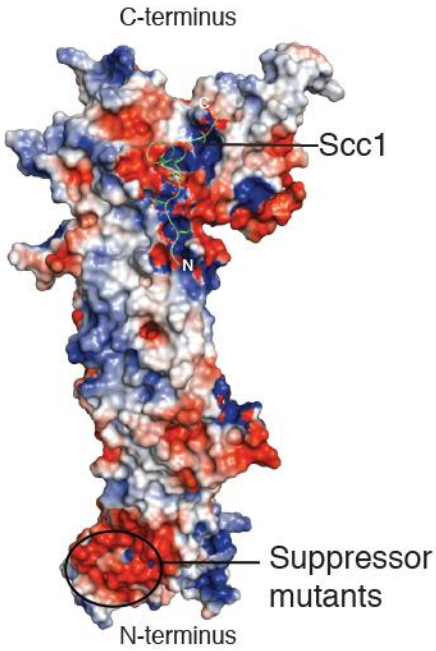

Figure 37 | Electrostatic surface potential of Pds5. Regions of positive and negative electrostatic potential are shown in blue and red from +3 to -3 V calculated with APBS and rendered using Pymol. The acidic patch showing the region where suppressor mutants are localised is indicated.

Calculation of the electrostatic surface potential shows that the conserved N–terminal region of Pds5 is highly negatively charged (Figure 38). It is therefore conceivable that this region of Pds5 monitors the lysine acetylation status of Smc3Hd. However, we found no evidence that Pds5 binds directly to the Smc3Hd while also bound to Scc1, and ablation of key residues on Pds5 and Scc1 alone is sufficient to preclude assembly of this ternary complex *in vitro* and *in vivo*. The SAXS data further suggest that, at least in the absence of acetylation, Pds5 is directed away from and does not engage the Smc3Hd directly.

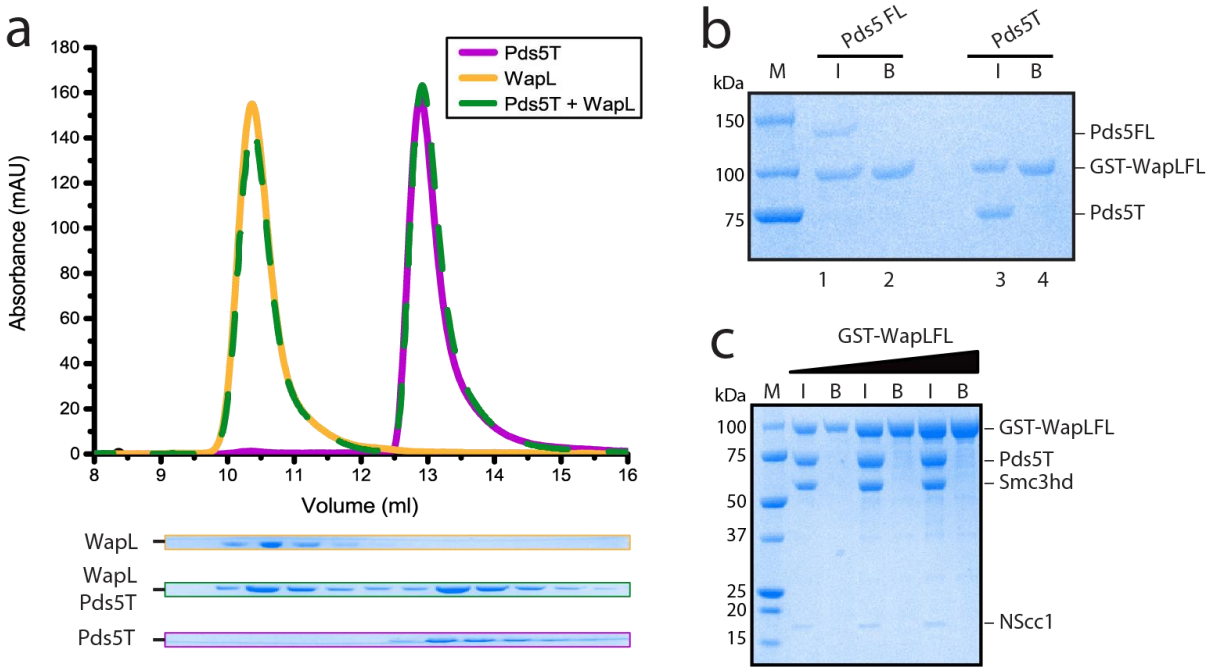

Figure 38 | Biochemical analysis of Wapl binding. (a) Size exclusion chromatography showing that full-length monodisperse Wapl does not interact directly with Pds5T. Below: samples from fractions across the chromatograms were analysed by SDS-PAGE. (b) Wapl does

not interact with full-length Pds5 or Pds5T. SDS-PAGE gel showing a pulldown of Pds5 full-length (lanes 1+2) or Pds5T (lanes 3+4) by full-length GST-Wapl. (c) Wapl does not interact with the ternary Pds5T-Smc3hd-NScc1 complex. SDS-PAGE gel showing a pulldown of the Pds5T-Smc3hd-NScc1 ternary complex with increasing amounts of full-length GST-Wapl. I (Input), B (Bound), (M) Marker.

Several studies have shown that Wapl directly interacts with Pds5 to execute the removal of cohesin from chromatin (Sutani et al., 2009, Rowland et al., 2009, Shintomi and Hirano, 2009). Such an interaction was proposed to occur through the conserved N–terminal domain of Pds5, as suppressor mutations in this region abolish co-localisation of Wapl and Cohesin *in vivo* (Chan et al., 2012). Hence, one possibility might be that the N terminus of Pds5 positions Wapl in the vicinity of the Smc3–Scc1 interface. However, we were not able to isolate a stable complex between Wapl and Pds5T or full–length Pds5 using biochemically well–defined protein preparations (Figure 38a, b), nor could we detect persistent interactions between Wapl and the Pds5T–Smc3Hd–NScc1 complex (Figure 38c).

A preponderance of evidence exists to suggest that the binding of Wapl to cohesin is likely a highly co–operative event, and so the finding that Pds5 does not directly interact with Wapl in our *in vitro* assay is not altogether irreconcilable with the notion that they might still interact functionally *in vivo*, yet the nature of their collaboration remains elusive (Huis in 't Veld et al., 2014, Hara et al., 2014, Ouyang et al., 2013, Gandhi et al., 2006, Shintomi and Hirano, 2009, Kueng et al., 2006).

The structure reveals that Pds5 contains a highly conserved and almost continuous surface spine that extends from the N terminus of Pds5 towards the Scc1 binding region. The positions of conserved surface residues along this spine correlate with those of *eco1-1* suppressor mutants, and are particularly enriched in a highly negative patch located in the Pds5 N terminus (Figures 33 & 37) (Chan et al., 2012, Sutani et al., 2009). Hence, it is possible that this patch might contribute to the efficient

disengagement of cohesin from chromatin by Pds5, in cooperation with other release factors such as Wapl. As deletion of Wapl alone is not sufficient to cause inviability in budding yeast, this may offer an explanation as to why alteration of this conserved spine does not impair cell growth (Chan et al., 2013, Lopez-Serra et al., 2013, Rowland et al., 2009, Sutani et al., 2009).

In metazoans, Pds5 is universally conserved and may act, through the conserved spine, as a crucial and indispensable regulator of the dynamic cellular population of cohesin and its higher–order transactions with chromatin (Haarhuis et al., 2013, Haarhuis et al., 2014, Yan et al., 2013). As Pds5 alone is not able to disengage Smc3 and Scc1, it is likely that this function, appropriately, is restricted to a very specific context in the cell and may depend on additional factors and biochemical events, such as Wapl and ATP hydrolysis. Indeed, it could be that the function of Sororin, a Pds5-binding metazoan cohesion factor, might be to confer an enhancement to cohesion by restricting access to this 'releasing' patch on Pds5, until it is required to participate in cohesin release during prophase, however this possibility remains to be investigated (Nishiyama et al., 2010, Nishiyama et al., 2013a).

4.2. The Structural Basis of Pds5 Function and its Recruitment to Cohesin

In agreement with previously published data showing that Pds5 colocalises and turns over with core cohesin components, and participates in the key functional steps of cohesion establishment and maintenance, we found that the specific abrogation of recruitment of Pds5 to cohesin results in a dramatic failure to maintain sister chromatid cohesion (Panizza et al., 2000, Hartman et al., 2000, Losada et al., 2005, Vaur et al., 2012, Carretero et al., 2013). Our work demonstrates Pds5 is physically positioned to act as a critical bifunctional regulator of the closure of the ring at the Smc3–Scc1 interface, and therefore of the stable establishment and maintenance of cohesion and, conversely, the dynamic release of cohesin. Moreover, the finding that cell survival and

cohesion maintenance correlate linearly with the extent to which the Pds5-Scc1 interface is disrupted, in support of prior literature (Chan et al., 2013), provides further evidence that Pds5, where conserved, is a constitutive subunit of the cohesin complex.

Future studies will be required to address at a mechanistic level how Pds5 might coordinate the transition between the opening and stable closure of the Smc3–Scc1 interface, and how these mechanisms might in turn facilitate different functions of the cohesin complex.

4.3. A cohesin releasing function at the Smc3-Scc1 interface: a revised view of the non-SMC protein interaction network

Whilst a cohesin release complex is convenient conceptual model, the nature of such an assembly has remained elusive. The results reported here, in addition to prior reports, suggest that it is unlikely to exist as a distinct, individual macromolecular complex, but instead may be an emergent property of the concerted, and perhaps ephemeral, actions of several factors (Chan et al., 2012, Hara et al., 2014, Huis in 't Veld et al., 2014, Losada et al., 2005, Nishiyama et al., 2013a, Ouyang et al., 2013, Rowland et al., 2009, Shintomi and Hirano, 2009).

Full-length Pds5, Scc3, and Wapl are intractable targets for isolation from *E.Coli.* Optimisation of these protocols for Pds5 and Wapl led to preparations which were highly pure, but wherein the proteins still do not migrate on size-exclusion in a manner consistent with their predicted molecular masses, implying that they harbour some degree of disorder (figure 14). Therefore, considerable effort was invested into defining and isolating elements of Scc3 and Pds5 more conducive to rigorous biochemical characterisation. Subsequently, both a Scc3 core construct, relatively easily identified through truncation of N- and C-terminal disorder, and an extended truncation of Pds5, which required more involved protein biochemistry and mass-spectroscopy, and ultimately led to structure solution, were determined (figures 15-17, 23). As reported in the literature, these constructs both encompass sequence elements to which Wapl binding has been attributed (Chan et al., 2012, Roig et al., 2014, Sutani et al., 2009).

However, despite their well-established functional relationships in the cell, we did not find any evidence in favour of a direct, robust association between Wapl and its purported functional partners (figures 20, 21, 38). Considerable inconsistencies and ambiguities between *in vitro* and *in vivo* experiments persist and obfuscate our imperfect grasp of these processes. Moreover, current models of the yeast system are predicated on biochemical studies with proteins that do not behave as well-ordered globular assemblies and so must be interpreted with caution.

It is probable that Pds5 and Scc3 each individually co-ordinate specific aspects of cohesin regulation, and that these functions are in turn potentially modulated by transient interactions with Wapl, which shuttles between different cohesin complexes (Chan et al., 2012, Hara et al., 2014, Ouyang et al., 2013, Rowland et al., 2009). Wapl has additionally been proposed to interact directly with the Smc3hd domain, however this result has thus far not proven reproducible (figure 20) (Chatterjee et al., 2013, Ouyang et al., 2013). Furthermore, the mode of Wapl binding to Smc3 proposed by a peptide co-crystal structure was confounded somewhat by the recent discovery that this direct mode of association is irreconcilable with the structure of the globular Smc3 head (Chatterjee et al., 2013, Gligoris et al., 2014).

Fusion of the Smc3-Scc1 interface antagonises Wapl function, hence it is possible that the accessibility of NScc1 and its engagement by Wapl is a key determinant of whether Cohesin is released from DNA (Eichinger et al., 2013, Buheitel and Stemmann, 2013, Chan et al., 2012). However, we did not observe any interaction *in vitro* between Wapl and NScc1-Pds5T, nor between Wapl and Smc3hd, implying that, if they do associate under less stringent conditions than those investigated herein, the strength of any such subcomplexes is probably too weak for Wapl to plausibly compete Scc1 from Smc3 (figures 20 & 38). Hence, release appears unlikely to occur via direct displacement of Smc3 from NScc1 by Wapl. The biological logic to disfavour such a mechanism is obvious, as this would effectively generate constitutively unstable Cohesin complexes, unable to support cohesion in a manner perhaps comparable to those with weakened exit gates (Huis in 't Veld et al., 2014).

Yet, the mutation of select surface residues, which would not obviously lead to structural perturbation, in Pds5, Scc3, and Smc3 reduces turnover of the cohesin complex in Eco1 deficient cells, so evidently these factors do partake in an intrinsic release pathway (Chan et al., 2012). Notably, supplementation of Pds5 or Wapl depleted extracts with recombinantly expressed Pds5 and Wapl is sufficient to permit sister chromatid resolution, indicating that they may cooperate in the same process (Losada et al., 2005). The aneuploidy which arises from Pds5 isoform deletion in mice, and Wapl depletion in humans may thus arise from the abolition of a single releasing function in which both participate (Carretero et al., 2013, Haarhuis et al., 2013). In Humans, and in Mice, Wapl is an indispensable regulator of genome architecture, thus, if release does indeed depend on Pds5, one would anticipate that it too must be involved in controlling the topology of our genome (Tedeschi et al., 2013, Haarhuis et al., 2013).

If Wapl does indeed engage Pds5 and Scc3 simultaneously, it is tempting to speculate that, since these factors are situated at opposite sides of Scc1, release function might somehow entail a contraction of the cohesin complex which brings the heads into close proximity to promote ATP hydrolysis. However, it is difficult to envisage how such a process might occur in the absence of stable Wapl-Pds5-Scc3 interactions.

As ATP hydrolysis has been shown to provide sufficient energy to disengage kleisin proteins from a bacterial SMC complex (Woo et al., 2009), cohesin might exploit a similar mechanism. However a recent study revealed that ATP hydrolysis alone does not appear to be sufficient to drive dissociation of cohesin from circular DNA, and so it could be that the function of these release factors is to translate energy from ATPase activity into ring opening (Camdere et al., 2015). Accordingly then, Pds5-Scc3-Wapl, in a manner analogous to the mechanism by which Scc2-4 is proposed to drive opening of the hinges for the initial entrapment of DNA (Hinshaw et al., 2015, Chao et al., 2015, Murayama and Uhlmann, 2014, Hu et al., 2011, Arumugam et al., 2003, Weitzer et al., 2003), might be required to transmit the conformational changes resulting from ATP hydrolysis to achieve transient opening of the Smc3-Scc1 interface. Direction of functional outcomes of ATP hydrolysis by associated non-SMC subunits might then be

a general principle of eukaryotic SMC complexes (Arumugam et al., 2003, Chao et al., 2015, Piazza et al., 2014).

4.4. Toward a molecular model for sister chromatid cohesion

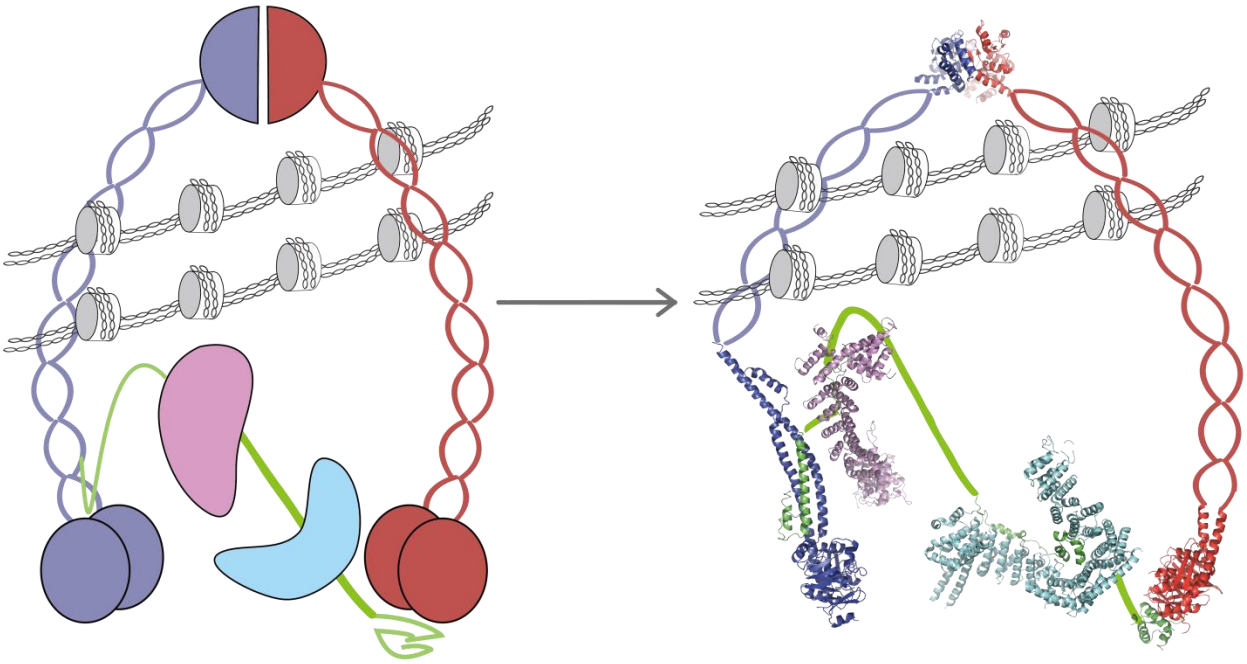

Figure 39 | Toward a molecular model of the cohesin complex. Schematic illustration of cohesin (left). Hypothetical model of the cohesin complex using existing structural information (right) with absent sections rendered as cartoons. Smc1-Scc1 (red and green; 1W1W); Smc3-Smc1 hinge complex (blue and red; 2WD5); Scc3-Scc1 (aquamarine and green; 4PJW); Smc3-Scc1 (blue and green; 4UX3); Pds5-Scc1 (violet and green; this study).

Whereas the identification of acetylated lysines on the ATPase head of Smc3 suggested that this modification might function as a direct switch to modulate the ATPase activity of cohesin, experimental evidence suggests that this modification does not detectably influence ATP hydrolysis of the Smc3-Smc1-Scc1 trimer in isolation (Ladurner et al., 2014). Instead, the converse is true: ATPase activity is actually

required for acetylation. In Metazoans, acetylation is essential yet not sufficient for the establishment of sister chromatid cohesion, given the additional requirement for Sororin. Thus it is entirely possible that Smc3 acetylation in itself may simply be a signalling event to indicate that such cohesin complexes have fulfilled loading and should be retained on DNA to participate in cohesion.

The Smc3hd only weakly stimulates ATP hydrolysis by Smc1 (Arumugam et al., 2006), thus it also remains to be seen whether Pds5, Scc3, or Wapl can enhance this function, in a manner comparable to the enhancement in ATP hydrolysis conferred to the condensin complex by its non-SMC subunits upon binding DNA (Piazza et al., 2014). The short residence time of Wapl on cohesin, along with the lack of interactions reported in this thesis disfavour any mechanism of release which requires a stable Pds5-Wapl assembly; however they do not exclude a transient, catalytic mode of cohesin disjuncture. Thus, in such a system, Pds5, Scc3 and Scc1 might collectively constitute a composite non-SMC subunit receptor for Wapl, which would in turn provide the stimulus for ATPase activity of the SMC heads. The function of acetylation then may be to further weaken the association of Wapl by masking a prospective binding surface on the Smc3 head, and so reduce the probability of ATP hydrolysis. In its essence, the most basic model of sister chromatid cohesion may simply entail the enrichment of cohesin on chromatin. In agreement with this prediction, a number of eukaryotic organisms, in fact lack the acetyltransferase whilst retaining the other non-SMC proteins including Pds5 and Wapl, and presumably are able to attain sufficient cohesion through stochastic processes (Peters and Nishiyama, 2012). However it is clear that from yeast to humans, efficient sister chromatid cohesion is achieved through the post-translational control of cohesion-associated regulatory factors (Ben-Shahar et al., 2008, Carretero et al., 2013, Chan et al., 2013, Hara et al., 2014, Hauf et al., 2005, Hou and Zou, 2005, Kitajima et al., 2005, Kitajima et al., 2006, Liu et al., 2013b, Nishiyama et al., 2013a, Unal et al., 2008, Waizenegger et al., 2000, Zhang et al., 2008).

Stable establishment of cohesion from yeast to humans may thus simply be conferred by rendering a subset of cohesin complexes insensate to release stimuli such as Wapl.

Moreover, that the prophase pathway should be so heavily reliant on mitotic kinases for its execution, and that centromeric cohesin might escape this process through recruitment of a phosphatase, is rather indicative of the existence of a signalling network which controls cohesion through the regulation of a putative, latent release function.

Establishment, maintenance and prophase dissolution of cohesion may therefore operate under the same principle: the control of functional surfaces in the cohesin complex through their post-translational modification. Whether these post-translational modifications then induce conformational changes in cohesin or are predicated upon them remains an open question.

Perhaps one of the most exciting elements of cohesin research is that these questions are not just conceptual challenges: they also represent significant technical challenges. Cohesin, as determined by electron microscopy, has an innate propensity toward conformational pleiotropy that, whilst presumably central to its function, considerably confounds conventional biophysical approaches. The field has made substantial advances toward a structural understanding of this complex: the ring model for cohesin predicted many years ago has now been validated through biochemical and structural characterisation of the putative ‘gates’ of the complex (Haering and Hochwagen, 2002, Gruber et al., 2003, Gruber et al., 2006, Gligoris et al., 2014, Huis in 't Veld et al., 2014); a molecular switch, the acetylation of Smc3, for cohesion has been described (Ben-Shahar et al., 2008, Unal et al., 2008, Zhang et al., 2008); the atomic details of the major cohesin regulatory factors, Pds5, Scc3, and Wapl, are now available (Chatterjee et al., 2013, Ouyang et al., 2013, Hara et al., 2014, Roig et al., 2014).

However, considerable questions remain as to the nature of cohesin function. How do accessory factors execute loading and unloading activities? How might cohesin accommodate chromatin? Are sister chromatids apportioned to distinct domains of cohesin, or is their entrapment relatively fluid? What is the architecture of DNA captured by cohesin? How is the ATPase activity fine-tuned to facilitate seemingly distinct functional events? Why do there appear to be separable entry and exit gates for DNA?

Are cohesin complexes engaged in sister chromatid cohesion structurally distinct from those which are not? How do cohesin complexes actually confer cohesion?

The high conservation of buried elements in the HEAT repeats of Scc3 and Pds5 may indicate that, in addition to providing interaction surfaces, the structure of these proteins may in itself be of mechanical significance. Whereas Scc3 occupies a considerable length of Scc1, and may confer additional strength to the ring, Pds5 is more flexibly positioned at the Smc3-Scc1 interface (Hara et al., 2014, Roig et al., 2014; this study). Our SAXS experiments support a degree of conformational flexibility (figure 36), and so it is possible that this may, in the context of the cell, serve a more directed purpose. It will be of great interest in future to study the topology of Pds5 at this interface, and whether events such as Smc3 acetylation or Wapl recruitment might manipulate this protein in order to effect structural alteration of the cohesin ring.

The results produced throughout this thesis work clarify the transactions between cohesin and its non-SMC regulators at the Smc3-Scc1 interface. Furthermore, the structural, biochemical and cell biological characterisation presented here provides atomic level insight into Pds5 and Scc1 function, and, together with existing structural models, establishes a framework for investigating further the molecular details of how these factors collaborate in the orchestration of sister chromatid cohesion. Defining the states, structures, and interactions, or lack thereof, of the cohesin complex and its regulators will be critical in the process of iteratively refining our understanding of this assembly, and ultimately the derivation of a molecular model for sister chromatid cohesion.

Acknowledgements

First and foremost, I thank my parents and family, for life and love. To you I owe all that I am and ever will be.

For his perpetual enthusiasm, I thank Daniel Panne. The subtlety of his mentorship is such that I may still be surprised with lessons decades from now. I would furthermore like to thank him for his somewhat questionable judgement in recruiting a PhD candidate with essentially no prior experience in structural biochemistry.

I would to express my gratitude to Dr Stephan Gruber, Dr Christian Häring, Prof Dr Andrea Musacchio, Dr Carlo Petosa, and Dr Joanna Timmins for taking the time to evaluate my thesis. I am also grateful to Dr Stephen Cusack, Dr Christian Häring, and Dr Saadi Khochbin for their valuable contributions to our annual thesis advisory committee meetings. I am especially indebted to Christian, who provided continual support to us throughout the duration of this thesis, and whose collaboration enabled us to situate the results of this thesis within their native biological context. Similarly, I give thanks to the members of the Häring Lab at EMBL Heidelberg, Marc Kschonsak and Jutta Metz, who contributed their time and expertise to the yeast work.

EMBL, and the Grenoble outstation, was an exceptional environment in which to have undertaken my PhD. Throughout these past four years, I have been fortunate to have encountered friendly, supportive and open attitudes in interactions with fellows and staff within and without the institute. The persistence, ingenuity and passion of my peers were a constant source of inspiration.

For stimulating late-night and weekend discussions, I thank Etienne, Lahari, Li Yan, Nie Yan, and Ramesh.

To Mattze I extend my considerable gratitude for showing me the (pink) light of cobalt, for sharing his expertise in limited proteolysis and crystallisation, and for his persistent,

ruthless encouragement. I would like to thank Stephanie Koo for her friendship and her mentorship. 스온, 고마워.

I am grateful to all members of the Panne lab, past and present, for discussions, criticism and support throughout the years. Special thanks go to Carmen, Emily, and Siyi for helping me to acclimatise to the lab. I thank Paul and Yan for being kindred spirits. Your eldritch poetry and companionship were welcome, if, regrettably, unforeseen experiences. Thanks also to Amédé for jokes and to Dr Jonathan Gaucher for being a joke.

If it were not for the excellent support of the EMBL, ESRF, IBS and PSB core facilities, this work would have been rather impractical. For invaluable assistance with mass spectrometry, I thank Drs Joanna Kirkpatrick (EMBL) and Luca Signor (IBS). The EMBL HTX Lab greatly accelerated the crystallographic work (thank you all!). It was also a considerable privilege to work in such proximity to the ESRF, so I extend my thanks to all the beamlines I visited (which probably encompasses all existing MX beamlines). I am particularly grateful for support from Adam, Andrew, Daniele, David, Martha, and Matt.

Appendix

6.1. Structure prediction and multiple-sequence alignments

6.1.2 Pds5

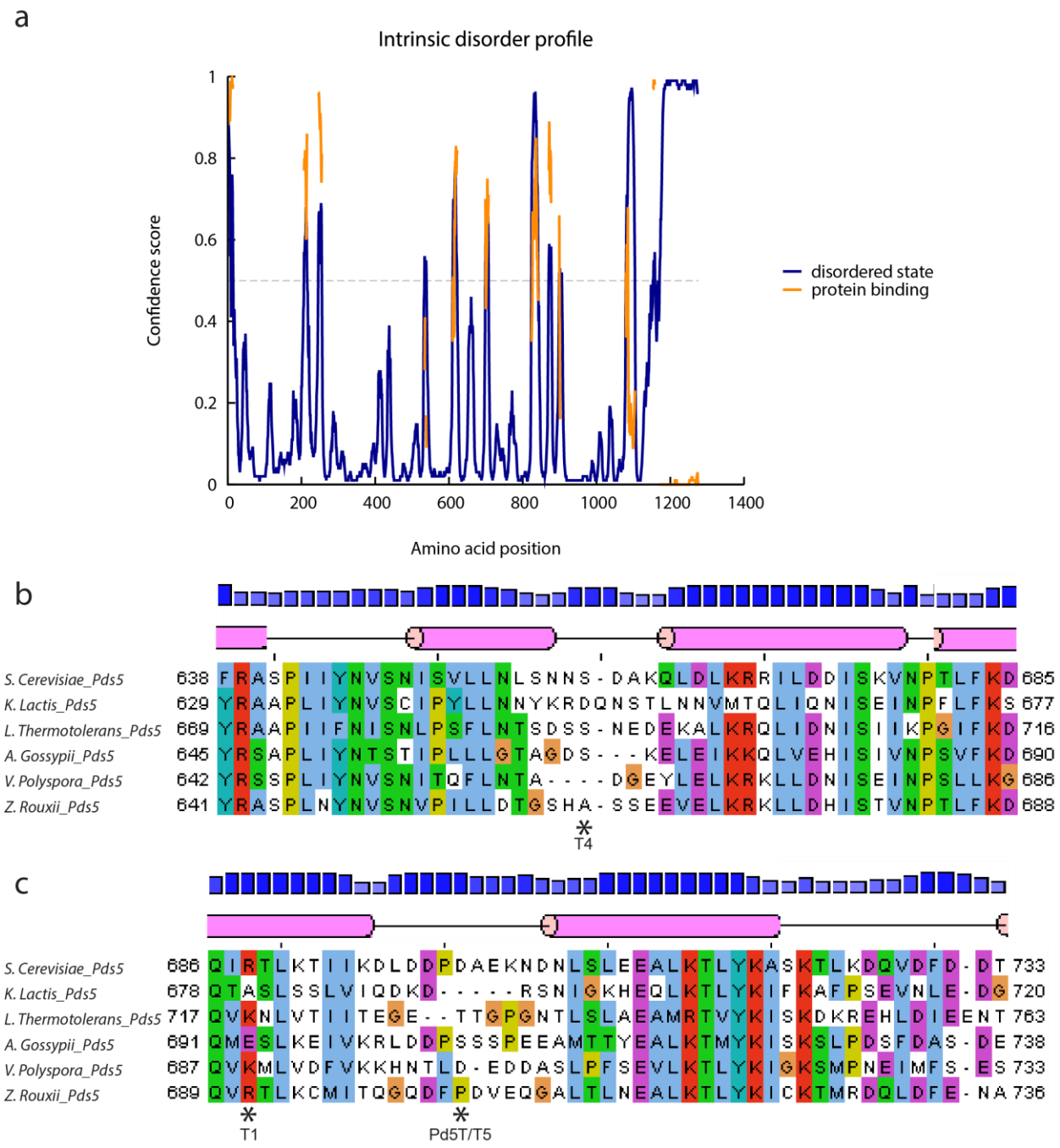

Figure 40 | Structural bioinformatics and construct design for Pds5. (a) Intrinsic disorder profile for Pds5 as predicted by Psipred. A confidence score above the dotted grey line indicates a disordered state. (b) Psipred structure prediction output for Pds5 overlaid above a multiple sequence alignment of fungal Pds5 proteins. Pink tubes indicate alpha helices. Blue bars indicate the confidence in structure assignment. The position of the C-terminal residue of Pds5T4 is marked with an asterisk. (c) Structure prediction of Pds5 overlaid above a multiple sequence alignment of Pds5 as in b. Positions for the C-terminal residue of Pds5T1 and Pds5T/Pds5T5 are marked with asterisks.
For brevity, not all Pds5 construct boundaries are shown. N-termini are as for the wild-type protein.

6.1.3. Scc1

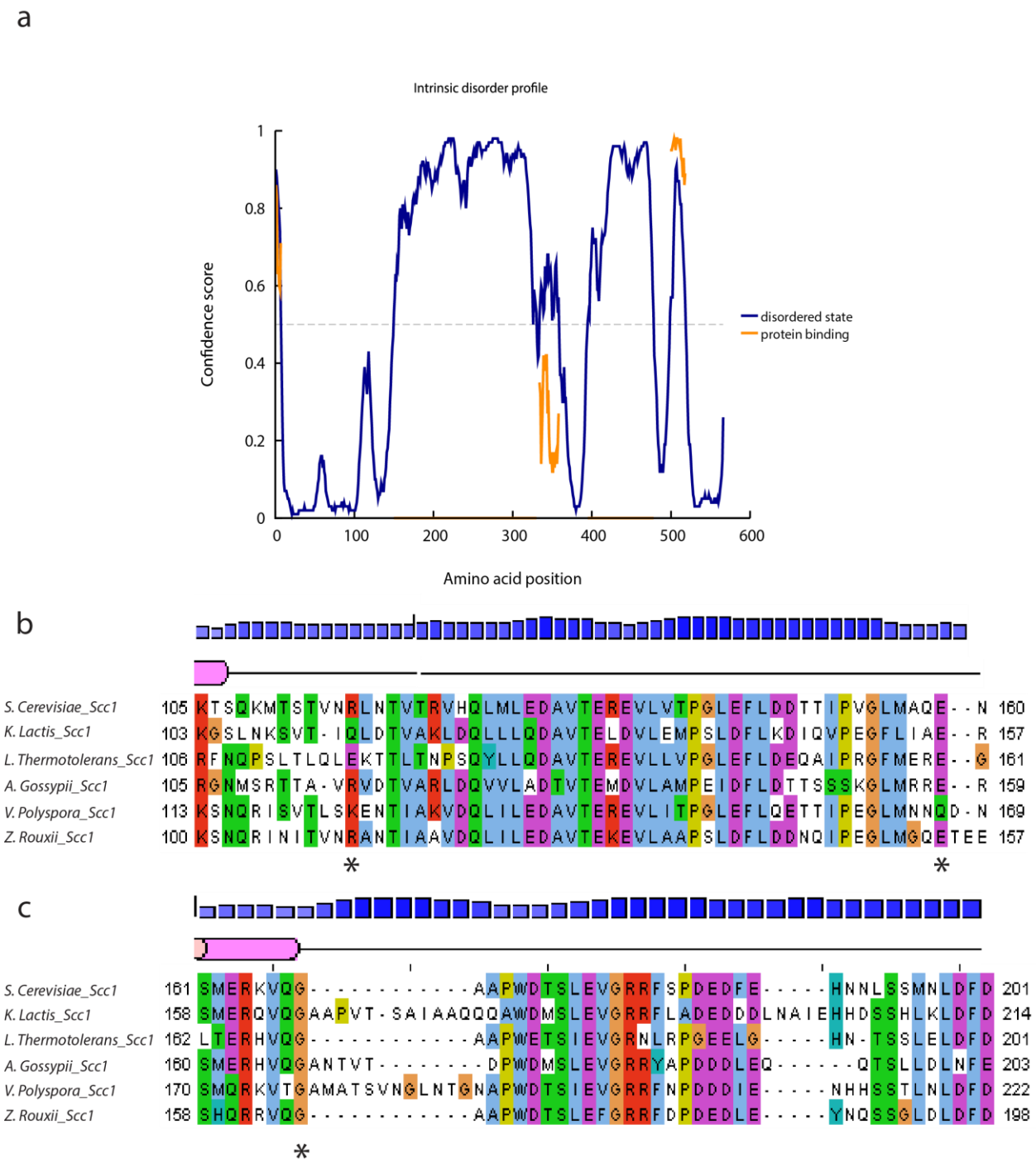

Figure 41 | Structural bioinformatics and construct design for Scc1. (a) Intrinsic disorder profile for Scc1 as predicted by Psipred. A confidence score above the dotted grey line indicates a disordered state. (b) Psipred structure prediction output for Scc1 overlaid above a multiple

sequence alignment of fungal Scc1 proteins. Pink tubes indicate alpha helices. Blue bars indicate the confidence in structure assignment. The positions of the N- and C-terminal boundaries of the Scc1 crystallisation construct are marked with asterisks. (c) Structure prediction of Scc1 overlaid above a multiple sequence alignment of Scc1 orthologues as in b. Position of the original NScc1$^{1\text{-}168}$ C-terminus is indicated with an asterisk.

6.1.4. Scc2

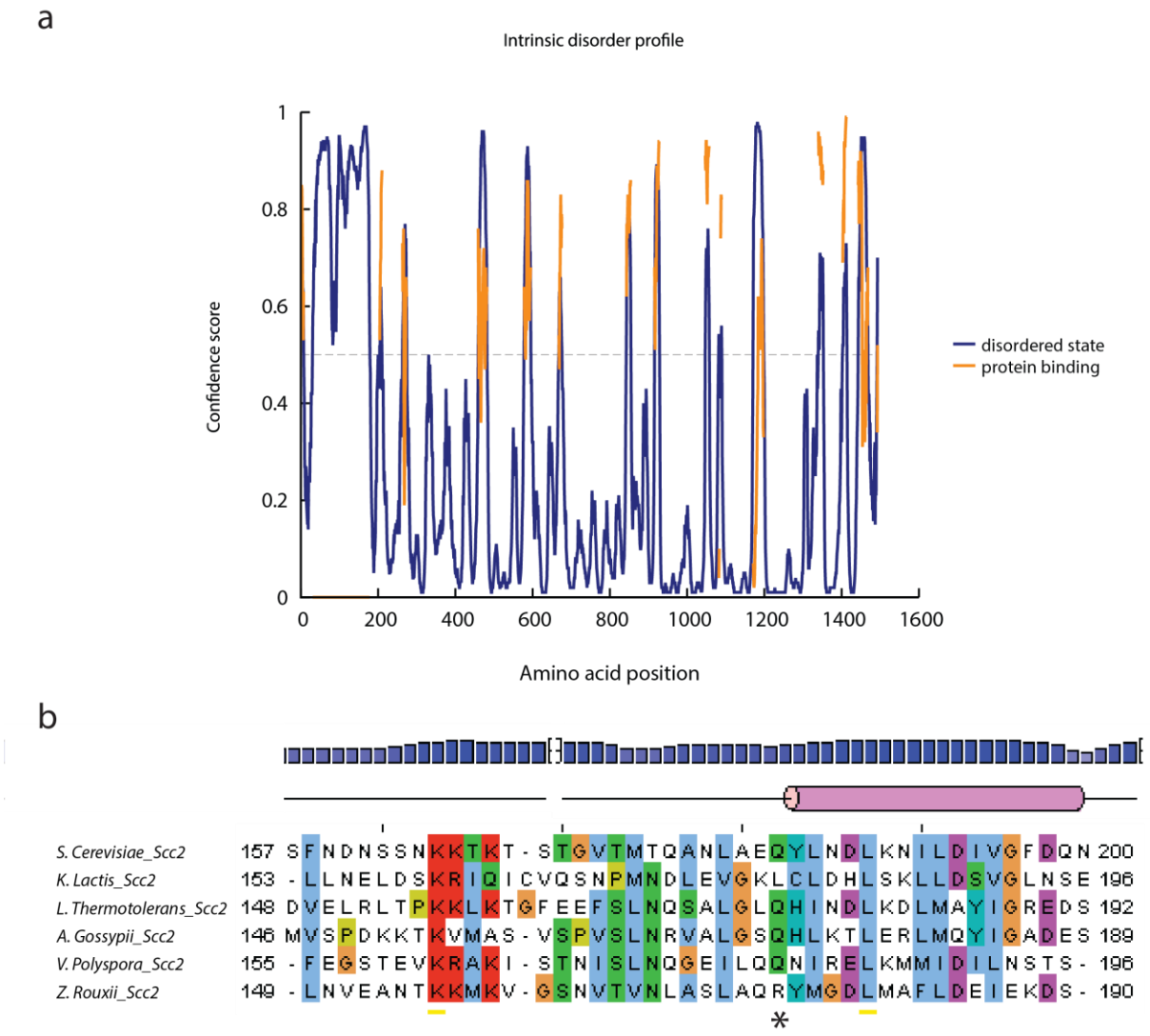

Figure 42 | Structural bioinformatics and construct design for Scc2. (a) Intrinsic disorder profile for Scc2 as predicted by Psipred. A confidence score above the dotted grey line indicates a disordered state. (b) Psipred structure prediction output for Scc2 overlaid above a multiple sequence alignment of fungal Scc2 proteins. Pink tubes indicate alpha helices. Blue bars

indicate the confidence in structure assignment. The position of the N-terminal residue of Scc2Long is indicated, the C-terminus is as the wild-type protein.

6.1.5. Scc3

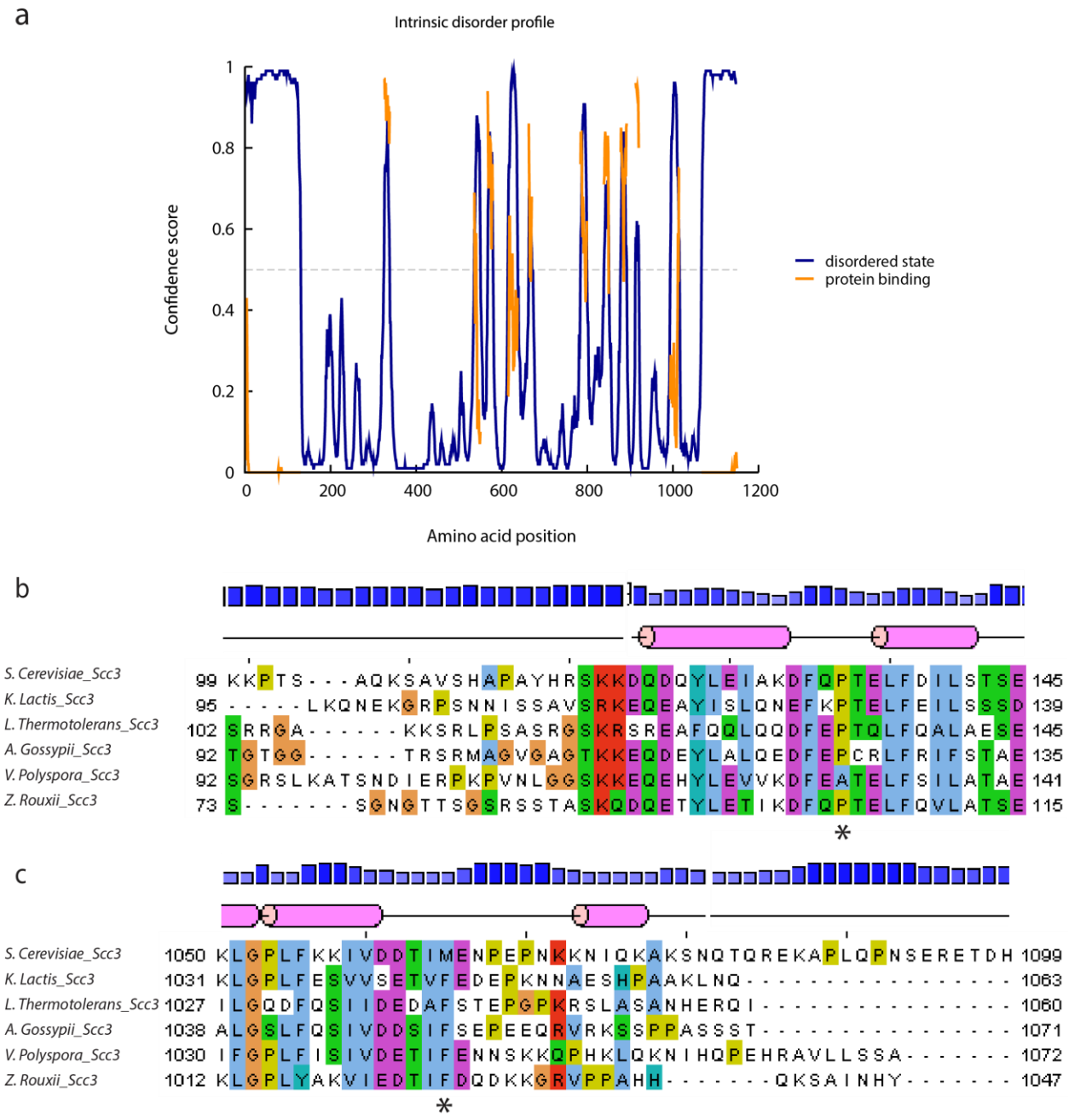

Figure 43 | Structural bioinformatics and construct design for Scc3. (a) Intrinsic disorder profile for Scc3 as predicted by Psipred. A confidence score above the dotted grey line indicates

a disordered state. (b) Psipred structure prediction output for Scc3 overlaid above a multiple sequence alignment of fungal Scc3 proteins. Pink tubes indicate alpha helices. Blue bars indicate the confidence in structure assignment. The position of the N-terminal boundary of Scc3Core is marked with an asterisk (c) Structure prediction of Scc1 overlaid above a multiple sequence alignment of Scc1 orthologues as in b. The position of the C-terminal boundary of Scc3Core is marked with an asterisk.

6.2. Crystallographic data collection, phasing, and refinement statistics

Appendix table 1: Data collection, phasing and refinement statistics

	Pds5T–Scc1 Native	Pds5T Native–Apo	Pds5T–Scc1 SAD	Pds5T–Scc1^{L128M} SAD
Data collection				
Space group	$P2_1$	I422	$P2_1$	$P2_1$
Cell dimensions				
a, *b*, *c* (Å)	147.23, 62.56, 155.94	283.69, 283.69, 172.79	147.30, 62.67, 156.20	148.61, 62.64, 156.89
Wavelength	0.965	0.999	0.965	0.965
Resolution (Å)	50-2.9	50-5.8	50-3.4	50-3.7
R_{sym} or R_{merge}	4.6 (71.3) *	2.3 (51.8) *	6.1 (41.2) *	19.8 (94.7) *
I / σI	9.14 (1.11) *	17.19 (1.57) *	10.1 (1.8) *	8.39 (1.56)*
CC (1/2)	99.9 (50.7) *	99.9 (61.89) *	99.7 (69.6) *	99.9 (66.6) *
Completeness (%)	96.3 (89.5) *	99.3 (98.5) *	96.4 (71) *	99.2 (93.1) *
Redundancy	2.58 (2.55) *	7.61 (7.99) *	1.99 (1.92) *	6.4 (5.1) *
Refinement				
Resolution (Å)	50-2.9	50-5.8		50- 3.7
No. reflections	59992	10082		29319
R_{work} / R_{free}	0.2656/0.2980	0.2490 / 0.3111		0.2128 / 0.2609
No. atoms	11116	10858		11160
Protein	1371	1337		1376
B-factors				
Protein	106	424		92
R.m.s deviations				
Bond lengths (Å)	0.003	0.003		0.008
Bond angles (°)	0.677	0.611		1.02

*Values in parentheses are for the highest-resolution shell.

6.3. Yeast Strains

Appendix Table 2: Yeast strains. All strains are derived from *S. cerevisiae* W303. *Nota bene: All strains were generated by the Häring Lab at EMBL Heidelberg and are included here for completeness.*

Strain	Genotype
Figures 30a and 32a	
C4307	MATa/α, pds5::natMX4/PDS5, ura3::PDS5-PK$_6$::URA3/ura3-1
C4308	MATa/α, pds5::natMX4/PDS5, ura3::PDS5^{D90A}-PK$_6$::URA3/ura3-1
C4309	MATa/α, pds5::natMX4/PDS5, ura3::PDS5^{D90R}-PK$_6$::URA3/ura3-1
C4310	MATa/α, pds5::natMX4/PDS5, ura3::PDS5^{A91R}-HRV3C$_3$-PK$_6$::URA3/ura3-1
C4311	MATa/α, pds5::natMX4/PDS5, ura3::PDS5^{D141A}-HRV3C$_3$-PK$_6$::URA3/ura3-1
C4312	MATa/α, pds5::natMX4/PDS5, ura3::PDS5^{D141R}-HRV3C$_3$-PK$_6$::URA3/ura3-1
C4313	MATa/α, pds5::natMX4/PDS5, ura3::PDS5^{E181A}-HRV3C$_3$-PK$_6$::URA3/ura3-1
C4314	MATa/α, pds5::natMX4/PDS5, ura3::PDS5^{E181R}-HRV3C$_3$-PK$_6$::URA3/ura3-1
C4315	MATa/α, pds5::natMX4/PDS5, ura3::PDS5^{R375E}-HRV3C$_3$-PK$_6$::URA3/ura3-1
C4316	MATa/α, pds5::natMX4/PDS5, ura3::PDS5^{R408D}-HRV3C$_3$-PK$_6$::URA3/ura3-1
C4317	MATa/α, pds5::natMX4/PDS5, ura3::PDS5^{Y457A}-HRV3C$_3$-PK$_6$::URA3/ura3-1
C4318	MATa/α, pds5::natMX4/PDS5, ura3::PDS5^{Y457D}-HRV3C$_3$-PK$_6$::URA3/ura3-1
C4319	MATa/α, pds5::natMX4/PDS5, ura3::PDS5^{Y458A}-HRV3C$_3$-PK$_6$::URA3/ura3-1
C4320	MATa/α, pds5::natMX4/PDS5, ura3::PDS5^{Y458E}-HRV3C$_3$-PK$_6$::URA3/ura3-1
C4321	MATa/α, pds5::natMX4/PDS5, ura3::PDS5^{I459E}-HRV3C$_3$-PK$_6$::URA3/ura3-1
C4322	MATa/α, pds5::natMX4/PDS5, ura3::PDS5^{Y457A,Y458A}-HRV3C$_3$-PK$_6$::URA3/ura3-1
C4323	MATa/α, pds5::natMX4/PDS5, ura3::PDS5^{Y457D,Y458E}-HRV3C$_3$-PK$_6$::URA3/ura3-1
C4324	MATa/α, pds5::natMX4/PDS5, ura3::PDS5^{Y457A,Y458A,I459A}-HRV3C$_3$-PK$_6$::URA3/ura3-1
C4325	MATa/α, pds5::natMX4/PDS5, ura3::PDS5^{K500E}-HRV3C$_3$-PK$_6$::URA3/ura3-1
C4326	MATa/α, pds5::natMX4/PDS5, ura3::PDS5^{A507L}-HRV3C$_3$-PK$_6$::URA3/ura3-1
C4327	MATa/α, pds5::natMX4/PDS5, ura3::PDS5^{R511A}-HRV3C$_3$-PK$_6$::URA3/ura3-1
C4328	MATa/α, pds5::natMX4/PDS5, ura3::PDS5^{W553A}-HRV3C$_3$-PK$_6$::URA3/ura3-1
Figures 30b and 32b	
C4329	MATa/α, scc1::kanMX/SCC1, trp1::SCC1-HA$_6$::TRP1/trp1-1
C4330	MATa/α, scc1::kanMX/SCC1, trp1::SCC1^{L128D}-HA$_6$::TRP1/trp1-1
C4331	MATa/α, scc1::kanMX/SCC1, trp1::SCC1^{D130R}-HA$_6$::TRP1/trp1-1
C4332	MATa/α, scc1::kanMX/SCC1, trp1::SCC1^{V137G}-HA$_6$::TRP1/trp1-1
C4333	MATa/α, scc1::kanMX/SCC1, trp1::SCC1^{V137D}-HA$_6$::TRP1/trp1-1
C4334	MATa/α, scc1::kanMX/SCC1, trp1::SCC1^{V137K}-HA$_6$::TRP1/trp1-1
C4335	MATa/α, scc1::kanMX/SCC1, trp1::SCC1^{L138K}-HA$_6$::TRP1/trp1-1
C4336	MATa/α, scc1::kanMX/SCC1, trp1::SCC1^{V137G,L138G}-HA$_6$::TRP1/trp1-1
Figure 34a	
C4342	MATa, SCC1-HA$_6$::HIS3, ura3::PDS5-HRV3C$_3$-PK$_6$::URA3
C4343	MATa, SCC1-HA$_6$::HIS3, ura3::PDS5^{R408D}-HRV3C$_3$-PK$_6$::URA3
C4344	MATa, SCC1-HA$_6$::HIS3, ura3::PDS5$^{Y457D,\ Y458E}$-HRV3C$_3$-PK$_6$::URA3
C4345	MATa, SCC1-HA$_6$::HIS3, ura3::PDS5^{I459E}-HRV3C$_3$-PK$_6$::URA3
C4346	MATa, SCC1-HA$_6$::HIS3, ura3::PDS5^{K500E}-HRV3C$_3$-PK$_6$::URA3

Figures 34b and 35

C4381	MATa, pds5::HIS3, leu2::pds5-101::LEU2, BMH1::PDS5- HRV3C$_3$-PK$_6$::natMX, cdc20::LEU2, trp1::pGAL-CDC20::TRP1, ura3::tetO::URA3, his3::tetR-GFP::HIS3
C4382	MATa, pds5::HIS3, leu2::pds5-101::LEU2, BMH1::PDS5^{R408D}-HRV3C$_3$-PK$_6$::natMX, cdc20::LEU2, trp1::pGAL-CDC20::TRP1, ura3::tetO::URA3, his3::tetR-GFP::HIS3
C4383	MATa, pds5::HIS3, leu2::pds5-101::LEU2, BMH1::PDS5^{Y457D,Y458E}-HRV3C$_3$-PK$_6$::natMX, cdc20::LEU2, trp1::pGAL-CDC20::TRP1, ura3::tetO::URA3, his3::tetR-GFP::HIS3
C4384	MATa, pds5::HIS3, leu2::pds5-101::LEU2, BMH1::PDS5^{I459E}-HRV3C$_3$-PK$_6$::natMX, cdc20::LEU2, trp1::pGAL-CDC20::TRP1, ura3::tetO::URA3, his3::tetR-GFP::HIS3
C4385	MATa, pds5::HIS3, leu2::pds5-101::LEU2, BMH1::PDS5^{K500E}-HRV3C$_3$-PK$_6$::natMX, cdc20::LEU2, trp1::pGAL-CDC20::TRP1, ura3::tetO::URA3, his3::tetR-GFP::HIS3

6.3. Construct table

Construct	Organism	Residues	Vector	Tag	Variants
Smc3hd-CScc1 & Smc1hd	*S. Cerevisiae*	Smc3 1-226-gsggs-991-1230-polyGS linker-Scc1 451-566 Smc1 1-214-gsggs-1024-1225	pET-Duet / pFastBac Dual	N-ter 6xHis (Smc3-Scc1) N-ter GST-TEV (Smc1hd)	Wt
Smc3hd-CScc1 & NScc1-Smc1hd	*S. Cerevisiae*	Smc3 1-226-gsggs-991-1230-polyGS linker-Scc1 451-566 Scc1 1-105-polyGS linker-Smc1 1-214-gsggs-1024-1225	pET-Duet / pFastBac Dual	N-ter 6xHis (Smc3-Scc1) N-ter GST-TEV (Scc1-Smc1hd)	Wt
Eco1	*S. Cerevisiae*	Full-length	pGEX-6T	N-ter GST-thrombin	C35A/C38A
Scc3	*S. Cerevisiae*	Full-length	pETM11	N-ter 6xHis-TEV	Wt
Scc3 Core	*S. Cerevisiae*	134-1064	pETM11	N-ter 6xHis-TEV	Wt
Scc2	*S. Cerevisiae*	Full-length	pETM11	N-ter 6xHis-TEV	Wt
Scc2 Long	*S. Cerevisiae*	183-1493	pETM11	N-ter 6xHis-TEV	Wt
Pds5	*S. Cerevisiae*	Full-length	pETM11	N-ter 6xHis-TEV	Wt
Pds5 Core L	*S. Cerevisiae*	1-656	pETM11	N-ter 6xHis-TEV	Wt
Pds5 Core M	*S. Cerevisiae*	1-611	pETM11	N-ter 6xHis-TEV	Wt
Pds5 Core S	*S. Cerevisiae*	1-530	pETM30	N-ter 6xHis-GST-TEV	Wt
Pds5 T1	*S. Cerevisiae*	1-688	pETM11	N-ter 6xHis-TEV	Wt
Pds5 T2	*S. Cerevisiae*	1-680	pETM11	N-ter 6xHis-TEV	Wt
Pds5 T3	*S. Cerevisiae*	1-684	pETM11	N-ter 6xHis-TEV	Wt
Pds5 T4	*S. Cerevisiae*	1-660	pETM11	N-ter 6xHis-TEV	Wt
Pds5 T5 / Pds5T	*S. Cerevisiae*	1-701	pETM11	N-ter 6xHis-TEV	Wt , R408D, Y457A, Y457D, Y458A, Y458E, Y457A/Y458A, Y457D/Y458E, I459E, K500E, A507L, R511A, W553A
Ag Pds5T	*A. Gossypii*	1-708	pETM11	N-ter 6xHis-TEV	Wt
H Pds5AT	*H. Sapiens*	1-692	pETM11	N-ter 6xHis-TEV	Wt
H Pds5BT	*H. Sapiens*	1-682	pETM11	N-ter 6xHis-TEV	Wt
Wapl	*S. Cerevisiae*	Full-length	pETM11 / pETM30	N-ter 6xHis-GST-TEV, C-ter Flag	Wt

WaplC	*S. Cerevisiae*	250-647	pETM30	N-ter 6xHis-GST-TEV, C-ter Flag	Wt
WaplN	*S. Cerevisiae*	1-249	pETM30	N-ter 6xHis-GST-TEV, C-ter Flag	Wt
NScc1	*S. Cerevisiae*	1-159	pAcyc-Duet	None / C-ter 6xHis	Wt , V137G/L138G
Scc1-Xtal	*S. Cerevisiae*	116-159	pAcyc-Duet	None	Wt , L128M
Smc3hd-Xtal	*S. Cerevisiae*	1-260-linker-971-1230	pAcyc-Duet	None	Wt

References

ADAMS, P. D., AFONINE, P. V., BUNKOCZI, G., CHEN, V. B., DAVIS, I. W., ECHOLS, N., HEADD, J. J., HUNG, L. W., KAPRAL, G. J., GROSSE-KUNSTLEVE, R. W., MCCOY, A. J., MORIARTY, N. W., OEFFNER, R., READ, R. J., RICHARDSON, D. C., RICHARDSON, J. S., TERWILLIGER, T. C. & ZWART, P. H. 2010. PHENIX: a comprehensive Python-based system for macromolecular structure solution. *Acta Crystallogr D Biol Crystallogr,* 66**,** 213-21.

ALEXANDRU, G., UHLMANN, F., MECHTLER, K., POUPART, M. A. & NASMYTH, K. 2001. Phosphorylation of the cohesin subunit Scc1 by Polo/Cdc5 kinase regulates sister chromatid separation in yeast. *Cell,* 105**,** 459-72.

ALUSHIN, G. M., RAMEY, V. H., PASQUALATO, S., BALL, D. A., GRIGORIEFF, N., MUSACCHIO, A. & NOGALES, E. 2010. The Ndc80 kinetochore complex forms oligomeric arrays along microtubules. *Nature,* 467**,** 805-10.

ANDERSON, D. E., LOSADA, A., ERICKSON, H. P. & HIRANO, T. 2002. Condensin and cohesin display different arm conformations with characteristic hinge angles. *J Cell Biol,* 156**,** 419-24.

ARUMUGAM, P., GRUBER, S., TANAKA, K., HAERING, C., MECHTLER, K. & NASMYTH, K. 2003. ATP Hydrolysis Is Required for Cohesin's Association with Chromosomes. *Current Biology,* 13**,** 1941-1953.

ARUMUGAM, P., NISHINO, T., HAERING, C. H., GRUBER, S. & NASMYTH, K. 2006. Cohesin's ATPase activity is stimulated by the C-terminal Winged-Helix domain of its kleisin subunit. *Curr Biol,* 16**,** 1998-2008.

BAUSCH, C., NOONE, S., HENRY, J. M., GAUDENZ, K., SANDERSON, B., SEIDEL, C. & GERTON, J. L. 2007. Transcription alters chromosomal locations of cohesin in Saccharomyces cerevisiae. *Mol Cell Biol,* 27**,** 8522-32.

BELLOWS, A. M., KENNA, M. A., CASSIMERIS, L. & SKIBBENS, R. V. 2003. Human EFO1p exhibits acetyltransferase activity and is a unique combination of linker histone and Ctf7p/Eco1p chromatid cohesion establishment domains. *Nucleic Acids Res,* 31**,** 6334-43.

BEN-SHAHAR, T., HEEGER, S., LEHANE, C., EAST, P., FLYNN, H., SKEHEL, M. & UHLMANN, F. 2008. Eco1-Dependent Cohesin Acetylation During Establishment of Sister Chromatid Cohesion. *Science,* 321**,** 563-566.

BERNARD, P., MAURE, J. F., PARTRIDGE, J. F., GENIER, S., JAVERZAT, J. P. & ALLSHIRE, R. C. 2001. Requirement of heterochromatin for cohesion at centromeres. *Science,* 294**,** 2539-42.

BIRKENBIHL, R. P. & SUBRAMANI, S. 1992. Cloning and characterization of rad21 an essential gene of Schizosaccharomyces pombe involved in DNA double-strand-break repair. *Nucleic Acids Res,* 20**,** 6605-11.

BLAT, Y. & KLECKNER, N. 1999. Cohesins bind to preferential sites along yeast chromosome III, with differential regulation along arms versus the centric region. *Cell,* 98**,** 249-59.

BORGES, V., LEHANE, C., LOPEZ-SERRA, L., FLYNN, H., SKEHEL, M., ROLEF BEN-SHAHAR, T. & UHLMANN, F. 2010. Hos1 deacetylates Smc3 to close the cohesin acetylation cycle. *Mol Cell,* 39**,** 677-88.

BORGES, V., SMITH, D. J., WHITEHOUSE, I. & UHLMANN, F. 2013. An Eco1-independent sister chromatid cohesion establishment pathway in S. cerevisiae. *Chromosoma,* 122**,** 121-34.

BRUNGER, A. T., ADAMS, P. D., FROMME, P., FROMME, R., LEVITT, M. & SCHRODER, G. F. 2012. Improving the accuracy of macromolecular structure refinement at 7 A resolution. *Structure,* 20**,** 957-66.

BUCHAN, D. W., MINNECI, F., NUGENT, T. C., BRYSON, K. & JONES, D. T. 2013. Scalable web services for the PSIPRED Protein Analysis Workbench. *Nucleic Acids Res,* 41**,** W349-57.

BUHEITEL, J. & STEMMANN, O. 2013. Prophase pathway-dependent removal of cohesin from human chromosomes requires opening of the Smc3–Scc1 gate. *The EMBO Journal,* 32**,** 666-676.

BURMANN, F., SHIN, H. C., BASQUIN, J., SOH, Y. M., GIMENEZ-OYA, V., KIM, Y. G., OH, B. H. & GRUBER, S. 2013. An asymmetric SMC-kleisin bridge in prokaryotic condensin. *Nat Struct Mol Biol,* 20**,** 371-9.

CAMDERE, G., GUACCI, V., STRICKLIN, J. & KOSHLAND, D. 2015. The ATPases of cohesin interface with regulators to modulate cohesin-mediated DNA tethering. *Elife,* 4.

CAMPBELL, C. S. & DESAI, A. 2013. Tension sensing by Aurora B kinase is independent of survivin-based centromere localization. *Nature,* 497**,** 118-21.

CANUDAS, S. & SMITH, S. 2009. Differential regulation of telomere and centromere cohesion by the Scc3 homologues SA1 and SA2, respectively, in human cells. *J Cell Biol,* 187**,** 165-73.

CARRETERO, M., RUIZ-TORRES, M., RODRIGUEZ-CORSINO, M., BARTHELEMY, I. & LOSADA, A. 2013. Pds5B is required for cohesion establishment and Aurora B accumulation at centromeres. *EMBO J,* 32**,** 2938-49.

CHAN, K. L., GLIGORIS, T., UPCHER, W., KATO, Y., SHIRAHIGE, K., NASMYTH, K. & BECKOUET, F. 2013. Pds5 promotes and protects cohesin acetylation. *Proc Natl Acad Sci U S A,* 110**,** 13020-5.

CHAN, K. L., ROIG, M. B., HU, B., BECKOUET, F., METSON, J. & NASMYTH, K. 2012. Cohesin's DNA exit gate is distinct from its entrance gate and is regulated by acetylation. *Cell,* 150**,** 961-74.

CHAO, W. C., MURAYAMA, Y., MUNOZ, S., COSTA, A., UHLMANN, F. & SINGLETON, M. R. 2015. Structural Studies Reveal the Functional Modularity of the Scc2-Scc4 Cohesin Loader. *Cell Rep,* 12**,** 719-25.

CHATTERJEE, A., ZAKIAN, S., HU, X.-W. & SINGLETON, M. R. 2013. Structural insights into the regulation of cohesion establishment by Wpl1. *The EMBO Journal,* 32**,** 677-687.

CIFERRI, C., PASQUALATO, S., SCREPANTI, E., VARETTI, G., SANTAGUIDA, S., DOS REIS, G., MAIOLICA, A., POLKA, J., DE LUCA, J. G., DE WULF, P., SALEK, M., RAPPSILBER, J., MOORES, C. A., SALMON, E. D. & MUSACCHIO, A. 2008. Implications for kinetochore-microtubule attachment from the structure of an engineered Ndc80 complex. *Cell,* 133**,** 427-39.

CIOSK, R., SHIRAYAMA, M., SHEVCHENKO, A., TANAKA, T., TOTH, A. & NASMYTH, K. 2000. Cohesin's binding to chromosomes depends on a separate complex consisting of Scc2 and Scc4 proteins. *Mol Cell,* 5**,** 243-54.

CLIFT, D., BIZZARI, F. & MARSTON, A. L. 2009. Shugoshin prevents cohesin cleavage by PP2A(Cdc55)-dependent inhibition of separase. *Genes Dev,* 23**,** 766-80.

COHEN-FIX, O., PETERS, J. M., KIRSCHNER, M. W. & KOSHLAND, D. 1996. Anaphase initiation in Saccharomyces cerevisiae is controlled by the APC-dependent degradation of the anaphase inhibitor Pds1p. *Genes Dev,* 10**,** 3081-93.

CUYLEN, S., METZ, J. & HAERING, C. H. 2011. Condensin structures chromosomal DNA through topological links. *Nat Struct Mol Biol,* 18**,** 894-901.

DARWICHE, N., FREEMAN, L. A. & STRUNNIKOV, A. 1999. Characterization of the components of the putative mammalian sister chromatid cohesion complex. *Gene,* 233**,** 39-47.

DAUM, J. R., POTAPOVA, T. A., SIVAKUMAR, S., DANIEL, J. J., FLYNN, J. N., RANKIN, S. & GORBSKY, G. J. 2011. Cohesion fatigue induces chromatid separation in cells delayed at metaphase. *Curr Biol,* 21**,** 1018-24.

DEARDORFF, M. A., BANDO, M., NAKATO, R., WATRIN, E., ITOH, T., MINAMINO, M., SAITOH, K., KOMATA, M., KATOU, Y., CLARK, D., COLE, K. E., DE BAERE, E., DECROOS, C., DI DONATO, N., ERNST, S., FRANCEY, L. J., GYFTODIMOU, Y., HIRASHIMA, K., HULLINGS, M., ISHIKAWA, Y.,

JAULIN, C., KAUR, M., KIYONO, T., LOMBARDI, P. M., MAGNAGHI-JAULIN, L., MORTIER, G. R., NOZAKI, N., PETERSEN, M. B., SEIMIYA, H., SIU, V. M., SUZUKI, Y., TAKAGAKI, K., WILDE, J. J., WILLEMS, P. J., PRIGENT, C., GILLESSEN-KAESBACH, G., CHRISTIANSON, D. W., KAISER, F. J., JACKSON, L. G., HIROTA, T., KRANTZ, I. D. & SHIRAHIGE, K. 2012. HDAC8 mutations in Cornelia de Lange syndrome affect the cohesin acetylation cycle. *Nature,* 489**,** 313-7.

DENISON, S. H., KAFER, E. & MAY, G. S. 1993. Mutation in the bimD gene of Aspergillus nidulans confers a conditional mitotic block and sensitivity to DNA damaging agents. *Genetics,* 134**,** 1085-96.

DOBIE, K. W., KENNEDY, C. D., VELASCO, V. M., MCGRATH, T. L., WEKO, J., PATTERSON, R. W. & KARPEN, G. H. 2001. Identification of chromosome inheritance modifiers in Drosophila melanogaster. *Genetics,* 157**,** 1623-37.

DOWEN, J. M., FAN, Z. P., HNISZ, D., REN, G., ABRAHAM, B. J., ZHANG, L. N., WEINTRAUB, A. S., SCHUIJERS, J., LEE, T. I., ZHAO, K. & YOUNG, R. A. 2014. Control of cell identity genes occurs in insulated neighborhoods in mammalian chromosomes. *Cell,* 159**,** 374-87.

DREIER, M. R., BEKIER, M. E., 2ND & TAYLOR, W. R. 2011. Regulation of sororin by Cdk1-mediated phosphorylation. *J Cell Sci,* 124**,** 2976-87.

EDWARDS, S., LI, C. M., LEVY, D. L., BROWN, J., SNOW, P. M. & CAMPBELL, J. L. 2003. Saccharomyces cerevisiae DNA polymerase epsilon and polymerase sigma interact physically and functionally, suggesting a role for polymerase epsilon in sister chromatid cohesion. *Mol Cell Biol,* 23**,** 2733-48.

EICHINGER, C. S., KURZE, A., OLIVEIRA, R. A. & NASMYTH, K. 2013. Disengaging the Smc3/kleisin interface releases cohesin from Drosophila chromosomes during interphase and mitosis. *EMBO J,* 32**,** 656-65.

EMSLEY, P. & COWTAN, K. 2004. Coot: model-building tools for molecular graphics. *Acta Crystallogr D Biol Crystallogr,* 60**,** 2126-32.

FARCAS, A. M., ULUOCAK, P., HELMHART, W. & NASMYTH, K. 2011. Cohesin's concatenation of sister DNAs maintains their intertwining. *Mol Cell,* 44**,** 97-107.

FEYTOUT, A., VAUR, S., GENIER, S., VAZQUEZ, S. & JAVERZAT, J. P. 2011. Psm3 acetylation on conserved lysine residues is dispensable for viability in fission yeast but contributes to Eso1-mediated sister chromatid cohesion by antagonizing Wpl1. *Mol Cell Biol,* 31**,** 1771-86.

FUNABIKI, H., YAMANO, H., KUMADA, K., NAGAO, K., HUNT, T. & YANAGIDA, M. 1996. Cut2 proteolysis required for sister-chromatid seperation in fission yeast. *Nature,* 381**,** 438-41.

GANDHI, R., GILLESPIE, P. J. & HIRANO, T. 2006. Human Wapl is a cohesin-binding protein that promotes sister-chromatid resolution in mitotic prophase. *Curr Biol,* 16**,** 2406-17.

GATTIKER, A., BIENVENUT, W. V., BAIROCH, A. & GASTEIGER, E. 2002. FindPept, a tool to identify unmatched masses in peptide mass fingerprinting protein identification. *Proteomics,* 2**,** 1435-44.

GAUSE, M., MISULOVIN, Z., BILYEU, A. & DORSETT, D. 2010. Dosage-sensitive regulation of cohesin chromosome binding and dynamics by Nipped-B, Pds5, and Wapl. *Mol Cell Biol,* 30**,** 4940-51.

GERLICH, D., KOCH, B., DUPEUX, F., PETERS, J. M. & ELLENBERG, J. 2006. Live-cell imaging reveals a stable cohesin-chromatin interaction after but not before DNA replication. *Curr Biol,* 16**,** 1571-8.

GILLESPIE, P. J. & HIRANO, T. 2004. Scc2 couples replication licensing to sister chromatid cohesion in Xenopus egg extracts. *Curr Biol,* 14**,** 1598-603.

GIMENEZ-ABIAN, J. F., SUMARA, I., HIROTA, T., HAUF, S., GERLICH, D., DE LA TORRE, C., ELLENBERG, J. & PETERS, J. M. 2004. Regulation of sister chromatid cohesion between chromosome arms. *Curr Biol,* 14**,** 1187-93.

GLIGORIS, T. G., SCHEINOST, J. C., BURMANN, F., PETELA, N., CHAN, K. L., ULUOCAK, P., BECKOUET, F., GRUBER, S., NASMYTH, K. & LOWE, J. 2014. Closing the cohesin ring: structure and function of its Smc3-kleisin interface. *Science,* 346**,** 963-7.

GLYNN, E. F., MEGEE, P. C., YU, H. G., MISTROT, C., UNAL, E., KOSHLAND, D. E., DERISI, J. L. & GERTON, J. L. 2004. Genome-wide mapping of the cohesin complex in the yeast Saccharomyces cerevisiae. *PLoS Biol,* 2**,** E259.

GRUBER, S., ARUMUGAM, P., KATOU, Y., KUGLITSCH, D., HELMHART, W., SHIRAHIGE, K. & NASMYTH, K. 2006. Evidence that Loading of Cohesin Onto Chromosomes Involves Opening of Its SMC Hinge. *Cell,* 127**,** 523-537.

GRUBER, S., HAERING, C. & NASMYTH, K. 2003. Chromosomal Cohesin Forms a Ring. *Cell,* 112**,** 765-777.

GUACCI, V., HOGAN, E. & KOSHLAND, D. 1994. Chromosome condensation and sister chromatid pairing in budding yeast. *J Cell Biol,* 125**,** 517-30.

GUACCI, V. & KOSHLAND, D. 2012. Cohesin-independent segregation of sister chromatids in budding yeast. *Mol Biol Cell,* 23**,** 729-39.

GUACCI, V., KOSHLAND, D. & STRUNNIKOV, A. 1997. A direct link between sister chromatid cohesion and chromosome condensation revealed through the analysis of MCD1 in S. cerevisiae. *Cell,* 91**,** 47-57.

HAARHUIS, J. H., ELBATSH, A. M. & ROWLAND, B. D. 2014. Cohesin and its regulation: on the logic of X-shaped chromosomes. *Dev Cell,* 31**,** 7-18.

HAARHUIS, J. H., ELBATSH, A. M., VAN DEN BROEK, B., CAMPS, D., ERKAN, H., JALINK, K., MEDEMA, R. H. & ROWLAND, B. D. 2013. WAPL-mediated removal of cohesin protects against segregation errors and aneuploidy. *Curr Biol,* 23**,** 2071-7.

HAERING, C. H., FARCAS, A. M., ARUMUGAM, P., METSON, J. & NASMYTH, K. 2008. The cohesin ring concatenates sister DNA molecules. *Nature,* 454**,** 297-301.

HAERING, C. H. & JESSBERGER, R. 2012. Cohesin in determining chromosome architecture. *Experimental Cell Research,* 318**,** 1386-1393.

HAERING, C. H., LOWE, J., HOCHWAGEN, A. & NASMYTH, K. 2002. Molecular architecture of SMC proteins and the yeast cohesin complex. *Mol Cell,* 9**,** 773-88.

HAERING, C. H., SCHOFFNEGGER, D., NISHINO, T., HELMHART, W., NASMYTH, K. & LOWE, J. 2004. Structure and stability of cohesin's Smc1-kleisin interaction. *Mol Cell,* 15**,** 951-64.

HAERING, C. L., J & HOCHWAGEN, A. N., K 2002. Molecular architecture of SMC proteins and the yeast cohesin complex. *Molecular Cell,* 9**,** 773-788.

HARA, K., ZHENG, G., QU, Q., LIU, H., OUYANG, Z., CHEN, Z., TOMCHICK, D. R. & YU, H. 2014. Structure of cohesin subcomplex pinpoints direct shugosin-Wapl antagonism in centromeric cohesion. *Nature Structural & Molecular Biology*.

HARTMAN, T., STEAD, K., KOSHLAND, D. & GUACCI, V. 2000. Pds5p is an essential chromosomal protein required for both sister chromatid cohesion and condensation in Saccharomyces cerevisiae. *J Cell Biol,* 151**,** 613-26.

HAUF, S., ROITINGER, E., KOCH, B., DITTRICH, C. M., MECHTLER, K. & PETERS, J. M. 2005. Dissociation of cohesin from chromosome arms and loss of arm cohesion during early mitosis depends on phosphorylation of SA2. *PLoS Biol,* 3**,** e69.

HEIDINGER-PAULI, J. M., ONN, I. & KOSHLAND, D. 2010. Genetic evidence that the acetylation of the Smc3p subunit of cohesin modulates its ATP-bound state to promote cohesion establishment in Saccharomyces cerevisiae. *Genetics,* 185**,** 1249-56.

HEIDINGER-PAULI, J. M., UNAL, E. & KOSHLAND, D. 2009. Distinct targets of the Eco1 acetyltransferase modulate cohesion in S phase and in response to DNA damage. *Mol Cell,* 34**,** 311-21.

HELLMUTH, S., BOTTGER, F., PAN, C., MANN, M. & STEMMANN, O. 2014. PP2A delays APC/C-dependent degradation of separase-associated but not free securin. *EMBO J,* 33**,** 1134-47.

HINSHAW, S. M., MAKRANTONI, V., KERR, A., MARSTON, A. L. & HARRISON, S. C. 2015. Structural evidence for Scc4-dependent localization of cohesin loading. *Elife,* 4.

HIRANO, T. 2006. At the heart of the chromosome: SMC proteins in action. *Nature Reviews Molecular Cell Biology,* 7**,** 311-322.

HOLLOWAY, S. L., GLOTZER, M., KING, R. W. & MURRAY, A. W. 1993. Anaphase is initiated by proteolysis rather than by the inactivation of maturation-promoting factor. *Cell,* 73**,** 1393-402.

HOLT, C. L. & MAY, G. S. 1996. An extragenic suppressor of the mitosis-defective bimD6 mutation of Aspergillus nidulans codes for a chromosome scaffold protein. *Genetics,* 142**,** 777-87.

HOLT, L. J., KRUTCHINSKY, A. N. & MORGAN, D. O. 2008. Positive feedback sharpens the anaphase switch. *Nature,* 454**,** 353-7.

HORNIG, N. C. & UHLMANN, F. 2004. Preferential cleavage of chromatin-bound cohesin after targeted phosphorylation by Polo-like kinase. *EMBO J,* 23**,** 3144-53.

HOU, F. & ZOU, H. 2005. Two human orthologues of Eco1/Ctf7 acetyltransferases are both required for proper sister-chromatid cohesion. *Mol Biol Cell,* 16**,** 3908-18.

HU, B., ITOH, T., MISHRA, A., KATOH, Y., CHAN, K. L., UPCHER, W., GODLEE, C., ROIG, M. B., SHIRAHIGE, K. & NASMYTH, K. 2011. ATP hydrolysis is required for relocating cohesin from sites occupied by its Scc2/4 loading complex. *Curr Biol,* 21**,** 12-24.

HUIS IN 'T VELD, P. J., HERZOG, F., LADURNER, R., DAVIDSON, I. F., PIRIC, S., KREIDL, E., BHASKARA, V., AEBERSOLD, R. & PETERS, J. M. 2014. Characterization of a DNA exit gate in the human cohesin ring. *Science,* 346**,** 968-72.

INDJEIAN, V. B., STERN, B. M. & MURRAY, A. W. 2005. The centromeric protein Sgo1 is required to sense lack of tension on mitotic chromosomes. *Science,* 307**,** 130-3.

IVANOV, D., SCHLEIFFER, A., EISENHABER, F., MECHTLER, K., HAERING, C. H. & NASMYTH, K. 2002. Eco1 is a novel acetyltransferase that can acetylate proteins involved in cohesion. *Curr Biol,* 12**,** 323-8.

JESSBERGER, R., RIWAR, B., BAECHTOLD, H. & AKHMEDOV, A. T. 1996. SMC proteins constitute two subunits of the mammalian recombination complex RC-1. *EMBO J,* 15**,** 4061-8.

KABSCH, W. 2010. Xds. *Acta Crystallogr D Biol Crystallogr,* 66**,** 125-32.

KAGEY, M. H., NEWMAN, J. J., BILODEAU, S., ZHAN, Y., ORLANDO, D. A., VAN BERKUM, N. L., EBMEIER, C. C., GOOSSENS, J., RAHL, P. B., LEVINE, S. S., TAATJES, D. J., DEKKER, J. & YOUNG, R. A. 2010. Mediator and cohesin connect gene expression and chromatin architecture. *Nature,* 467**,** 430-5.

KENNA, M. A. & SKIBBENS, R. V. 2003. Mechanical link between cohesion establishment and DNA replication: Ctf7p/Eco1p, a cohesion establishment factor, associates with three different replication factor C complexes. *Mol Cell Biol,* 23**,** 2999-3007.

KERREBROCK, A. W., MIYAZAKI, W. Y., BIRNBY, D. & ORR-WEAVER, T. L. 1992. The Drosophila mei-S332 gene promotes sister-chromatid cohesion in meiosis following kinetochore differentiation. *Genetics,* 130**,** 827-41.

KING, R. W., PETERS, J. M., TUGENDREICH, S., ROLFE, M., HIETER, P. & KIRSCHNER, M. W. 1995. A 20S complex containing CDC27 and CDC16 catalyzes the mitosis-specific conjugation of ubiquitin to cyclin B. *Cell,* 81**,** 279-88.

KITAJIMA, T. S., HAUF, S., OHSUGI, M., YAMAMOTO, T. & WATANABE, Y. 2005. Human Bub1 defines the persistent cohesion site along the mitotic chromosome by affecting Shugoshin localization. *Curr Biol,* 15**,** 353-9.

KITAJIMA, T. S., SAKUNO, T., ISHIGURO, K., IEMURA, S., NATSUME, T., KAWASHIMA, S. A. & WATANABE, Y. 2006. Shugoshin collaborates with protein phosphatase 2A to protect cohesin. *Nature,* 441**,** 46-52.

KOSHLAND, D. & HARTWELL, L. H. 1987. The structure of sister minichromosome DNA before anaphase in Saccharomyces cerevisiae. *Science,* 238**,** 1713-6.

KUENG, S., HEGEMANN, B., PETERS, B. H., LIPP, J. J., SCHLEIFFER, A., MECHTLER, K. & PETERS, J. M. 2006. Wapl controls the dynamic association of cohesin with chromatin. *Cell,* 127**,** 955-67.

KULEMZINA, I., SCHUMACHER, M. R., VERMA, V., REITER, J., METZLER, J., FAILLA, A. V., LANZ, C., SREEDHARAN, V. T., RATSCH, G. & IVANOV, D. 2012. Cohesin rings devoid of Scc3 and Pds5 maintain their stable association with the DNA. *PLoS Genet,* 8**,** e1002856.

KURLANDZKA, A., RYTKA, J., GROMADKA, R. & MURAWSKI, M. 1995. A new essential gene located on Saccharomyces cerevisiae chromosome IX. *Yeast,* 11**,** 885-90.

KURLANDZKA, A., RYTKA, J., ROZALSKA, B. & WYSOCKA, M. 1999. Saccharomyces cerevisiae IRR1 protein is indirectly involved in colony formation. *Yeast,* 15**,** 23-33.

LADURNER, R., BHASKARA, V., HUIS IN 'T VELD, P. J., DAVIDSON, I. F., KREIDL, E., PETZOLD, G. & PETERS, J. M. 2014. Cohesin's ATPase activity couples cohesin loading onto DNA with Smc3 acetylation. *Curr Biol,* 24**,** 2228-37.

LAFONT, A. L., SONG, J. & RANKIN, S. 2010. Sororin cooperates with the acetyltransferase Eco2 to ensure DNA replication-dependent sister chromatid cohesion. *Proc Natl Acad Sci U S A,* 107**,** 20364-9.

LARIONOV, V. L., KARPOVA, T. S., KOUPRINA, N. Y. & JOURAVLEVA, G. A. 1985. A mutant of Saccharomyces cerevisiae with impaired maintenance of centromeric plasmids. *Curr Genet,* 10**,** 15-20.

LENGRONNE, A., KATOU, Y., MORI, S., YOKOBAYASHI, S., KELLY, G. P., ITOH, T., WATANABE, Y., SHIRAHIGE, K. & UHLMANN, F. 2004. Cohesin relocation from sites of chromosomal loading to places of convergent transcription. *Nature,* 430**,** 573-8.

LENGRONNE, A., MCINTYRE, J., KATOU, Y., KANOH, Y., HOPFNER, K. P., SHIRAHIGE, K. & UHLMANN, F. 2006. Establishment of sister chromatid cohesion at the S. cerevisiae replication fork. *Mol Cell,* 23**,** 787-99.

LIEBERMAN-AIDEN, E., VAN BERKUM, N. L., WILLIAMS, L., IMAKAEV, M., RAGOCZY, T., TELLING, A., AMIT, I., LAJOIE, B. R., SABO, P. J., DORSCHNER, M. O., SANDSTROM, R., BERNSTEIN, B., BENDER, M. A., GROUDINE, M., GNIRKE, A., STAMATOYANNOPOULOS, J., MIRNY, L. A., LANDER, E. S. & DEKKER, J. 2009. Comprehensive mapping of long-range interactions reveals folding principles of the human genome. *Science,* 326**,** 289-93.

LIU, H., JIA, L. & YU, H. 2013a. Phospho-H2A and cohesin specify distinct tension-regulated Sgo1 pools at kinetochores and inner centromeres. *Curr Biol,* 23**,** 1927-33.

LIU, H., RANKIN, S. & YU, H. 2013b. Phosphorylation-enabled binding of SGO1-PP2A to cohesin protects sororin and centromeric cohesion during mitosis. *Nat Cell Biol,* 15**,** 40-9.

LOPEZ-SERRA, L., KELLY, G., PATEL, H., STEWART, A. & UHLMANN, F. 2014. The Scc2-Scc4 complex acts in sister chromatid cohesion and transcriptional regulation by maintaining nucleosome-free regions. *Nat Genet,* 46**,** 1147-51.

LOPEZ-SERRA, L., LENGRONNE, A., BORGES, V., KELLY, G. & UHLMANN, F. 2013. Budding yeast Wapl controls sister chromatid cohesion maintenance and chromosome condensation. *Curr Biol,* 23**,** 64-9.

LOSADA, A., HIRANO, M. & HIRANO, T. 1998. Identification of Xenopus SMC protein complexes required for sister chromatid cohesion. *Genes Dev,* 12**,** 1986-97.

LOSADA, A., HIRANO, M. & HIRANO, T. 2002. Cohesin release is required for sister chromatid resolution, but not for condensin-mediated compaction, at the onset of mitosis. *Genes Dev,* 16**,** 3004-16.

LOSADA, A., YOKOCHI, T. & HIRANO, T. 2005. Functional contribution of Pds5 to cohesin-mediated cohesion in human cells and Xenopus egg extracts. *J Cell Sci,* 118**,** 2133-41.

LOSADA, A., YOKOCHI, T., KOBAYASHI, R. & HIRANO, T. 2000. Identification and characterization of SA/Scc3p subunits in the Xenopus and human cohesin complexes. *J Cell Biol,* 150**,** 405-16.

LYONS, N. A., FONSLOW, B. R., DIEDRICH, J. K., YATES, J. R., 3RD & MORGAN, D. O. 2013. Sequential primed kinases create a damage-responsive phosphodegron on Eco1. *Nat Struct Mol Biol,* 20**,** 194-201.

LYONS, N. A. & MORGAN, D. O. 2011. Cdk1-dependent destruction of Eco1 prevents cohesion establishment after S phase. *Mol Cell,* 42**,** 378-89.

MARSTON, A. L., THAM, W. H., SHAH, H. & AMON, A. 2004. A genome-wide screen identifies genes required for centromeric cohesion. *Science,* 303**,** 1367-70.

MCGUINNESS, B. E., HIROTA, T., KUDO, N. R., PETERS, J. M. & NASMYTH, K. 2005. Shugoshin prevents dissociation of cohesin from centromeres during mitosis in vertebrate cells. *PLoS Biol,* 3**,** e86.

MEGEE, P. C., MISTROT, C., GUACCI, V. & KOSHLAND, D. 1999. The centromeric sister chromatid cohesion site directs Mcd1p binding to adjacent sequences. *Mol Cell,* 4**,** 445-50.

MICHAELIS, C., CIOSK, R. & NASMYTH, K. 1997. Cohesins: chromosomal proteins that prevent premature separation of sister chromatids. *Cell,* 91**,** 35-45.

MINAJIGI, A., FROBERG, J. E., WEI, C., SUNWOO, H., KESNER, B., COLOGNORI, D., LESSING, D., PAYER, B., BOUKHALI, M., HAAS, W. & LEE, J. T. 2015. Chromosomes. A comprehensive Xist interactome reveals cohesin repulsion and an RNA-directed chromosome conformation. *Science,* 349.

MINAMINO, M., ISHIBASHI, M., NAKATO, R., AKIYAMA, K., TANAKA, H., KATO, Y., NEGISHI, L., HIROTA, T., SUTANI, T., BANDO, M. & SHIRAHIGE, K. 2015. Esco1 Acetylates Cohesin via a Mechanism Different from That of Esco2. *Curr Biol,* 25**,** 1694-706.

MISHRA, A., HU, B., KURZE, A., BECKOUET, F., FARCAS, A. M., DIXON, S. E., KATOU, Y., KHALID, S., SHIRAHIGE, K. & NASMYTH, K. 2010. Both interaction surfaces within cohesin's hinge domain are essential for its stable chromosomal association. *Curr Biol,* 20**,** 279-89.

MOLDOVAN, G. L., PFANDER, B. & JENTSCH, S. 2006. PCNA controls establishment of sister chromatid cohesion during S phase. *Mol Cell,* 23**,** 723-32.

MONACO, S., GORDON, E., BOWLER, M. W., DELAGENIERE, S., GUIJARRO, M., SPRUCE, D., SVENSSON, O., MCSWEENEY, S. M., MCCARTHY, A. A., LEONARD, G. & NANAO, M. H. 2013. Automatic processing of macromolecular crystallography X-ray diffraction data at the ESRF. *J Appl Crystallogr,* 46**,** 804-810.

MURAYAMA, Y. & UHLMANN, F. 2014. Biochemical reconstitution of topological DNA binding by the cohesin ring. *Nature,* 505**,** 367-71.

MURRAY, A. W. & SZOSTAK, J. W. 1985. Chromosome segregation in mitosis and meiosis. *Annu Rev Cell Biol,* 1**,** 289-315.

NASMYTH, K. 2011. Cohesin: a catenase with separate entry and exit gates? *Nat Cell Biol,* 13**,** 1170-7.

NERUSHEVA, O. O., GALANDER, S., FERNIUS, J., KELLY, D. & MARSTON, A. L. 2014. Tension-dependent removal of pericentromeric shugoshin is an indicator of sister chromosome biorientation. *Genes Dev,* 28**,** 1291-309.

NISHIYAMA, T., LADURNER, R., SCHMITZ, J., KREIDL, E., SCHLEIFFER, A., BHASKARA, V., BANDO, M., SHIRAHIGE, K., HYMAN, A., MECHTLER, K. & PETERS, J.-M. 2010. Sororin Mediates Sister Chromatid Cohesion by Antagonizing Wapl. *Cell,* 143**,** 737-749.

NISHIYAMA, T., SYKORA, M. M., HUIS IN 'T VELD, P. J., MECHTLER, K. & PETERS, J. M. 2013a. Aurora B and Cdk1 mediate Wapl activation and release of acetylated cohesin from chromosomes by phosphorylating Sororin. *Proceedings of the National Academy of Sciences,* 110**,** 13404-13409.

NISHIYAMA, T., SYKORA, M. M., HUIS IN 'T VELD, P. J., MECHTLER, K. & PETERS, J. M. 2013b. Aurora B and Cdk1 mediate Wapl activation and release of acetylated cohesin from chromosomes by phosphorylating Sororin. *Proc Natl Acad Sci U S A,* 110**,** 13404-9.

O'DONOVAN, D. J., STOKES-REES, I., NAM, Y., BLACKLOW, S. C., SCHRODER, G. F., BRUNGER, A. T. & SLIZ, P. 2012. A grid-enabled web service for low-resolution crystal structure refinement. *Acta Crystallogr D Biol Crystallogr,* 68**,** 261-7.

OIKAWA, K., OHBAYASHI, T., KIYONO, T., NISHI, H., ISAKA, K., UMEZAWA, A., KURODA, M. & MUKAI, K. 2004. Expression of a novel human gene, human wings apart-like (hWAPL), is associated with cervical carcinogenesis and tumor progression. *Cancer Res,* 64**,** 3545-9.

ONN, I., GUACCI, V. & KOSHLAND, D. E. 2009. The zinc finger of Eco1 enhances its acetyltransferase activity during sister chromatid cohesion. *Nucleic Acids Res,* 37**,** 6126-34.

ORGIL, O., MATITYAHU, A., ENG, T., GUACCI, V., KOSHLAND, D. & ONN, I. 2015. A conserved domain in the scc3 subunit of cohesin mediates the interaction with both mcd1 and the cohesin loader complex. *PLoS Genet,* 11**,** e1005036.

OUYANG, Z., ZHENG, G., SONG, J., BOREK, D. M., OTWINOWSKI, Z., BRAUTIGAM, C. A., TOMCHICK, D. R., RANKIN, S. & YU, H. 2013. Structure of the human cohesin inhibitor Wapl. *Proceedings of the National Academy of Sciences,* 110**,** 11355-11360.

PANIZZA, S., TANAKA, T., HOCHWAGEN, A., EISENHABER, F. & NASMYTH, K. 2000. Pds5 cooperates with cohesin in maintaining sister chromatid cohesion. *Curr Biol,* 10**,** 1557-64.

PARELHO, V., HADJUR, S., SPIVAKOV, M., LELEU, M., SAUER, S., GREGSON, H. C., JARMUZ, A., CANZONETTA, C., WEBSTER, Z., NESTEROVA, T., COBB, B. S., YOKOMORI, K., DILLON, N., ARAGON, L., FISHER, A. G. & MERKENSCHLAGER, M. 2008. Cohesins functionally associate with CTCF on mammalian chromosome arms. *Cell,* 132**,** 422-33.

PEPLOWSKA, K., WALLEK, A. U. & STORCHOVA, Z. 2014. Sgo1 regulates both condensin and Ipl1/Aurora B to promote chromosome biorientation. *PLoS Genet,* 10**,** e1004411.

PEREIRA, G. & SCHIEBEL, E. 2003. Separase regulates INCENP-Aurora B anaphase spindle function through Cdc14. *Science,* 302**,** 2120-4.

PERNOT, P., ROUND, A., BARRETT, R., DE MARIA ANTOLINOS, A., GOBBO, A., GORDON, E., HUET, J., KIEFFER, J., LENTINI, M., MATTENET, M., MORAWE, C., MUELLER-DIECKMANN, C., OHLSSON, S., SCHMID, W., SURR, J., THEVENEAU, P., ZERRAD, L. & MCSWEENEY, S. 2013. Upgraded ESRF BM29 beamline for SAXS on macromolecules in solution. *J Synchrotron Radiat,* 20**,** 660-4.

PETERS, J.-M. & NISHIYAMA, T. 2012. Sister Chromatid Cohesion. *Cold Spring Harbor Perspectives in Biology*.

PETOUKHOV, M. V., FRANKE, D., SHKUMATOV, A. V., TRIA, G., KIKHNEY, A. G., GAJDA, M., GORBA, C., MERTENS, H. D., KONAREV, P. V. & SVERGUN, D. I. 2012. New developments in the program package for small-angle scattering data analysis. *J Appl Crystallogr,* 45**,** 342-350.

PIAZZA, I., RUTKOWSKA, A., ORI, A., WALCZAK, M., METZ, J., PELECHANO, V., BECK, M. & HAERING, C. H. 2014. Association of condensin with chromosomes depends on DNA binding by its HEAT-repeat subunits. *Nat Struct Mol Biol,* 21**,** 560-8.

RANKIN, S., AYAD, N. G. & KIRSCHNER, M. W. 2005. Sororin, a substrate of the anaphase-promoting complex, is required for sister chromatid cohesion in vertebrates. *Mol Cell,* 18**,** 185-200.

RAO, H., UHLMANN, F., NASMYTH, K. & VARSHAVSKY, A. 2001. Degradation of a cohesin subunit by the N-end rule pathway is essential for chromosome stability. *Nature,* 410**,** 955-9.

REMESEIRO, S., CUADRADO, A., CARRETERO, M., MARTINEZ, P., DROSOPOULOS, W. C., CANAMERO, M., SCHILDKRAUT, C. L., BLASCO, M. A. & LOSADA, A. 2012a. Cohesin-SA1 deficiency drives

aneuploidy and tumourigenesis in mice due to impaired replication of telomeres. *EMBO J,* 31**,** 2076-89.

REMESEIRO, S., CUADRADO, A., GOMEZ-LOPEZ, G., PISANO, D. G. & LOSADA, A. 2012b. A unique role of cohesin-SA1 in gene regulation and development. *EMBO J,* 31**,** 2090-102.

RESNICK, T. D., SATINOVER, D. L., MACISAAC, F., STUKENBERG, P. T., EARNSHAW, W. C., ORR-WEAVER, T. L. & CARMENA, M. 2006. INCENP and Aurora B promote meiotic sister chromatid cohesion through localization of the Shugoshin MEI-S332 in Drosophila. *Dev Cell,* 11**,** 57-68.

ROIG, M. B., LOWE, J., CHAN, K. L., BECKOUET, F., METSON, J. & NASMYTH, K. 2014. Structure and function of cohesin's Scc3/SA regulatory subunit. *FEBS Lett,* 588**,** 3692-702.

ROJAS, J. R., TRIEVEL, R. C., ZHOU, J., MO, Y., LI, X., BERGER, S. L., ALLIS, C. D. & MARMORSTEIN, R. 1999. Structure of Tetrahymena GCN5 bound to coenzyme A and a histone H3 peptide. *Nature,* 401**,** 93-8.

ROWLAND, B. D., ROIG, M. B., NISHINO, T., KURZE, A., ULUOCAK, P., MISHRA, A., BECKOUET, F., UNDERWOOD, P., METSON, J., IMRE, R., MECHTLER, K., KATIS, V. L. & NASMYTH, K. 2009. Building sister chromatid cohesion: smc3 acetylation counteracts an antiestablishment activity. *Mol Cell,* 33**,** 763-74.

SANYAL, A., LAJOIE, B. R., JAIN, G. & DEKKER, J. 2012. The long-range interaction landscape of gene promoters. *Nature,* 489**,** 109-13.

SCHLEIFFER, A., KAITNA, S., MAURER-STROH, S., GLOTZER, M., NASMYTH, K. & EISENHABER, F. 2003. Kleisins: a superfamily of bacterial and eukaryotic SMC protein partners. *Mol Cell,* 11**,** 571-5.

SCHMITZ, J., WATRIN, E., LENART, P., MECHTLER, K. & PETERS, J. M. 2007. Sororin is required for stable binding of cohesin to chromatin and for sister chromatid cohesion in interphase. *Curr Biol,* 17**,** 630-6.

SCHRODER, G. F., LEVITT, M. & BRUNGER, A. T. 2010. Super-resolution biomolecular crystallography with low-resolution data. *Nature,* 464**,** 1218-22.

SHINTOMI, K. & HIRANO, T. 2009. Releasing cohesin from chromosome arms in early mitosis: opposing actions of Wapl-Pds5 and Sgo1. *Genes Dev,* 23**,** 2224-36.

SIEVERS, F. & HIGGINS, D. G. 2014. Clustal omega. *Curr Protoc Bioinformatics,* 48**,** 3 13 1-3 13 16.

SJOGREN, C. & NASMYTH, K. 2001. Sister chromatid cohesion is required for postreplicative double-strand break repair in Saccharomyces cerevisiae. *Curr Biol,* 11**,** 991-5.

SKIBBENS, R. V., CORSON, L. B., KOSHLAND, D. & HIETER, P. 1999. Ctf7p is essential for sister chromatid cohesion and links mitotic chromosome structure to the DNA replication machinery. *Genes Dev,* 13**,** 307-19.

SODING, J., BIEGERT, A. & LUPAS, A. N. 2005. The HHpred interactive server for protein homology detection and structure prediction. *Nucleic Acids Res,* 33**,** W244-8.

SOLOMON, D. A., KIM, T., DIAZ-MARTINEZ, L. A., FAIR, J., ELKAHLOUN, A. G., HARRIS, B. T., TORETSKY, J. A., ROSENBERG, S. A., SHUKLA, N., LADANYI, M., SAMUELS, Y., JAMES, C. D., YU, H., KIM, J. S. & WALDMAN, T. 2011. Mutational inactivation of STAG2 causes aneuploidy in human cancer. *Science,* 333**,** 1039-43.

STEAD, K., AGUILAR, C., HARTMAN, T., DREXEL, M., MELUH, P. & GUACCI, V. 2003. Pds5p regulates the maintenance of sister chromatid cohesion and is sumoylated to promote the dissolution of cohesion. *J Cell Biol,* 163**,** 729-41.

STEGMEIER, F., VISINTIN, R. & AMON, A. 2002. Separase, polo kinase, the kinetochore protein Slk19, and Spo12 function in a network that controls Cdc14 localization during early anaphase. *Cell,* 108**,** 207-20.

STROM, L., KARLSSON, C., LINDROOS, H. B., WEDAHL, S., KATOU, Y., SHIRAHIGE, K. & SJOGREN, C. 2007. Postreplicative formation of cohesion is required for repair and induced by a single DNA break. *Science,* 317**,** 242-5.

STRUNNIKOV, A. V., LARIONOV, V. L. & KOSHLAND, D. 1993. SMC1: an essential yeast gene encoding a putative head-rod-tail protein is required for nuclear division and defines a new ubiquitous protein family. *J Cell Biol,* 123**,** 1635-48.

STUDIER, F. W. 2005. Protein production by auto-induction in high density shaking cultures. *Protein Expr Purif,* 41**,** 207-34.

SUDAKIN, V., GANOTH, D., DAHAN, A., HELLER, H., HERSHKO, J., LUCA, F. C., RUDERMAN, J. V. & HERSHKO, A. 1995. The cyclosome, a large complex containing cyclin-selective ubiquitin ligase activity, targets cyclins for destruction at the end of mitosis. *Mol Biol Cell,* 6**,** 185-97.

SUMARA, I., VORLAUFER, E., GIEFFERS, C., PETERS, B. H. & PETERS, J. M. 2000. Characterization of vertebrate cohesin complexes and their regulation in prophase. *J Cell Biol,* 151**,** 749-62.

SUMARA, I., VORLAUFER, E., STUKENBERG, P. T., KELM, O., REDEMANN, N., NIGG, E. A. & PETERS, J. M. 2002. The dissociation of cohesin from chromosomes in prophase is regulated by Polo-like kinase. *Mol Cell,* 9**,** 515-25.

SUN, Y., KUCEJ, M., FAN, H. Y., YU, H., SUN, Q. Y. & ZOU, H. 2009. Separase is recruited to mitotic chromosomes to dissolve sister chromatid cohesion in a DNA-dependent manner. *Cell,* 137**,** 123-32.

SUTANI, T., KAWAGUCHI, T., KANNO, R., ITOH, T. & SHIRAHIGE, K. 2009. Budding yeast Wpl1(Rad61)-Pds5 complex counteracts sister chromatid cohesion-establishing reaction. *Curr Biol,* 19**,** 492-7.

SVENSSON, O., MALBET-MONACO, S., POPOV, A., NURIZZO, D. & BOWLER, M. W. 2015. Fully automatic characterization and data collection from crystals of biological macromolecules. *Acta Crystallogr D Biol Crystallogr,* 71**,** 1757-67.

TAKAHASHI, T. S., YIU, P., CHOU, M. F., GYGI, S. & WALTER, J. C. 2004. Recruitment of Xenopus Scc2 and cohesin to chromatin requires the pre-replication complex. *Nat Cell Biol,* 6**,** 991-6.

TANAKA, K., HAO, Z., KAI, M. & OKAYAMA, H. 2001. Establishment and maintenance of sister chromatid cohesion in fission yeast by a unique mechanism. *EMBO J,* 20**,** 5779-90.

TANAKA, K., YONEKAWA, T., KAWASAKI, Y., KAI, M., FURUYA, K., IWASAKI, M., MURAKAMI, H., YANAGIDA, M. & OKAYAMA, H. 2000. Fission yeast Eso1p is required for establishing sister chromatid cohesion during S phase. *Mol Cell Biol,* 20**,** 3459-69.

TANAKA, T., COSMA, M. P., WIRTH, K. & NASMYTH, K. 1999. Identification of cohesin association sites at centromeres and along chromosome arms. *Cell,* 98**,** 847-58.

TANG, T. T., BICKEL, S. E., YOUNG, L. M. & ORR-WEAVER, T. L. 1998. Maintenance of sister-chromatid cohesion at the centromere by the Drosophila MEI-S332 protein. *Genes Dev,* 12**,** 3843-56.

TANG, Z., SUN, Y., HARLEY, S. E., ZOU, H. & YU, H. 2004. Human Bub1 protects centromeric sister-chromatid cohesion through Shugoshin during mitosis. *Proc Natl Acad Sci U S A,* 101**,** 18012-7.

TEDESCHI, A., WUTZ, G., HUET, S., JARITZ, M., WUENSCHE, A., SCHIRGHUBER, E., DAVIDSON, I. F., TANG, W., CISNEROS, D. A., BHASKARA, V., NISHIYAMA, T., VAZIRI, A., WUTZ, A., ELLENBERG, J. & PETERS, J.-M. 2013. Wapl is an essential regulator of chromatin structure and chromosome segregation. *Nature,* 501**,** 564-568.

TERRET, M. E., SHERWOOD, R., RAHMAN, S., QIN, J. & JALLEPALLI, P. V. 2009. Cohesin acetylation speeds the replication fork. *Nature,* 462**,** 231-4.

TOTH, A., CIOSK, R., UHLMANN, F., GALOVA, M., SCHLEIFFER, A. & NASMYTH, K. 1999. Yeast cohesin complex requires a conserved protein, Eco1p(Ctf7), to establish cohesion between sister chromatids during DNA replication. *Genes Dev,* 13**,** 320-33.

TSUKAHARA, T., TANNO, Y. & WATANABE, Y. 2010. Phosphorylation of the CPC by Cdk1 promotes chromosome bi-orientation. *Nature,* 467**,** 719-23.

UHLMANN, F., LOTTSPEICH, F. & NASMYTH, K. 1999. Sister-chromatid separation at anaphase onset is promoted by cleavage of the cohesin subunit Scc1. *Nature,* 400**,** 37-42.

UHLMANN, F. & NASMYTH, K. 1998. Cohesion between sister chromatids must be established during DNA replication. *Curr Biol,* 8**,** 1095-101.

UNAL, E., HEIDINGER-PAULI, J. M., KIM, W., GUACCI, V., ONN, I., GYGI, S. P. & KOSHLAND, D. E. 2008. A molecular determinant for the establishment of sister chromatid cohesion. *Science,* 321**,** 566-9.

UNAL, E., HEIDINGER-PAULI, J. M. & KOSHLAND, D. 2007. DNA double-strand breaks trigger genome-wide sister-chromatid cohesion through Eco1 (Ctf7). *Science,* 317**,** 245-8.

VAUR, S., FEYTOUT, A., VAZQUEZ, S. & JAVERZAT, J. P. 2012. Pds5 promotes cohesin acetylation and stable cohesin-chromosome interaction. *EMBO Rep,* 13**,** 645-52.

VERNI, F., GANDHI, R., GOLDBERG, M. L. & GATTI, M. 2000. Genetic and molecular analysis of wings apart-like (Wapl), a gene controlling heterochromatin organization in Drosophila melanogaster. *Genetics,* 154**,** 1693-710.

WAIZENEGGER, I. C., HAUF, S., MEINKE, A. & PETERS, J. M. 2000. Two distinct pathways remove mammalian cohesin from chromosome arms in prophase and from centromeres in anaphase. *Cell,* 103**,** 399-410.

WANG, F., YODER, J., ANTOSHECHKIN, I. & HAN, M. 2003. Caenorhabditis elegans EVL-14/PDS-5 and SCC-3 are essential for sister chromatid cohesion in meiosis and mitosis. *Mol Cell Biol,* 23**,** 7698-707.

WATRIN, E., SCHLEIFFER, A., TANAKA, K., EISENHABER, F., NASMYTH, K. & PETERS, J. M. 2006. Human Scc4 is required for cohesin binding to chromatin, sister-chromatid cohesion, and mitotic progression. *Curr Biol,* 16**,** 863-74.

WEITZER, S., LEHANE, C. & UHLMANN, F. 2003. A model for ATP hydrolysis-dependent binding of cohesin to DNA. *Curr Biol,* 13**,** 1930-40.

WENDT, K. S., YOSHIDA, K., ITOH, T., BANDO, M., KOCH, B., SCHIRGHUBER, E., TSUTSUMI, S., NAGAE, G., ISHIHARA, K., MISHIRO, T., YAHATA, K., IMAMOTO, F., ABURATANI, H., NAKAO, M., IMAMOTO, N., MAESHIMA, K., SHIRAHIGE, K. & PETERS, J. M. 2008. Cohesin mediates transcriptional insulation by CCCTC-binding factor. *Nature,* 451**,** 796-801.

WINN, M. D., BALLARD, C. C., COWTAN, K. D., DODSON, E. J., EMSLEY, P., EVANS, P. R., KEEGAN, R. M., KRISSINEL, E. B., LESLIE, A. G., MCCOY, A., MCNICHOLAS, S. J., MURSHUDOV, G. N., PANNU, N. S., POTTERTON, E. A., POWELL, H. R., READ, R. J., VAGIN, A. & WILSON, K. S. 2011. Overview of the CCP4 suite and current developments. *Acta Crystallogr D Biol Crystallogr,* 67**,** 235-42.

WOO, J.-S., LIM, J.-H., SHIN, H.-C., SUH, M.-K., KU, B., LEE, K.-H., JOO, K., ROBINSON, H., LEE, J., PARK, S.-Y., HA, N.-C. & OH, B.-H. 2009. Structural Studies of a Bacterial Condensin Complex Reveal ATP-Dependent Disruption of Intersubunit Interactions. *Cell,* 136**,** 85-96.

XIONG, B., LU, S. & GERTON, J. L. 2010. Hos1 is a lysine deacetylase for the Smc3 subunit of cohesin. *Curr Biol,* 20**,** 1660-5.

XU, Z., CETIN, B., ANGER, M., CHO, U. S., HELMHART, W., NASMYTH, K. & XU, W. 2009. Structure and function of the PP2A-shugoshin interaction. *Mol Cell,* 35**,** 426-41.

YAMAGISHI, Y., HONDA, T., TANNO, Y. & WATANABE, Y. 2010. Two histone marks establish the inner centromere and chromosome bi-orientation. *Science,* 330**,** 239-43.

YAN, J., ENGE, M., WHITINGTON, T., DAVE, K., LIU, J., SUR, I., SCHMIERER, B., JOLMA, A., KIVIOJA, T., TAIPALE, M. & TAIPALE, J. 2013. Transcription factor binding in human cells occurs in dense clusters formed around cohesin anchor sites. *Cell,* 154**,** 801-13.

ZHANG, J., SHI, X., LI, Y., KIM, B. J., JIA, J., HUANG, Z., YANG, T., FU, X., JUNG, S. Y., WANG, Y., ZHANG, P., KIM, S. T., PAN, X. & QIN, J. 2008. Acetylation of Smc3 by Eco1 is required for S phase sister chromatid cohesion in both human and yeast. *Mol Cell,* 31**,** 143-51.

ZHANG, N., JIANG, Y., MAO, Q., DEMELER, B., TAO, Y. J. & PATI, D. 2013. Characterization of the interaction between the cohesin subunits Rad21 and SA1/2. *PLoS ONE,* 8**,** e69458.

ZOU, H., MCGARRY, T. J., BERNAL, T. & KIRSCHNER, M. W. 1999. Identification of a vertebrate sister-chromatid separation inhibitor involved in transformation and tumorigenesis. *Science,* 285**,** 418-22.